May 2019

A Viable Residential DC Microgrid for Low Income Communities – Architecture, Protection and Education

Karthik Palaniappan
University of Wisconsin-Milwaukee

A VIABLE RESIDENTIAL DC MICROGRID FOR LOW INCOME COMMUNITIES – ARCHITECTURE, PROTECTION AND EDUCATION

by

Karthik Palaniappan

A Dissertation Submitted in

Partial Fulfillment of the

Requirements for the Degree of

Doctor of Philosophy

in Engineering

at

The University of Wisconsin-Milwaukee

May 2019

ABSTRACT

A VIABLE RESIDENTIAL DC MICROGRID FOR LOW INCOME COMMUNITIES IN MILWAUKEE – ARCHITECTURE, PROTECTION AND EDUCATION

by

Karthik Palaniappan

The University of Wisconsin-Milwaukee, 2019
Under the Supervision of Professor Robert M. Cuzner

The availability of fossil fuels in the future and the environmental effects such as the carbon footprint of the existing methodologies to produce electricity is an increasing area of concern. In rural areas of under-developed parts of the world, the problem is lack of access to electrification. DC microgrids have become a proven solution to electrification in these areas with demonstrated exceptional quality of power, high reliability, efficiency, and simplified integration between renewable energy sources (principally solar PV) and energy storage. In the United States, a different problem occurs that can be addressed with the same DC microgrid approach that is finding success internationally. In disinvested, underserved communities with high unemployment and low wages, households contribute a significant portion of their income towards the fixed cost of their electrical utility connection, which by law must be supplied to every household. In order to realize such a microgrid in these communities, there are three major areas which need to be accounted for. Firstly, there needs to be a custom architecture for the community under consideration and it needs to be economical to match the needs of the underserved community. Secondly, DC microgrid for home energy interconnection is potentially less complex and less expensive to deploy, operate and maintain however, faster protection is a key element to ensuring resilience, viability and adoptability. Lastly, these types of efforts will

be sustainable only if the people in the community are educated and invested in the same as they are the key stakeholders in these systems.

This dissertation presents an approach to make the DC Microgrid economically feasible for low income households by reducing the cost they incur on electric bills. The approach is to overlay a DC system into homes that have a utility feed in order to incorporate renewable energy usage into an urban setting for the express purpose of driving down individual household utility costs. The results show that the incorporation of a certain level of "smart" appliances and fixtures into the renovation of vacated homes and the use of a microgrid to enable sharing of renewable energy, such as solar power combined with energy storage, between homes in the proposed architecture yields the least expensive option for the patrons. The development of solid state circuit breakers that interface between the microgrid and the home DC power panels helps in faster protection of the DC system. In this dissertation, a SiC JFET based device is designed and built to protect against DC faults at a faster rate than the available solutions. The prototype is tested for verification and used to discriminate against short circuit faults and the results show the successful fault discrimination capabilities of the device. A basic system level simulation with the protection device is implemented using Real Time Hardware in the loop platform. Finally, as a part of engaging the community members, the high school kids in the area who might potentially be living in some of the houses in this community are being educated about the microgrid, appliances and other technologies to get a better understanding of STEM and hopefully inspiring them to pursue a career in STEM in the future.

I dedicate this dissertation to my son.

TABLE OF CONTENTS

LIST OF FIGURES

LIST OF TABLES

LIST OF NOMENCLATURE

AC	Alternating Current
ALP	Aggregated Load Profile
ASGP	Aggregated Solar Generation Profile
CB	Circuit Breakers
CDC	Community Development Corporation
CHIL	Computer Hardware-in-the-Loop
DC	Direct Current
DC MG	DC Micro Grid
DER	Distributed Energy Resources
DOE	Department Of Energy
DSM	Demand Side Management
FPGA	Field Programmable Gate Array
HEMS	Home Energy Management System
HIL	Hardware-in-the-Loop
JFET	Junction Field Effect Transistor
L(i)	Load Data from ALP
MCB	Miniature Circuit Breakers
MCCB	Molded Case Circuit Breakers
MEMS	Microgrid Energy Management System
MOV	Metal Oxide Varistor
NLP	Net Load Profile
NREL	National Renewable Energy Laboratories
PCC	Point of Common Coupling
RECS	Residential Energy Consumption Survey
S(i)	Solar Data from ASGP
SiC	Silicon Carbide
SSCB	Solid State Circuit Breaker
TCE	Thermal Coefficient of Expansion
USP	Unit Size Panel
WBG	Wide Band Gap

ACKNOWLEDGEMENTS

Service to mankind is service to God – Sai Baba

As humans, I believe we are on earth for a purpose and it is not possible to always find out what it is. This quote has always stuck in my head since the time I heard it and I believe that my purpose in this world is to serve mankind in whatsoever way possible during my lifetime. I have been very lucky and extremely fortunate to be associated with a university like UWM which shares a similar vision, of serving the community through technology and research.

I have to start by thanking my advisor Dr. Robert M Cuzner for not only being a great advisor and a mentor but also for being such an inspiration. I have been blessed to spend so much time with him the past few years and I will cherish those moments for the rest of my life. The technical depth in the topics he has discussed with me is unparalleled and the humanitarianism in him so contagious. I cannot imagine working on this topic without his support and for that I am very thankful to him till eternity. I am very proud to be the first PhD student graduating from his lab and I have him to thank for being there for me every step of the way from publishing my first conference paper to a journal. I hope I made you proud and wish to continue making you proud in my future endeavors.

I would like to thank Dr. Adel Nasiri for being the backbone of the Center for Sustainable Electrical Energy Systems from its time of inception. It is because of his vision that the center exists and lot of us were able to do experiments as a part of our graduate work in the initial days, I can never forget that. I have no words to thank Dr. David Yu, he has been with me the entire time at UWM starting from the first day I came here as an undergraduate student till today and without him I would probably be lost. I would like to thank Dr. Tian Zhao not only for kindly

accepting and being a part of the committee but also for being a pillar of support for the project since its inception and his guidance. I have to thank Dr. Ahmed S Mohamed Sayed Ahmed from Rockwell Automation for being a part of the committee and providing valuable suggestions and inputs. The time he had spent with me since the internship and his approach towards the various topics surrounding Power are affable and for that I thank him for being a part of my life.

I would like to thank all my friends and colleagues in our lab for all the countless hours we spent together in the lab while working on different things. It was definitely an enjoyable experience going through life with them on a daily basis. The numerous discussion and debates on different topics always kept me going and it contributed to a lot of things I learned along the way. And I would like to thank David McClanahan for being there for me through the years since my first day at UWM.

Finally, I would like to thank my wife, parents, aunt and in-laws for all the help they have provided to me in the past few years to get me this far. If not for them I do not think I will be able to peacefully finish my work and get to this stage in my life. I am very thankful to God for blessing me with such wonderful people in my life and I wish to repay them in whichever way possible in the coming years.

Chapter 1 Introduction

The existing approach to providing electricity is expensive. As a result, more than 1.2 billion people around the world live without electricity and the World Bank estimates that it will take a trillion dollars through 2030 to solve this energy poverty [1]. Additionally, the availability of fossil fuels in the future and the environmental effects, such as the carbon footprint of the existing methodologies to produce electricity and declining fossil fuel-based resources are an increasing areas of concern worldwide. Simultaneous solutions to the energy poverty and environmental crises are being addressed through the incorporation of wind and solar Photovoltaic (PV) energy sources into electrification projects. In the United States, electricity is universally available and, perhaps as a result, U.S. households are the highest consumers of electrical power. A unique corollary to the energy poverty of largely rural areas internationally exists within the U.S. and other developed country urban areas [2], [3]. Households in disinvested and underserved urban areas, which are largely minority populations, face high unemployment and low wages. The fixed cost of the ever-present electrical connection to these households becomes a proportionally significant burden when compared to the average middle-income household. At the same time, because of a well-established utility grid structure in the U.S., the trend for renewable energy penetration is distributed energy resources (DERs) applied locally to areas, communities and, in the case of solar PV, to individual households. It is middle to upper-middle income households that participate directly in addressing the environmental solution through individual residence installation of solar PV systems and future adoption of managed solar PV plus battery energy storage systems. DER will refer to the combination of renewable energy sources (solar PV for the residential application) with energy storage.

Populations in largely low-income, disinvested areas within the U.S. are shut out from the opportunity to contribute to and participate in DER deployment due to high cost of installation combined with lack of educational and occupational opportunity—contributing to an ever widening "energy technology disparity gap". This is partly due to the fact that, in the U.S. both power generation and grid operation are controlled and owned by the utility power company and autonomy and independence from the grid through DER is a function of the ability of the energy consumer to finance the DER installation and subsidize its payment through energy savings over time. A microgrid is defined by the U.S. Department of Energy (DOE) as "a group of interconnected loads and distributed energy resources (DERs) with clearly defined electrical boundaries that acts as a single controllable entity with respect to the electric utility grid.". The opportunity to participate in DER deployment within these urban areas will likely be made available through community-based, "behind-the-grid" approaches rather than the conventional individual solar PV installations seen in suburban areas that directly interface with the utility grid through the household AC distribution system. The concept of a collaboratively managed community or residential microgrid within the undeserved areas, where low income households can become prosumers rather than consumers within a shared DER infrastructure is a phenomenal opportunity to address the inherent inequity of the U.S. energy poverty manifestation and to improve quality of life in general.

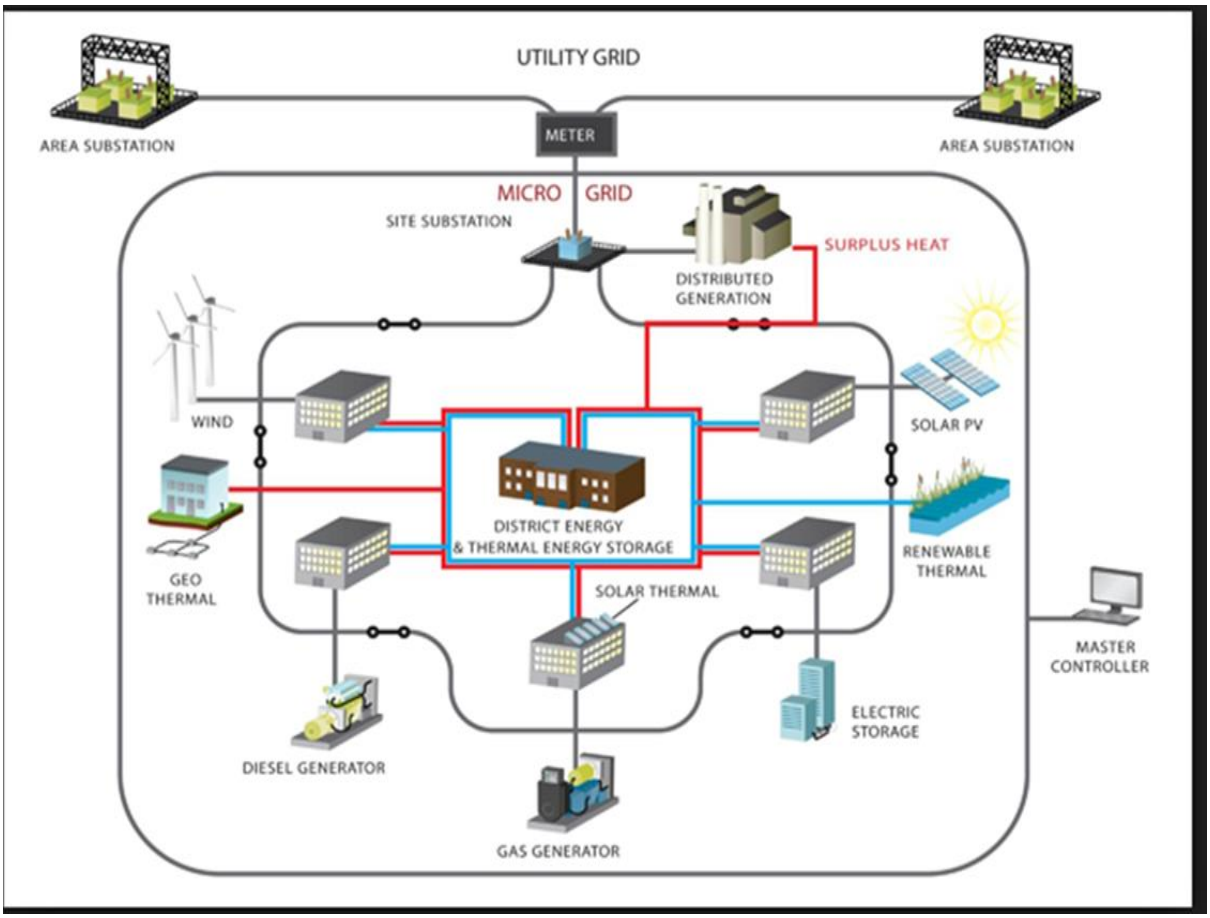

Figure 1-1 - Typical Generic Microgrid

Community microgrids have emerged as an alternative to address the rising societal demands for electric infrastructures that are able to provide premium reliability and power quality levels while at the same time being economically and environmentally friendly [34] - [36]. Community microgrids aim primarily at supplying electricity to a group of houses within a neighborhood or several connected neighborhoods in close proximity. Community microgrids enable unique opportunities for every day consumers to optimize shared renewable energy generation and storage between participants [38], [39], [45]. Additionally, since high efficiency loads are DC fed and electronic conversion usually implies a DC link through which energy is transferred or stored, DC electrification is increasingly proposed as a means of providing more direct, lower

complexity and lower loss energy transfer [45]-[48]. A novel residential DC microgrid is developed as part of an effort to revitalize under-served neighborhoods in Milwaukee as a means of alleviating the high relative cost of utility services to low income households while simultaneously developing a more affordable and accessible approach to smart interconnected renewable energy installations [73].

The main focus of this work is protection and it is not possible to design a protection system independent of the architecture. In DC Microgrids, protection is the greatest impediment.

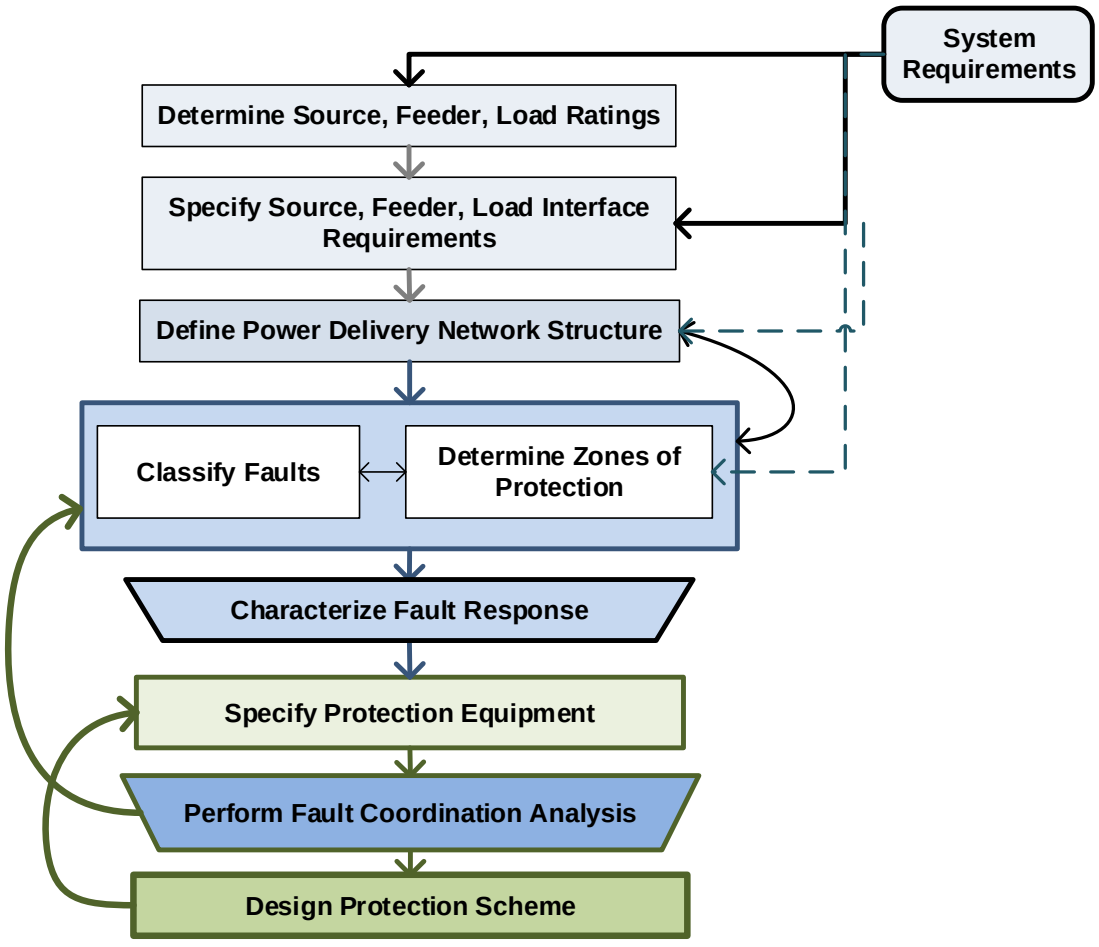

Figure 1-2 - Protective System Design Flowchart

A typical conventional protective system design practice is as given in the flow chart in Figure 1-2. The first requirement to the design process is to determine the feeder and load ratings and to find the requirements. This is to be followed by the fault classification and characterization, this step helps in identifying the protection equipment over which the fault coordination analysis is performed and the protection scheme is designed. This dissertation follows this approach very closely with the architecture selected first, followed by the protective design and the protection system.

The protective design process is initiated by the choice of the neighborhood and the corresponding architecture. The intention is to use the DC microgrid to offload the household loads from the household utility supply while avoiding energy export at the individual residences. Each single family property has a detached garage where solar panels and batteries will be installed. The commercial property will have rooftop solar panels and battery energy storage and is designated as a single point of interface between the DC microgrid and the utility at a hub location where excess energy from the combined, shared renewables of the interconnected dwellings can be sold back to the utility. The primary objective is to drive down individual dwelling utility costs through energy sharing between the PV solar generation and battery energy storage. The PV/battery systems and associated controls would be distributed between the commercial building and the single family properties using low cost, commercially available components. Feedback sensing will be accomplished through wired communications between microgrid sensing points at the detached garages and a centralized microgrid controller at the hub, for the purposes of energy management and handling of fault conditions, such as ground faults, that require some level of communications for location and coordination.

Home Energy Management Systems (HEMS) at the dwellings are intended to operate autonomously from the microgrid and should be based upon an open source, common platform. Similarly, there will be Microgrid Energy Management Systems (MEMS) distributed at microgrid feeder points based upon the same hardware/firmware platform. A secured server at the hub will interface to the web so that individual dwellings can monitor and adjust their energy usage and smart energy controls based on feedback from the microgrid controller available through the cloud. The objective is for all of the participants to contribute to a self-optimizing system that balances the randomness of solar power generation with energy storage buffers, energy pricing and the stochastic nature of demanded load as distributed between the dwellings.

1.1 Research Motivation

There are three main reasons to pursue this research, developed of viable energy sharing concepts that can extend to a much wider user base, DC system protection and focusing on the community.

1.1.1 Develop Feasible Energy Sharing Concepts

- Direct the concept of residential solar to household cost savings through collaborative energy sharing via a residential microgrid rather than net metering.
- Develop a concept that extends adoptability to low income areas in the U.S.
- Develop low cost implementations by building up international efforts such as DC electrification in India and the IEEE Smart Village Initiative.

1.1.2 DC Protection

- Protection is the greatest technical barrier to large scale adoption of the DC microgrid concept
- Lack of standards
- Lack of hardware and system implementations that enable safe and reliable operation
- Protective coordination and selectivity issues
- Lack of understanding of how systems will behave under various fault scenarios

1.1.3 Address Human Usage Aspect

- Scalable, safe solutions for incorporating the Solar PV plus battery in the individual homes and building up the microgrid from there.
- Community engagement through STEM education of students in target neighborhood that introduces them to energy and Internet of Things concepts.
- Development of stakeholders necessary for sustaining the microgrid through education and training.

1.2 Scientific Contributions

- Development of a viable architecture for a DC residential microgrid
- Address maximizing benefits of the microgrid by extending part of the DC architecture into the home and combining with smart fixtures and appliances
    - Detailed load analysis.
    - Comparison of conventional, smart AC and smart DC homes.

        - Optimize the number if panels and energy storage per house within the community for economic reasons.
- Development of a viable protective system approach
        - Building and analyzing an ultra-fast Silicon Carbide solid state circuit breaker.
        - Generalizing the SSCB to be able to use at different parts of the microgrid so as to coordinate the faults.
        - Short circuit fault discrimination using the SSCB.
        - Experimental test and verification of the fault discrimination and coordination capabilities of the SSCB.
- Validation of some system performance using Hardware-in-the-Loop (HIL) platform and novel Computer Hardware-in-the-Loop (CHIL) test platforms proposed.
- Development of technical content based on the various components of the microgrid to educate students from Low Income neighborhoods to pursuit STEM.

1.3 Thesis Organization

Chapter 2 presents the existing literature related to DC systems, community microgrids and DC protection devices. Chapter 3 is a brief introduction of the community where the novel DC microgrid is proposed. Chapter 4 deals with the development of a feasible architectural frame work for the community. It starts from the selection and definition of various loads in the individual houses and scales up to the community. The optimal sizing of the solar panels and batteries for the individual houses and hence the community is arrived at as detailed in [4]. Chapter 5 delves into the solid state protection device design and simulations associated with the same as described in [5]. Chapter 6 provides details on the protection design implementation.

Chapter 7 discusses the experimental results of the hardware tests conducted with the device from the previous chapter. Chapter 8 introduces a basic real time Hardware in the loop set up for the DC microgrid set up and presents a novel high end system. Chapter 9 talks about the societal impacts of the project and Chapter 10 summarizes the conclusion of this dissertation and mentions future research topics.

Chapter 2 Review

2.1 DC Systems

DC systems will accelerate the adoption and insertion of power electronics into the electric grid by enabling effective utilization of energy saving loads and integration between renewable energy resources and storage. DC systems will be less complex and less expensive to deploy, operate and maintain and more efficient power delivery and more effective energy dispatch. DC power systems have been widely used for a long time in vehicles and boats; DC has long powered traditional telephone service (and more recently USB and power over Ethernet (PoE)) in buildings. The number of native DC end-uses is on the rise too, with the proliferation of LED lighting and consumer electronics. Nearly all office equipment -- monitors, computers, copiers, and servers -- are now natively DC. A large and growing number of DC based appliances provide compelling reliability, power quality, and efficiency reasons for directly using DC power from renewable energy systems or batteries, rather than converting first to AC and then back to DC. With both building-sited photovoltaic (PV) power and DC-based product usage rapidly growing, and given the critical need for improved energy efficiency, it is time to adopt DC power for mainstream applications. The main factors that support the use of the DC systems are the ease of DC generation and storage, DC loads. Electric Vehicles, Efficiency and Conversion stage reduction as shown in Figure 2-1 [8].

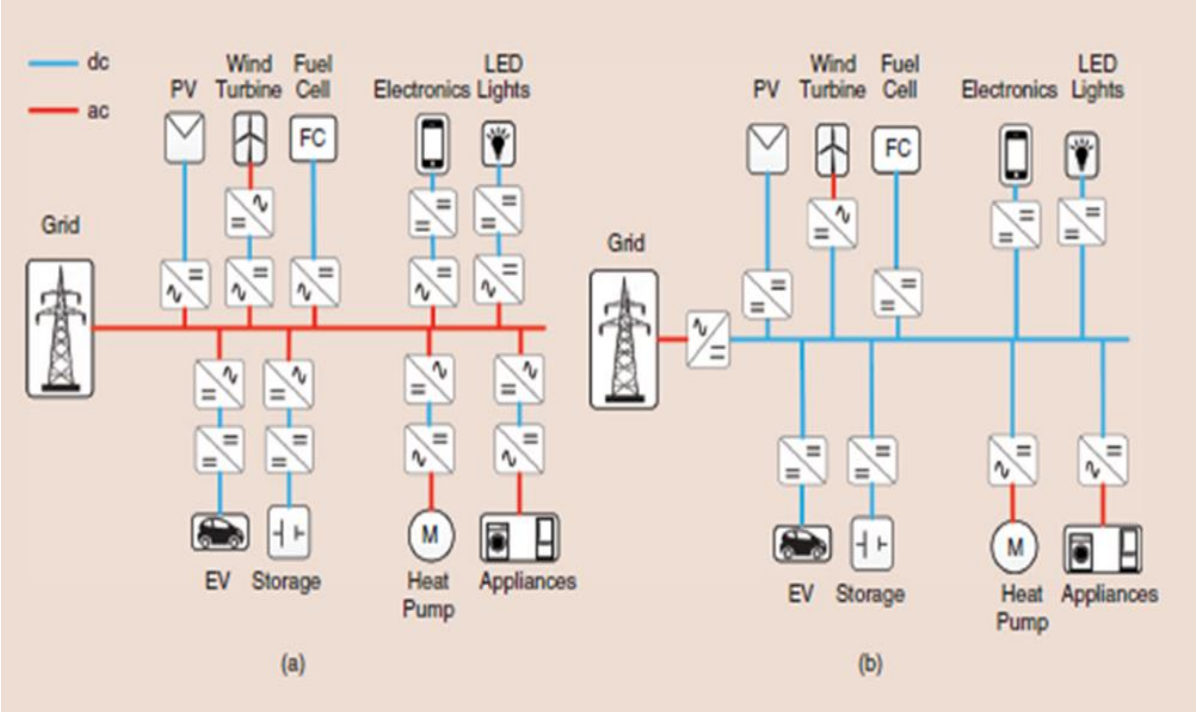

Figure 2-1 - Conversion stages are reduced when switching from (a) ac to (b) dc distribution systems for residential applications

2.1.1 DC Distribution

An efficient distribution system is a key factor for sustainable energy systems. Today, there is an open discussion on whether to use ac or dc electrical power systems. This matter can be traced back to the battle between Edison and Tesla/Westinghouse more than a century ago [6]. The technology available back then made the ac option far more advantageous; consequently, electrical power systems worldwide are ac based. Today's scenario is different, and dc-based power systems offer interesting advantages in terms of simplicity, cost, and efficiency [7].

Figure 2-2 - Worldwide Demonstration Sites for DC Distribution in Buildings

The authors in [8] focus on DC solution in residential and commercial building application and list a few examples of demonstration sites as shown in Figure 2-1.

- NextHome (Detroit, MI) is a demonstration DC test bed developed by NextEnergy. The NextHome features PV generation and supplies direct-DC power for LED lighting, ceiling fans, floor heating, home appliances, and includes battery storage and bi-directional EV charging [9].
- The project's goal in Chino, CA is to demonstrate the benefits of DC distribution in commercial buildings, by implementing a PV powered, direct DC, 380 Volt distribution system powering lighting and forklift chargers [10].
- Bosch has implemented a DC microgrid demonstration project, funded by the U.S. Department of Defense, in Fort Bragg, NC, which includes a 15kW PV array powering

44 DC induction lights, 4 DC ceiling fans, and a 100 kW Li-Ion battery storage system. A side-by-side equivalent AC system reportedly uses 8% more electricity compared to the DC microgrid. A highlight of the Bosch DC power system configuration is that maximum power point tracking (MPPT) is not performed directly after the PV array, but rather at the AC/DC gateway converter, allowing for higher system efficiency [11].

- Philips has implemented a grid-connected, PV-powered DC test bed installation for an office LED lighting system at the Eindhoven (Netherlands) High Tech Campus, and compared its energy performance against an equivalent AC system. The site has demonstrated 2% electricity savings and 5% potential savings for the DC system. [12].
- Fraunhofer has built a DC office building test bed, which includes a grid connected, 380V direct-DC system, battery storage, DC lighting, EV charger, and a 24V DC nanogrid for electronic loads. The DC system demonstrated electricity savings ranging at about 2.7%-5.5% over an equivalent AC system [13].
- The Beijing University of Civil Engineering and Architecture (BUCEA) is conducting research to demonstrate the energy and non-energy benefits of DC distribution in buildings. Researchers at BUCEA have estimated 11% savings from shifting to an all-DC system from the current AC-system [14].
- NTT Facilities is developing a demonstration DC microgrid for an office building in Hokkaido, Japan. The DC system includes a PV array Li-Ion battery storage, LED lighting, a refrigerator, electronics, and an EV. NTT researchers report that the DC system yields 4.2% electricity savings compared to the same system powered by AC [15].

- A DC microgrid has been implemented at Xiamen University in China. The direct-DC system consists of a 150kW PV array, 30kW air conditioning system, 40kW EV charging station, and 20kW LED lighting. Researchers concluded that efficient DC microgrid applications should include a bi-directional inverter and battery storage, and that a hybrid DC-AC building distribution system would be more suitable for today's commercial buildings [16].

2.1.2 DC Testbeds

There have been a numerous microgrid implementations and mainly functioning to supply power or for research in the laboratories to analyze the operation of the microgrid in detail. The following table, Table 2-1 comprises of a list of DC microgrid testbeds in the US as listed in [17]. A point to note is that they are all radial structures and not mesh.

Table 2-1 - DC Microgrid Testbeds in the US

Location	**Renewable DG**	**Non Renewable DG**	**Load**	**Storage**
University of Miami, Florida [18]	PV, Fuel Cell	None	Residential	Battery
Sandia National Lab, Washington DC [19]	PV, Wind	Diesel	Residential, Static	Battery
UT Arlington [20]	PV, Wind, Fuel Cell	Diesel, Gas	Residential, Static	Battery
FIU Testbed [21]	PV, Wind, Fuel Cell	Motor Driven Generator	Residential, Motor	Flywheel
Hawaii Hydrogen Power Park [22]	PV, Wind, Fuel Cell	None	Residential, Static	Battery

2.2 Community DC Microgrids

The U.S. low-income household spends from 10%-20% of total household monthly income on utility costs while middle-income households only spend 3% [26], [27]. Low-income households also have low access to energy efficiency programs [26], [28]. This presents a stark example of the "energy technology disparity gap" within the U.S. As a solution, the rising societal demands to provide premium reliability and power quality levels can be addressed by community microgrids [29]-[36]. Community microgrids aim primarily at supplying electricity to a group of consumers, or with the introduction of cloud-based interactive energy trading, prosumers, within in a neighborhood or several connected neighborhoods in close proximity. A residential community microgrid enable unique opportunities for participants to manage and share independently DERs [37]-[45]. Net zero energy usage can be achieved within the community or residential microgrid through energy export to the utility at a single shared point of connection. This portal for energy export may be a designated "hub" residence or a commercial property that also participates through a shared connection to the microgrid. All of this is aided by integration of stored energy, such as distributed batteries, collectively owned energy storage units or even utility-owned energy storage to off-set the effects of weather- or time-of-day- related energy availability. The presence of energy storage within the microgrid will certainly increase the resiliency of electricity availability among the microgrid participants.

The microgrid infrastructure must include communications and controls that "smooth down" the intermittent output of renewable energy sources, enable optimal dispatch of power from these sources as well as optimal exchange of energy between participants on the grid to both reduce and level out the use of power from the utility by the neighborhood(s) [45]. It is also possible for the microgrid to be disconnected from the main electrical grid and supply power to all the participants

independent of what the utility is doing. The resulting resiliency provided by the community microgrid would enable the neighborhood(s) to ride through high impact, low probability events such as intense seasonal storms, flooding, tornados, damaged power plant generation and transmission lines and terrorist attacks.

The DC Microgrid (DC MG) is an obvious choice for enabling integration and collaborative management of DERs, particularly in "behind-the-grid" solutions where, depending upon the architecture, the DC MG may be collaboratively owned and operated by prosumers, or by some other entity such as a community energy cooperative that may also include participation from the utility company or for non-U.S. implementations participation from the grid operator or government-owned grid. The "behind-the-grid" DC MG will provide some level of independence and autonomy for the actual energy users. The DC MG has been used to electrify homes in rural off grid communities across the world and individual dwellings and entire villages and hamlets have been electrified at relatively low cost and without the need for the existence or development of any supporting electrical infrastructure. The most significant and underappreciated advantage to DC-enabled homes is that they can wired into a low installation cost DC community microgrid that enables the shared use of renewable energy sources, such as solar, between a group of homes [49]-[54].

The DC MG has demonstrated exceptional quality of power, higher reliability, better efficiency, and improved energy utilization on site. The safe and reliable distribution of DC is a key component to the success of DC MG deployment and this aspect is being addressed technologically in other areas, such commercial and navy ship, as well as aircraft electrifications [55]-[57]. A recognition of lessons learned in DC distribution will certainly increase the viability of expansive DC MG deployment.

Typical household loads are increasingly becoming natively DC. The DC MG will also be instrumental and integral to the adoption and insertion of power electronics into the electric grid by enabling effective utilization of energy saving loads and integration between renewable energy resources and storage. Today, many loads and sources are natively DC, such as solar cells, batteries, LED lighting or by the application of electronic controls that converts AC motors in a DC operated speed controlled drive system. Thus, modern buildings benefit from DC power grids to realize a more efficient power exchange between DC sources, storage and loads [25]. DC systems are innately less complex and less expensive to deploy, operate and maintain and are more efficient for power delivery and effective for energy dispatch. In [23], low voltage DC grid prototype with some DC loads are explored. Buildings collect needed energy from building environment to realize a net-zero energy needed balance during a year [24]. Battery energy storage units can make solar energy available at night and a utility grid access allows an exchange of electric energy with other buildings and power sources such as wind parks outside of cities.

The technology to generate and distribute electricity is evolving to match the loads being fed. The most commonly used, like cell phones, computers and TV are all native DC devices. Today many household loads operate on a DC backbone and the future trend toward highly energy efficient loads, such as LED lighting, speed controlled fans and variable torque washers and dryers, will eventually move all household loads to a native DC source of supply. AC supplies would necessarily include their own AC to DC converters, which waste between 7-12% of the energy used [58], [59]. On the other hand, a DC powered smart home, or rather DC-enabled home, will have the best chance of operating with net-zero energy [60]-[66], with attendant effective energy use and reductions in greenhouse gases. Today, such a home is only accessible to those who can

afford the luxury of being environmentally responsible. At the same time, most ironically, the detriments that come with climate change tends to have the greatest impact on the poor [67].

Utility costs are a major impediment to economic mobility. Adoption of cost saving/environmentally friendly technologies such as Solar PV plus batteries is out of reach of low income households—creating an ever-widening disparity gap. While the achievement of a DC enabled net-zero energy consuming home by itself may be far off for the common person, a net-zero energy community is more likely to be within the realm of possibility soon. The proposed residential DC MG concept of this paper can be a model for adoptable, organic growth of community-based DC MG across a wide range of communities. The focus is on the low-income household because of the aforementioned greater need and it is also believed that populations within disinvested, underserved areas will be more open to the concept of collaborative energy sharing than other areas because altruistic motivations that raise the opportunities of the community as whole, as opposed to the individual, will be more accepted [68], [69]. Initiation of this project will depend upon initial investment through local or federal government grants. The model for sustainability and future ownership is yet to be developed.

This work proposes a unique community DC MG implementation which includes a commercial property that hosts a single AC/DC interface to the utility for the DC MG [70]. The DC MG is based upon a resilient electrical architecture that radially distributes out the DC MG out to other dwellings from the commercial property "hub" [5]. Each single family property has its own solar PV and battery energy storage installed in detached garages [73]. The commercial property includes apartment dwellings that are serviced by solar PV and battery energy storage installed on the roof of the building. The DC MG will be embedded within an urban neighborhood. The authors

are working with developers in an underserved area in Milwaukee, Wisconsin to implement this DC MG.

2.3 Protection Devices

Microgrids are the key technology to meet the requirements of commercial applications of renewable energy and distributed generations (DGs) in the power distribution systems [39]. The implementation of microgrids provides an accessible way to address the environment problems of greenhouse, air pollution and the depletion of traditional energy resources. Compared to an AC microgrid, the DC microgrid presents a more effective mean of integrating distributed energy sources and supplying high quality power to urban or remote rural areas[40], [41].

However, the short circuit fault protection for DC microgrids is a critical challenge that must be addressed in order to ensure large scale deployment. The response time of electromechanical circuit breakers to sudden inception of a short circuit fault is several hundreds of microseconds in DC systems. Also, the power electronic devices are only able to bear the fault current to 2-3 times of the nominal load current while electromechanical circuit breakers depend upon much higher surge currents to enable fault discrimination [42][42]. Moreover, the introduction of distributed generation into the microgrid poses special challenges to fault discrimination [43].

It is well recognized that reliable DC protection is likely the main impediment to widespread deployment of DC microgrids [74]-[99]. While AC fault protection design is based upon commercial component and sub-system selection and a proven set of design rules that can be scaled according to system volt-ampere (VA) levels, the same cannot be said about DC fault protection. The DC microgrid fault characteristic is dominated by bus connected capacitance and cable impedance between capacitive sources of fault energy and the fault location [74]-[92]. Also, achievement of accurate and reliable fault discrimination in DC microgrids is a significant

challenge given both the demanding speed of response and the dynamically changing configurations. Present day solutions rely upon relaying and communications between Fault Isolating Devices (FIDs) and grid feeding converters [74] - [95]. However, due to the demand for high speed of response of the FIDs, the success of accurately isolating a fault to its location is diminished by sensing and communications delays and increasing reliability involve increasing costs beyond what would be acceptable for residential distribution systems.

Table 2-2 - Commercially Available LV DC Protection Devices Data

Type	**Manufacturer**	**Un (V)**	**I_n (A)**	**I_{sc} (Ka)**
Fuse	Ferraz Shawnut	500 - 1000	1 - 600	100
Fuse	IFO Electric	250 - 550	2 - 630	120
MCCB	ABB	250 - 750	25 - 800	16 - 70
MCCB	Eaton	250 - 750	15 - 630	10 - 42
MCCB	Siemens	250 - 600	26 - 630	20 - 32
CB	Secheron	900 - 3600	1000 - 6000	80

As mentioned in [76], to ensure reliable operation of the LV DC microgrid, it is important to have a well-functioning protection system. As a starting point, knowledge from existing protection systems for high-power LV dc power systems, for example, in generating stations and traction power systems [77], [78] can be used. However, these systems utilize grid-connected rectifiers with current- limiting capability during dc faults. In contrast, an LV dc microgrid must be connected to an ac grid through converters with bidirectional power flow and, therefore, a different protection system design is needed. Short-circuit current calculations for LV dc systems have been treated in [79] and fault detection in [80]. However, the protection devices have not been considered. So far, the influence of protection devices on the system performance has only been considered in studies of high-voltage (HV) dc applications, such as electric ships and HV dc transmission systems [81] – [83]. Protection devices commercially available for LV dc

systems are fuses, molded-case circuit breakers (MCCB), LV power CBs, and isolated-case CBs [85]. Some of these models are specially designed for dc, but most can be used in ac and dc applications. However, the ratings for ac and dc operation are different, and must be carefully considered when designing the protection system. Table 2-2 lists some examples of commercially available protection devices for LV dc systems, together with their nominal voltage and current, and short-circuit-current-interruption capability.

2.4 Summary

In this chapter, a thorough literature review of the existing systems was presented. The chapter started with discussing the different types of DC systems, their importance and increased interest in these systems. The various DC distributions in buildings around the world are presented and DC Microgrid testbed around the US and details on them are presented. Then, details about the DC Community microgrids and their state of the art was presented. Lastly, there is a discussion on the challenge of DC protection and how it is being tackled today and the literature on that was discussed.

Chapter 3 An Introduction to the Proposed Community

This project will be executed in the Garden Homes District in Milwaukee, WI, USA. Milwaukee's Garden Homes neighborhood, the area consists of older homes with detached garages. At one time, as shown in Figure 3-1, this area was a thriving industrial community where workers lived with their families near businesses and factories that employed them until a lasting recession drove businesses out of this area, leaving behind an impoverished community and multiple vacated homes. They are all almost abandoned as shown in Figure 3-2.

Figure 3-1 - Garden Homes District - Then

These vacated homes will be refurbished with a large part of their electrical system designed to directly deliver DC to household loads so that they are compatible with the DC microgrid concept presented in this paper. Within this neighborhood there are several vacant single family homes that are being purchased and renovated by a non-profit community development corporation (CDC). The intent is to sell these homes to owner-occupant buyers which will help

to stabilize the neighborhood. The CDC's efforts are coordinated with the microgrid development and the goal is to have homes concurrently sell or lease as the community microgrid project is ongoing. The average dwelling size is 1200 ft2 (140 m2). Typical service to such a home is 230Vac/60Hz, 100-200A. The intent is to provide an option for each renovated home to connect into a 380Vdc service coming from the detached garage. Each detached garage will be equipped with combined solar PV and battery storage. Homes sharing adjacent lots will also be inter-connected by a 380Vdc microgrid.

Figure 3-2 - Garden Homes District – Now

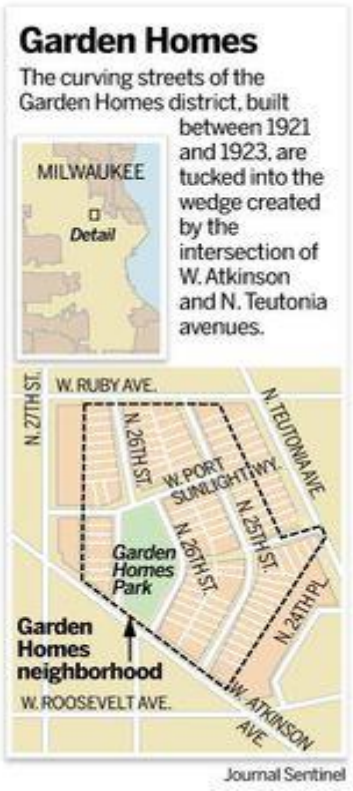

Figure 3-3 - Garden Homes Neighborhood

A couple of excerpts from [84] as shared below can detail the level of desperation in this neighborhood as seen in Figure 3-3 - Garden Homes Neighborhood.

"How do you save this neighborhood — I don't know," said LaPierre.

"Just because it is historic, just because it has this great history to it, doesn't make it immune to what is happening across the city. Somebody has got to figure out how to put it all back together...the last chapter has not been written."

3.1 Summary

The proposed community under consideration for this project is introduced in this chapter. The history of the location and its current status is indicated.

Chapter 4 Economically Feasible Architecture Development

This chapter focuses on development of a feasible DC MG architecture for the proposed community. The proposed radially distributed architecture consists of a single utility interface through which excess energy from the microgrid can be exported. The interconnected homes have an AC interface to the utility but the intention is to prohibit energy export at the homes and only export through this single interface. This is done by executing a bottoms up approach where the system architecture is arrived at by focusing on the individual loads and thereby the individual homes in the community. The load profiles for the low income houses and the optimal installation of PV panels and energy storage at each of the homes are determined. And thereby a feasible architecture(s) for distributing DC within homes and the level of DC distribution that can be viably accomplished given present-day commercial solutions within the home is determined.

As mentioned in [70] a notional distribution and modeling of load demand between AC, DC, smart AC, smart DC was performed and real data from currently existing loads i.e., AC and DC which are available in the market are used and compared that to the previous notional results. The load distributions using actual data for the Wisconsin households as provided by the Department of Energy (DOE) [100], [101] are analyzed. The source of load data is from Building America research program sponsored by the DOE. The optimization of the installed solar PV and battery energy storage at each location is performed using this data. The AC loads consist mainly of the range and other necessary appliances which do not have an equivalent commercially available DC-fed appliance or fixture market or an equivalent AC-fed energy-saving appliance or fixture that can be easily modified to be DC-fed. Natively DC electronic loads that are DC-fed have a higher efficiency compared to natively DC electronic loads that are AC-fed due to the absence of power conversion losses and reduced distribution losses. Such loads include LED lighting, personal

computers, mobile chargers, flat-panel televisions, air conditioning, brush-less DC motor powered fans, etc. The conversion from AC to DC loads is very crucial since, as the percentage of kW-hr consumed by natively DC loads will continue to increase within households. Conventional AC household distribution combined with either conventional AC, Smart AC loads and replacement of natively DC-fed loads with DC-powered loads, with an associated penetration of DC distribution into the home are considered with respect to costs the energy costs incurred by each of the houses. The goal is to reduce the utility cost payed by the members of the community by importing power consumption from the load perspective first and then design the "behind-the-grid" DC MG with optimally designed levels of solar PV and storage integration based upon the concept of sharing loads. The amount of energy consumed by the community during the different seasons, will aid in drawing inferences to design the most favorable microgrid with minimal cost as a criterion. The energy consumption of the 9 dwellings in the community is broken down into different categories such as minimal, maximum, anonymous and moderate power consumption. The parameters taken into consideration for categorizing the power usage are human behavior such as working family, size of the family, and size of the house. Also, the final economical implementation of energy storage management within the households and DC MG can be accomplished with common platform Home Energy Management System (HEMS) and a Microgrid Energy Management System (MEMS) hardware [102].

Details of the proposed implementation are provided in Section 1. The loads within the participating households, comparison between homes with only AC distribution and homes with a feasible level of DC distribution and direct DC-fed loads, as well as the advantages of using one over the other, are presented in Section 2. Section 3 describes a method used in Matlab to

achieve the optimal solar and battery installations for each participant and Section 4 discusses the envisioned energy management methodology within the DC MG.

4.1 Details of the Dwellings

The layout of the property with the 9 dwellings is shown in Figure 4-1. The commercial building "hub" distributes 380Vdc to the connected homes, enabling a sharing of distributed solar power and battery energy storage among the homes. The houses in the community connect to the 380Vdc microgrid feed through the shared easement. There may be a mix of distribution among the houses. For example, homes that have already been re-furbished with conventional AC distribution will include an interface to the DC microgrid like the interface between rooftop solar PV and home electrical in conventional installations. However, this approach is not ideal as it carries with it the overhead of DC to AC conversion and complicates the interface between the utility and the community microgrid. As shown in Figure 4-2 the preferred approach for each group of interconnected homes is to have a designated lead dwelling (in this case the commercial property) that provides the interface to the utility for energy import and export while each of the homes has the DC portion of its loads fed independently from its own energy resources and the microgrid. This approach enables radially distributed feeds to each dwelling, which is advantageous from a protection standpoint [73] and management of DC MG utility interface at one common point. Each house will have a standard 240Vac connection to the utility but power panel distribution within the homes will be set up so that there is no possibility of mixing utility and renewable energy in each individual home except through the lead house. In this way, cumulative surcharges for renewable energy installation in each home can be avoided. The interaction between renewable and utility will be contained to the community microgrid. Energy management controls will be

developed for the community microgrid that will manage the usage of utility energy with optimal rates and the availability of solar power.

Figure 4-1 - Property map showing the connected dwellings (gray)

As a back-up and to support a level of conventional plug-in appliance operation, consistent with the needs of flexibility and the availability of viable DC appliances, each home still maintains its own 240Vac connection to the utility. Interlocking controls between the home DC MG interface and home interfacing inverter ensure that DC MG power is only used to offload loads within the home. In this way, the complications of utility/renewable management are contained within the DC MG and at the hub interface. One of the benefits of DC MG is that the power can be distributed between the homes with minimal public infrastructure investment and minimal utility involvement [33]. For example, DC cables can be buried underground as the interconnected homes are on the same city block (as shown in Figure 4-2) and can be integrated into existing infrastructures such

as un-used pipes. Perhaps the most significant and underappreciated advantage to DC-enabled homes combined with a DC MG is the enabling of shared use of renewable energy sources, such as solar, between a group of homes.

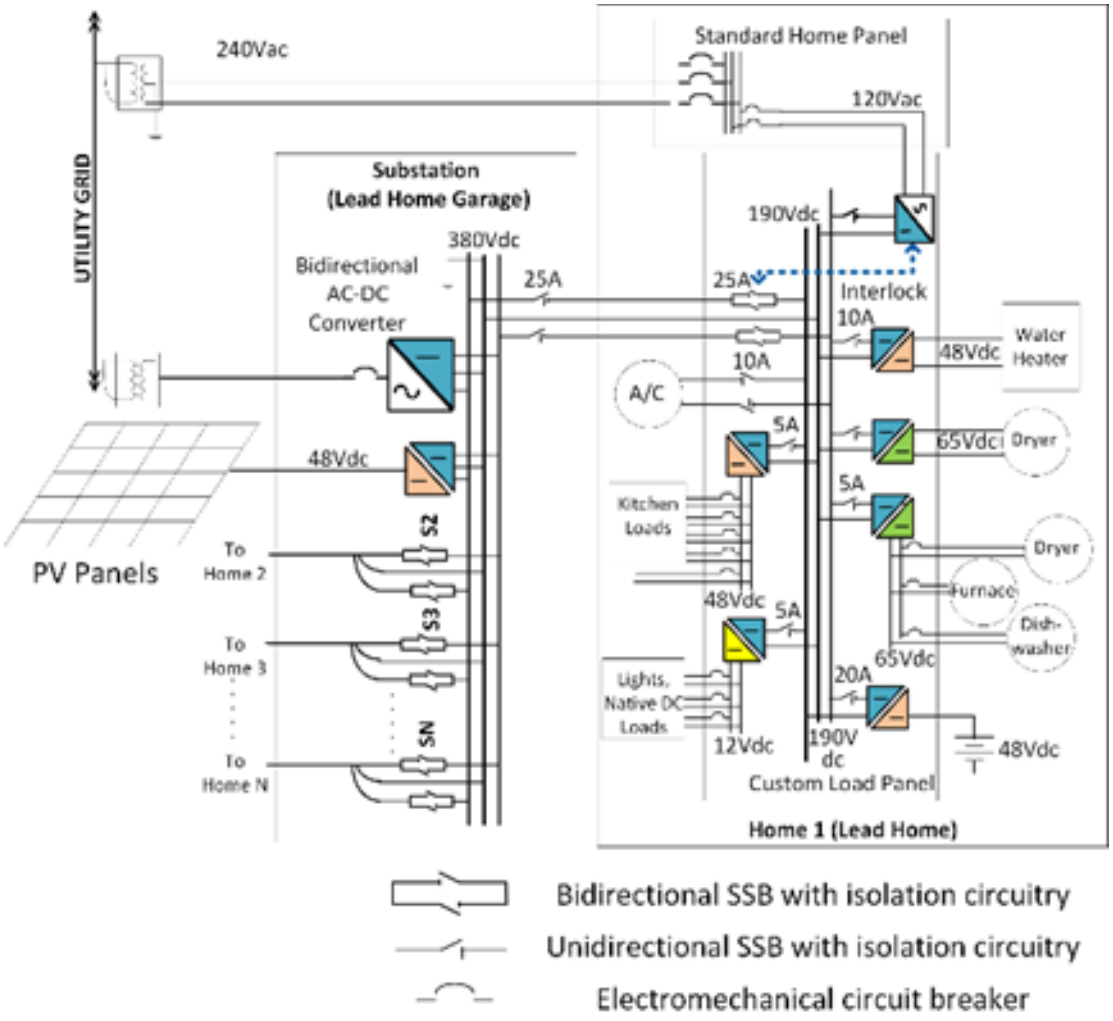

Figure 4-2 - Notional lead dwelling distribution system

A five year living laboratory residential DC MG project will provide a proving ground for development of communication and protection technologies that are necessary for the viable, safe and effective implementation of distributed energy resources (DERs) in a DC distribution system [73].

Table 4-1 - Power consumption of various loads.

Load	AC Load	Appliance Factor	Human Usage Factor	Power Conv. Factor	Smart AC Home Load	DC Home Load
	(kW)	h_a	h_u	h_h	(kW)	(kW)
Central A/C	3.45	1	0.5	1.1	1.90	
Blower Motor	0.19	1	1	1.1	0.21	
Level 1 DC A/C	1.20	1	1	0.92	1.10	0.56
Level 2 DC A/C	1.20	1	1	0.92	1.10	0.56
Level 1 DC Circ. Fan	0.75	1	1	0.92	0.69	0.01
Level 2 DC Circ. Fan	0.75	1	1	0.92	0.69	0.01
Range	6.00	0.6	0.5	1.1	1.98	1.98
Water Heater	5.50	1	0.5	0.92	3.02	2.53
Dryer	5.00	0.6	0.8	1.1	2.64	2.64
Washer	0.50	0.3	0.9	1.1	0.12	0.12
Heating (Gas)	0.32	1	1	1.0	0.32	0.32
Duct Fans		1	1	1.10	0.024	0.021
Dishwasher	1.10	1	1	1.1	1.2	1.21
Refrigerator	0.50	1	0.3	1.1	0.2	0.17
Freezer	0.35	1	1	0.92	0.4	0.17
Kitchen Loads	4.5	1	0.3	1.1	1.5	1.49
Electronic Loads	0.75	0.4	0.3	0.92	0.09	0.08
Lights (Kitchen)	0.08	1.0	0.5	1.00	0.040	0.020
Lights (Common Room)	0.34	1.00	0.50	1.10	0.187	0.009
Lights (Bath)	0.06	1.00	0.50	1.10	0.033	0.005
Lights (Bedroom 1+Bath)	0.18	1.00	0.50	1.10	0.099	0.012
Lights (Bedroom 2 & 3)	0.24	1.00	0.50	1.10	0.132	0.014
Lights (Basement)	0.08	1.00	0.50	1.10	0.044	0.007
Worst Case Peak Load	**33.04**				**17.35**	**11.61**

4.2 Load Selection and Comparison

The homes in the DC MG can achieve more benefits if smart DC loads are incorporated into the home [65]. The loads consuming more power in the house are taken into consideration and analyzed by comparing existing AC loads with Smart AC loads and DC loads as stated below. As mentioned in the previous section, a number of loads are still used as AC either because of their minimal power consumption or because there is no DC equivalent commercially available. The smart AC loads used are converted to energy efficient devices by using additional factors to account for expected reductions in power consumption. The factors considered are Appliance Factor, Human Usage Factor and Power Conversion Factor as shown in Table 4-1. The Appliance Factor is selected to be an efficiency value associated with the AC appliance under consideration. Human Usage Factor is derived based on the human understanding of an appliance and how the human operates the equipment efficiently. Power Conversion Factor is to account for the losses in converters involved for a proper operation of the equipment. All of these factors are values between 0 and 1. The Appliance and Power Conversion Factors are derived from various studies online and published studies of smart AC and DC loads [61], [64]-[65]. For now, the Human Usage Factor is assumed to be 0.5 or 1 for most appliances and will evolve over time based on individual usage. Table 4-1 lists the various devices assumed to be in the houses under consideration. Smart AC loads for the appliances is calculated as the product of traditional AC load times the three factors listed in the previous paragraph. The power for the DC loads indicates the power an equivalent DC equipment might consume.

Table 4-2: Seasonal Utility Costs

Loads	**Summer Utility Home Monthly Cost**			**Winter Utility Home Monthly Cost**		
	AC	**Smart AC**	**DC Home**	**AC**	**Smart AC**	**DC Home**
Central A/C	$136.62	$75.14	---	---	---	---
Blower Motor	$7.39	$8.12	---	---	---	---
A/C 1	---	---	$22.18	---	---	---
A/C 2	---	---	$22.18	---	---	---
Ceiling Fan 1	---	---	$0.55	---	---	---
Ceiling Fan 2	---	---	$0.55	---	---	---
Range	$66.00	$21.78	$21.78	$105.60	$34.85	$34.85
Water Heater	$72.59	$39.93	$33.33	$72.59	$39.93	$33.33
Dryer	$11.00	$5.81	$5.81	$11.00	$5.81	$5.81
Washer	$0.55	$0.14	$0.14	$0.55	$0.14	$0.14
Heating (Gas)	---	---	---	$12.77	$12.77	$12.77
Duct Fans	---	---	---	$	$0.93	$0.85
Dishwasher	$1.21	$1.33	$1.33	$1.21	$1.33	$1.33
Refrigerator	$8.25	$2.72	$2.72	$8.25	$2.72	$2.72
Freezer	$2.31	$2.54	$1.12	$2.31	$2.54	$1.12
Kitchen Loads	$39.60	$13.07	$13.07	$49.50	$16.34	$16.34
Electronic Loads	$21.12	$2.65	$2.22	$24.75	$3.10	$2.60
Lights (Kitchen)	$0.79	$1.85	$0.09	$1.41	$3.29	$0.16
Lights (Common Room)	$4.49	$0.44	$0.07	$5.98	$0.58	$0.09
Lights (Bath)	$0.20	$0.33	$0.04	$0.20	$0.33	$0.04
Lights (Bedroom 1+Bath)	$1.19	$0.87	$0.09	$1.58	$1.16	$0.12
Lights (Bedroom 2 & 3)	$2.38	$0.44	$0.07	$3.17	$0.58	$0.09
Total Utility Bill	$375.68	$177.15	$127.33	$308.26	$134.51	$112.35
Average Savings per Month	---	$198.53	$248.35	---	$173.74	$195.91
% of Income	**18.80**	**8.90**	**6.40**	**15.40**	**6.70**	**5.60**

Analysis of some of the load in Table 4-1 is considered. The commercial DC Air Conditioner (A/C) makes use of solar power and can run be run directly from a solar panel without the need to have an inefficient inverter to convert the DC to AC [103]. In this case, the home 48Vdc distribution feeds the A/C units directly. Also, 48Vdc brushless fan motors are distributed to three rooms in each how and their operation is coordinated with the A/C units using a ventilation/environmental control system that optimizes operation against a range of user defined settings in order to minimize energy consumption. The traditional Air conditioner has a power consumption of 3.45 kW whereas the DC Air conditioner have 0.56 kW. The DC A/C, when AC supplied is 1.10 kW which is almost double the DC fed Air conditioner. Another load to point out is the dryer, the traditional AC load is about 5 kW whereas the Smart AC load is only about half of that, assuming that the dryer utilizes heat pump technology, which reheats the air internally without taking the cold air from outside.

Each home was assumed to have an income based upon U.S. minimum wage ($7.25 USD/hour). The monthly utility costs for summer and winter are listed in Table 4-2 and the monthly energy bill is expressed in the final row as a percentage of monthly income. It can be observed that the saving per month is substantial when using a house with DC loads compared to a house with AC loads. The comparison with a house with Smart AC loads is comparable as well but still a little higher than the DC loads. The table indicated the percentage of monthly income a family would pay for utilities. In summer the utility costs go from almost 19% to 6.4% if all DC loads are used when possible in the house. Adding solar and PV to this will yield a substantial benefit for the community as the DC MG can enable a driving down of costs per household collectively. The optimal installation is discussed in the next section. The capital cost of DC equipment is a bit higher than the equivalent AC equipment in case of larger systems like Air conditioners,

refrigerators etc., but the cost of the smaller systems like Lights, Fans and so on are comparable. When the systems are installed as a whole, as seen in [109], the cost of the overall installed system becomes significantly less. The potential operation and maintenance costs are significantly lesser and as stated in [110], there could be up to 30% reduction in a 25-year Lifetime costs of a DC system compared to an AC system.

The DOE dataset contains hourly load profile data for 16 commercial building types (based off the DOE commercial reference building models) and residential buildings (based off the Building America House Simulation Protocols [106]). This dataset also uses the Residential Energy Consumption Survey (RECS) for statistical references of building types by location [107]. The data from there was used to populate Table 4-3. This table lists the typical consumption of all the loads in a given house in Wisconsin during the summer and winter season in the AC column. The DC column in the table represents the consumption of a commercially available DC load to fulfill the purpose filled by the AC load. The data presented in this table is for a base house. There are similar databases for the high usage and low usage houses which will be used as a part of the community to get our 9 dwellings. The appliances were not converted into DC because they were generally like ranges and other things which do not have a DC counterpart commercially available.

Table 4-3: Seasonal DOE Load Consumption Data

Loads	**Summer Home Consumption in kW**		**Winter Home Consumption in kW**	
	AC	**DC**	**AC**	**DC**
Cooling	0.050	0.036	---	---
Interior Lighting	0.145	0.046	0.273	0.088
Exterior Lighting	0.031	0.009	0.059	0.018
Appliances	0.237	---	0.239	---
Miscellaneous	0.353	0.136	0.461	0.178
Total	**18.80**	**8.90**	**15.40**	**6.70**

4.3 Optimal Residential Solar and Battery Sizing

In this section, an optimization approach is presented to determine the number of the solar panels and the capacity of the battery energy storage for each house comparing the previous data with the current DOE dataset for base house in Wisconsin. Key data/parameters for this optimization approach include, the load profile, solar generation profile, installation cost of solar systems and battery energy storage systems. In this work, we assume that, by using advanced DC MG management strategy, the energy generated by the solar panels, energy storage capacity and the stored energy can be shared among all the houses, which lead to an integrated DC MG.

The typical load profile has been recorded for each house within the DC MG at different seasons, which are further used to obtain the aggregated load profile (ALP) for the overall DC MG. The ALP is defined as the total energy consumed by loads (in kWh) of all the houses in the DC MG vs. hour of day. The aggregated solar generation profile (ASGP) are obtained by a similar manner. Considering the baseline case that a unit size solar panel, i.e., a 300 W solar panel, is installed on each house, the ASGP is then defined as the total energy generated by the unit size panel (USP) of all the houses in the DC MG vs. hour of day. As shown in Figure 4-3, which represents the case in summer, by varying the number of unit size panels installed on each house, the net load profile (NLP), i.e., ALP – ASGP*(# of the USP), can be plotted. It is clear that the net loads consumption is reduced with the increasing of the number of USP installed per house. For instance, the purple profile with circle markers represent the NLP when 9 USP are installed on top of each house. Between 8:00 am to 6:00 pm, the total energy generated by the solar panels are higher than the total energy consumed by the loads. If the extra energy can be stored in battery energy storage system and then utilized to supply the loads in other hours of the day, the total utility bill will be further reduced.

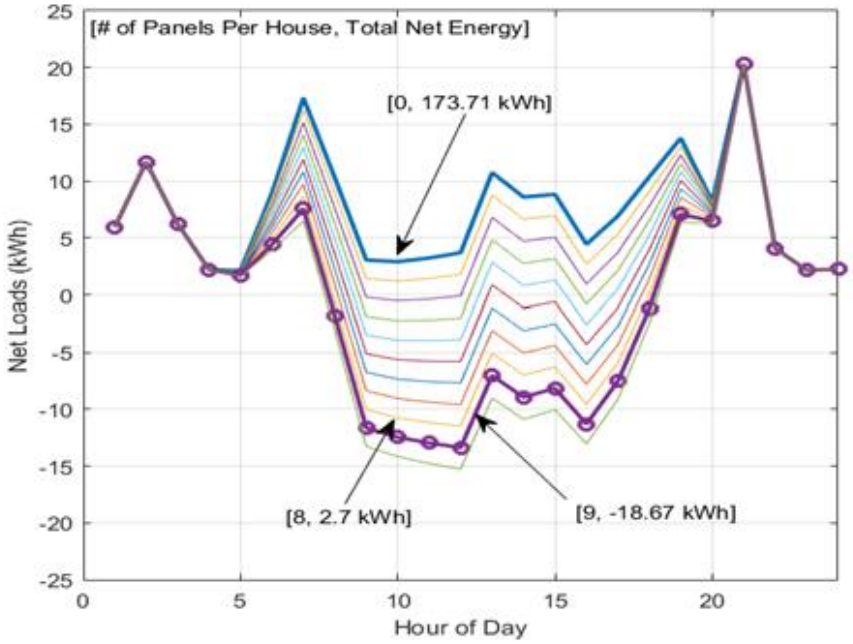

Figure 4-3 - The net loads profiles of the cases with different number of solar panels

The DOE database was used to create a notional community with the average data in WI households. The data has the houses divided into base, low and high with respect to the amount of energy a household uses throughout the year. This database gives us the data for these households on every hour in everyday i.e., 8760 hours. This is the most comprehensive data available and they use the reported data so it is as close to the actual reality as possible. As shown in Figure 4-4, represents the case of a base house in Wisconsin. It can be observed that with a fewer number of panels we are able to achieve the Net Zero capabilities with that data. It appears that the custom approach was more conservative than an actual average household usage in WI.

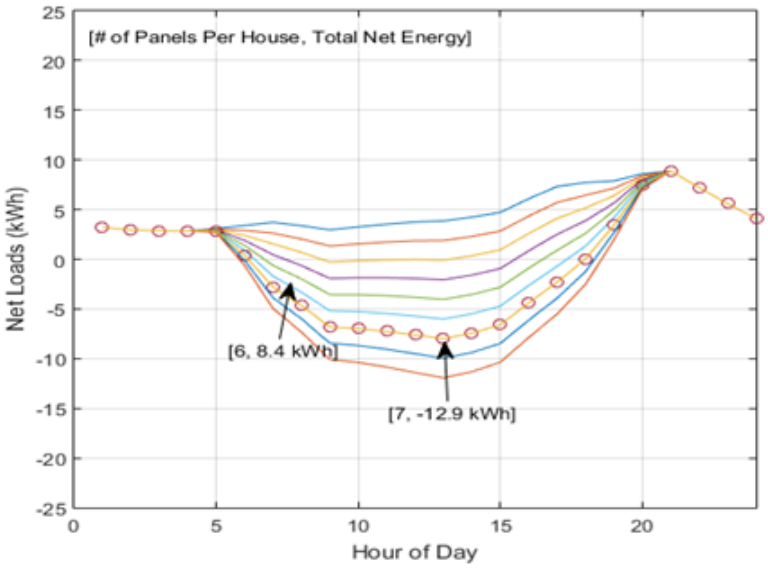

Figure 4-4 - The net loads profiles of the cases with different number of solar panels with the DOE dataset

In this work, the unit cost of the residential solar PV installation is assumed to be $ 2.93 per watt dc, per NREL's recent US solar PV system cost benchmark report [104]. This unit cost includes the costs related to modules, converter/charger, structural and electric balance of system, sales tax, installation labor etc. According to another NREL's report on residential solar PV with energy storage [105], the reported battery cost is $471/kWh, which is selected to calculate the cost, including installation and permitting, for battery system in this work. In addition, the utility unit electricity cost is assumed to be $ 0.11 per kWh. In this project, the specific constraints for the installation cost are: total installation cost, PV and battery, < $10 K and total installation cost of the Hub (commercial property) < $30K. The objective of this optimization is to minimize the utility bill for the DC MG.

Figure 4-5 illustrates the block diagram of the proposed optimization algorithm. L[i] and S[i] are load data from ALP and solar generation data from ASGP at hour i. By varying the number of USP, i.e., P#, and capacity of the battery energy storage, i.e., B# (in kWh), installed in each house, the corresponding net energy consumed by the load can be obtained. Typical results for different

seasons are shown in Figure 4-6. For the worst case, i.e., in winter with the least solar generation, by using optimized PV-battery combination, the total energy consumed by each home is 71.39/9*30 = 238 kWh, which corresponds to $ 26.18 on utility bill.

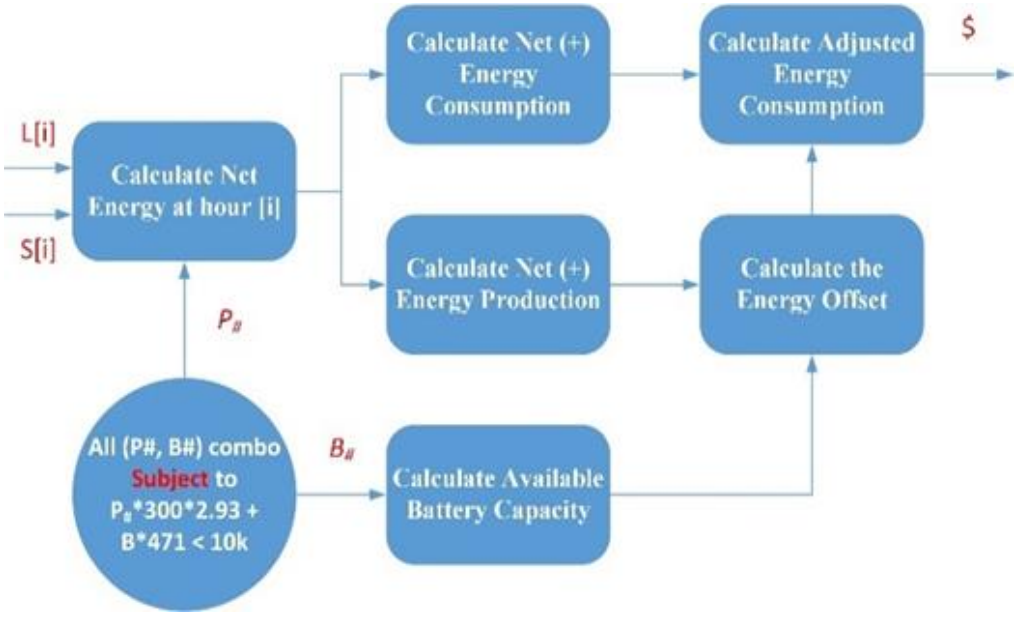

Figure 4-5 - Block diagram of the proposed optimization algorithm

The optimal results for the combination for battery and solar panel required for the DOE database set is as listed in Table 4-4. The typical results for the various seasons of the base house in WI is as shown in Figure 4-7. The total energy consumed by each home in the worst case is calculated by looking at the winter where the contribution of the solar panel and battery is the least out of all the seasons. The Total energy consumed at that time by each home is 52/9*30 = 173 kWh, which corresponds to $ 19.03 on utility bill, hence showing that our previous estimate was conservative a well.

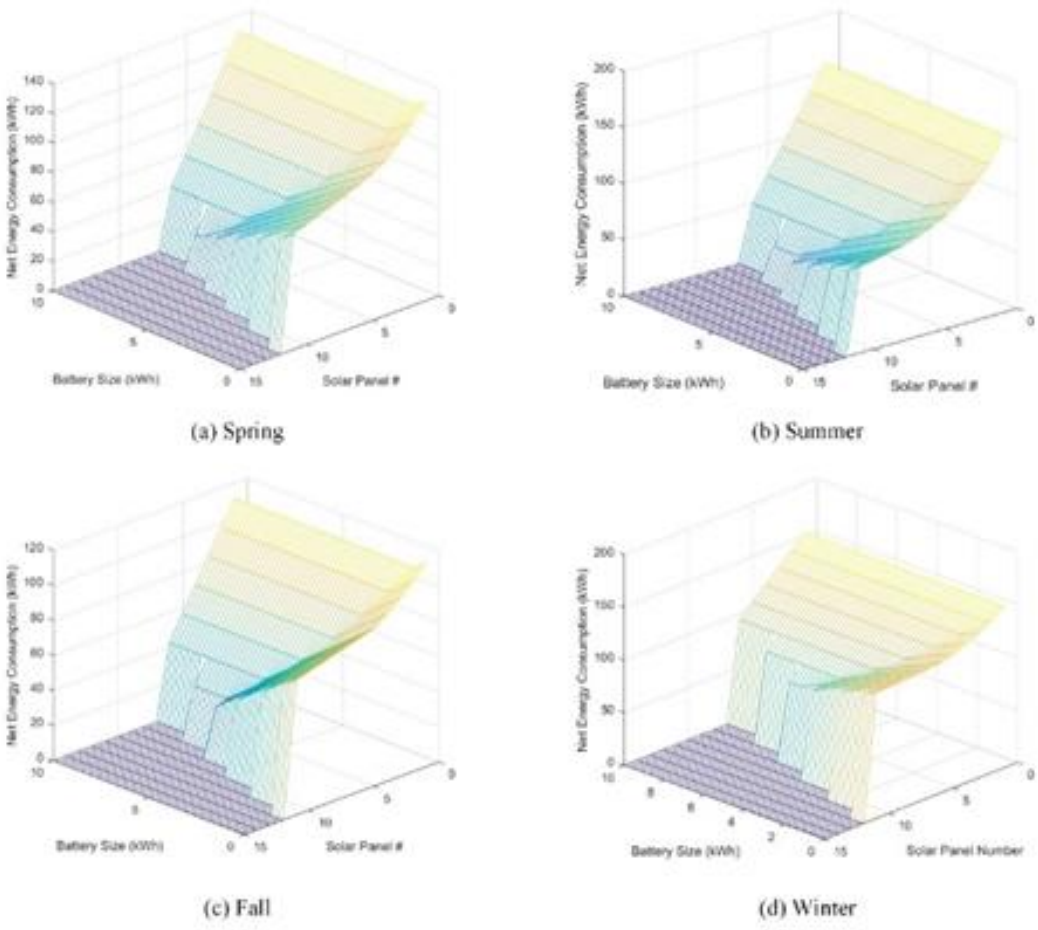

Figure 4-6 - The net energy consumption versus the capacity of battery and the number of solar panels for different seasons

Table 4-4: Optimal results for Different seasons with DOE Data

Season	**Battery (kWh/Home)**	**No of Panels**	**Net Energy (kWh/Day)**
Spring	6.4	8	10
Summer	4.4	6	9
Fall	6.6	9	28
Winter	6	9	52

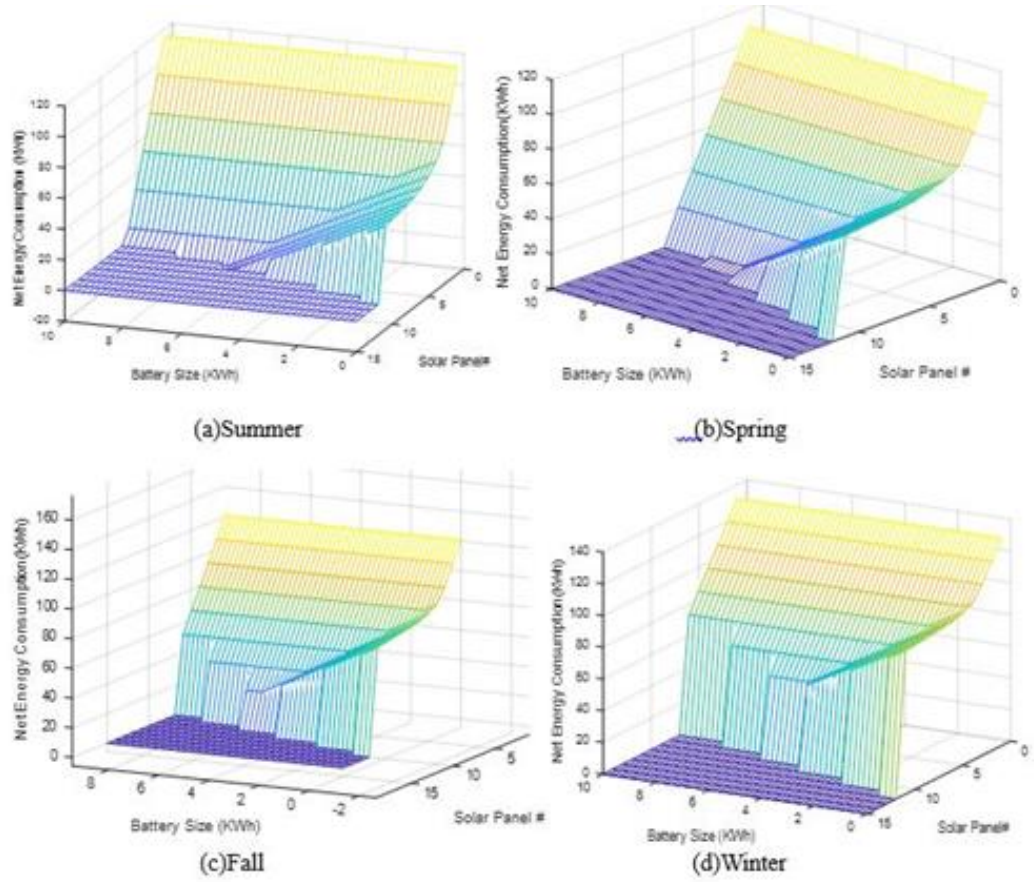

Figure 4-7 - The net energy consumption versus the capacity of battery and the number of solar panels for different seasons with the DOE dataset

4.4 Smart Home Energy Management

The home renovation will include installation of a level of fixtures and appliances that directly use the DC through Point of Load Converters. Figure 4-8 shows the implementation the community DC MG for the mixed AC-DC home with the load distribution described in Table 4-1. This is the envisioned layout for the first home to be re-furbished in the DC community microgrid. The other homes will have an identical layout with the exception that their detached garages will not have an interface to the 240Vac power. The lead house interface to the utility is through a bidirectional AC to DC converter to enable import of energy to the microgrid as well as export of energy to the grid. Home DC power is routed through a "smart" DC electrical panel that has

intelligence to control how energy is dispatched to loads, informed both by a smart home energy management system and a self-learning energy controller that is autonomously tuned over time. The system uses a combination of artificial intelligence and internet of things concepts, to coordinate energy management of the microgrid with the energy-usage habits of the home occupants. Home occupants receive feedback from a secure internet site to give them an opportunity to interact with the system to improve their energy usage. The system also provides complete transparency to the microgrid energy providing and sharing service while maintaining privacy of all participants.

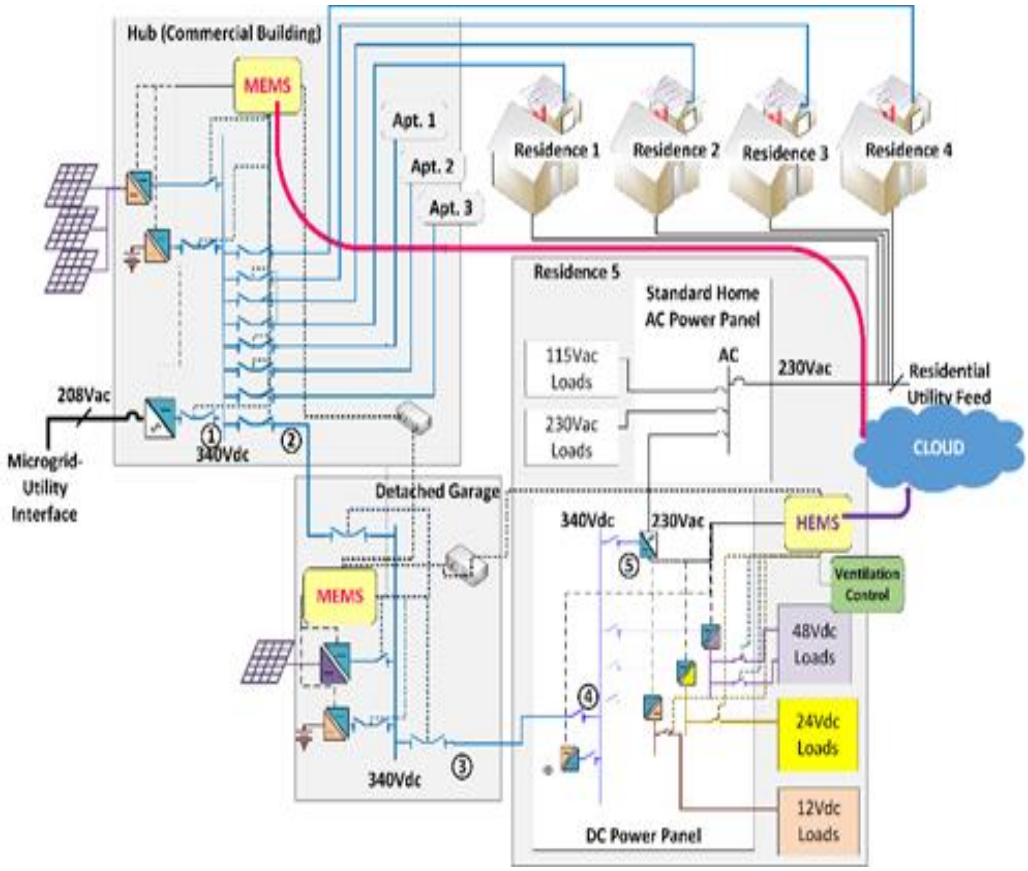

Figure 4-8 - Notional implementation of the DC MG

Distributed microgrid controls smooth out intermittent generation by using the diverse energy usage patterns within the homes (sending energy where it is needed most at any given time) and storing excess energy in batteries so that it can be cooperatively dispatched for use during low generation times or times when utility rates are higher. Net unused energy is sold back to the utility (if it is beneficial) through a single managed portal at the hub house garage AC to DC converter. The present research says that it is beneficial from the customer and the utility point of view to store the excess generated power first rather than trying to send it back to the grid. This is because the incentive received for sending energy back to grid, is 0.05-0.07$ per kW. Smart energy meters will be installed for real time energy usage monitoring and smart energy management among the houses.

The customer can adjust power consumption in real time through a Home Energy Management System (HEMS). Studies show that having simple access to such information helps consumers reduce their energy use by up to 15% [66]. The HEMS and Microgrid Energy Management System (MEMS) use a common hardware platform. They would use cloud bases, open source programming. The user will be able to give his inputs to the HEMS where some local controls will be implemented and it will report back to the MEMS which has information about all the houses in the MG. The MEMS will then choose the optimal path for the energy between the various houses based on the controls and algorithms in that layer. MEMS will also incorporate Demand Side Management (DSM) techniques between the various houses in the DC MG. DSM focuses on changing customer behavior to benefit both the community micro grid and utility company (supplying energy during low solar irradiance). Benefits include saving electricity, reducing peak load, and controlling demand [108].

4.5 Summary

An economically feasible architecture for the proposed community is proposed in this chapter. This is done by taking a bottoms up approach. The load profiles for the individual dwellings are built first using the individual appliances in each of the dwellings and the user profile associated with them. The dwellings were categorized into high, medium and low use in terms of their energy consumption requirements. Then, based on the location of each of the dwellings i.e., more sun/ less sun/ shading on the dwelling and so on the amount of available solar power for each of the houses were determined. The information obtained along with the constraint of battery storage availability and cost was fed into an optimization algorithm to find the optimal solar and battery power requirement for each of the homes with cost as the optimizing function. Lastly, a novel smart home management system for the community with HEMS and MEMS is proposed.

Chapter 5 Protection System Design

Microgrids require protective systems and power converters interfacing to distributed energy sources and loads to work in a coordinated fashion under all kinds of fault conditions. Achievement of reliable fault discrimination in microgrids is one of the main factors that drives up development costs of microgrids because each system becomes a custom design because of the following:

- Multiple potential energy paths during fault scenarios
- Impacts of source and load capacitances and cabling creates a complex interdependence between system layout, stability and fault response
- Time-trip requirements are compressed in much shorter time scales leading to need for fast activing protective device and low latency fault detection and location

Future microgrid relaying systems will require optimal allocation of protective functions between converters and protective devices, high speed communications at secondary control layer levels of the system and distributed knowledge of the dynamically changing system configuration. This chapter will talk about the challenges and requirements of DC Microgrid protection and propose a solution.

5.1 Protection Requirements and Challenges in Microgrids

5.1.1 Protection Requirements

- Respond reliably to both main grid and microgrid faults
- Isolate the smallest part of the microgrid closest to the fault location
- Predictability and scalability of response with increased DER penetration
- Segmentation should be supported by both DERs and Switchgear

5.1.2 Challenges to Meeting Requirements

- Availability of sufficient short-circuit current during islanded operation
- Contribution of capacitor discharge at fault inception
- Controllable islands of different size and content can be formed as a result of faults in the main grid or inside the microgrid
- Unpredictability of fault current directions and number of potential fault current paths
- Dependence on communications vs. reliability of communications based fault protection
- Fault ride-through requirements vs. converter voltage collapse
- DC injection into the AC grid
- Creation of multiple ground potentials within a non-isolated system
- Difficulty of ground fault detection, location and isolation
- Ground faults cause increased system stresses and extensive losses of system power

5.1.3 Challenges in a DC Microgrid Setting

There a couple of challenges in addition to a traditional setting in DC Microgrids. Traditional mechanical circuit breakers, in power distribution system, are widely used for all kinds of fault protections but in DC microgrids, mechanical circuit breakers have a couple of problems to address yet.

- Long clearing time: Typical molded case mechanical circuit breakers have long response time to a fault (around several tens of milliseconds). However, the protection for power electronic devices require in a range of several hundreds of microseconds.

- Arc extinguishing: In a DC microgrid, the DC bus voltage never pass through zero comparing to AC, so when turning off the circuit breaker, arc is generated at that moment. Arcing is very dangerous and may cause fire or damage to both devices and people. As well, it will greatly shorten the lifetime of the mechanical circuit breakers.

DC microgrid for home energy interconnection is potentially less complex and less expensive to deploy, operate and maintain however, faster protection is a key element to ensuring resilience, viability and adoptability. Nowadays, relays, reclosers, and fuses with time -coordinated characteristics that respond to phase and residual currents protect most distribution system. Sequencing and reclosing schemes of relays and reclosers use instantaneous elements, which are generally difficult to coordinate. Schemes that use instantaneous elements must balance the pros and cons of sensitivity, fuse-saving, trip-saving, cost and complexity.

5.2 Need for Newer Protection Solutions for the DC Microgrid

The zero crossing in an AC system provides opportunity electromechanical circuit breaker arc to extinguish. Upstream & downstream circuit breakers can coordinate because AC reactance limits currents. In contrast a DC System has no zero crossing so electromechanical circuit breakers must be de-rated. It becomes virtually impossible for upstream & downstream circuit breakers to coordinate due to current limitation of upstream source.

5.2.1 DC Protection Design Criterion

The basic design criteria for a DC Protective systems as described in [42] are:

- Reliability—Predictability of the protective system response to faults and dependability to not trip spuriously on transients or noise.

- Speed—Fault is removed from the system and normal operating voltages is rapidly restored.
- Performance—Continuity of service to the loads; where a lower performing system loses a significant portion of its loads when a fault occurs.
- Economics—Installation and recurring costs; generally, in opposition to performance, i.e. a good performing system generally costs more.
- Simplicity—Quantity of parts, zones of protection, level control de-centralization needed to ensure its reliability.

These form a set of important criteria which need to be fulfilled by the proposed solution and another need is the ability to discriminate and coordinate faults as mentioned earlier, between upstream and downstream in a DC setup.

5.2.2 Traditional Time Trip Curves

The time trip curve helps set the breakers in the system for coordination and discrimination in an AC system. These curves are used by the breakers to decide which breaker turns on and how the current gets routed to the different parts of the system in case of a fault situation. A typical curve is as shown in Figure 5-1 . The horizontal axis is the current in Amperes and the vertical axis is the time in Seconds. The curve illustrates a 400A circuit breaker ahead of a 90A breaker. Any fault above 1500A on the load side of the 90A breaker will open both breakers. The 90A breaker will generally unlatch before the 400A breaker. However, before the 90A breaker can separate its contacts and clear the fault current, the 400A breaker has unlatched and also will open.

Assume a 4000A short circuit exists on the load side of the 90A circuit breaker.

The sequence of events would be as follows:

1. The 90A breaker will unlatch (Point A) and free the breaker mechanism to start the actual opening process.
2. The 400A breaker will unlatch (Point B) and it, too, would begin the opening process. Once a breaker unlatches, it will open. At the unlatching point, the process is irreversible.
3. At Point C, the 90A breaker will have completely interrupted the fault current.
4. At Point D, the 400A breaker also will have completely opened the circuit.

In cases where several breakers are in series, the larger upstream breaker may start to unlatch before the smaller downstream breaker has cleared the fault. This means that for faults in this range, a main breaker may open when it would be desirable for only the feeder breaker to open." This is typically referred to in the industry as a "cascading effect."

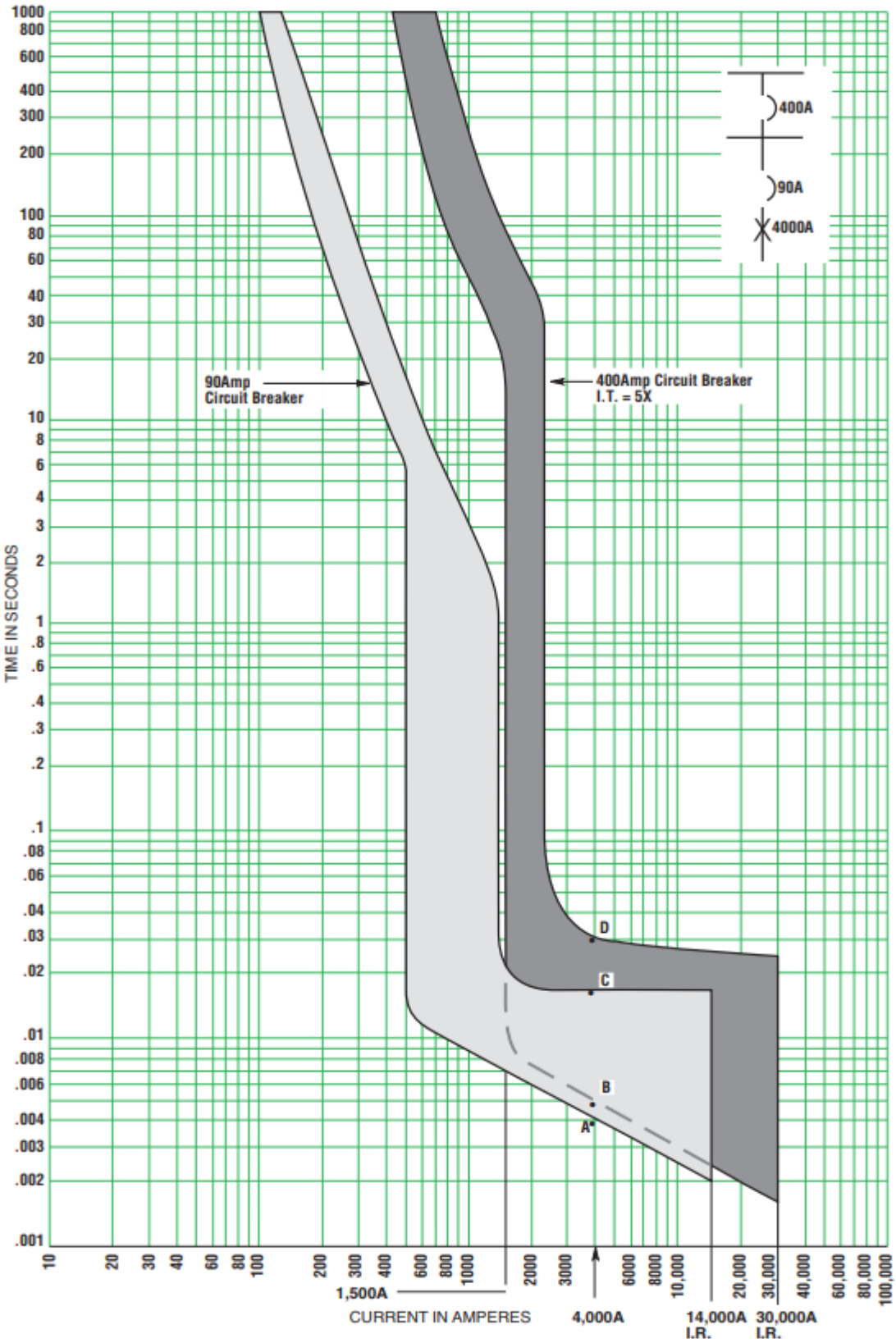

Figure 5-1 – Typical Time Trip Curve Example

The traditional overcurrent protection has some limitations [114].

- Phase overcurrent relays must be set above the maximum load current. Therefore, maximum load expectations limit the sensitivity and speed of the protection for phase-to-phase and three-phase faults.
- Protection settings must be checked against load levels frequently and seasonally, because load growth and extreme temperatures can result in load current tripping on faulted circuits when energy is most needed.
- Ground overcurrent relays must be set above the maximum load unbalance expected on the feeder. Unbalance, whether from uneven loading of the three phases, from single-phase switching operations, or from blown fuses, limits the sensitivity of ground protection.

Overcurrent protection coordinates by current, time, or both. Figure 5-2 depicts a radial system with two inverse-time overcurrent devices. To ensure selectivity, the upstream (backup) device must wait for the downstream (primary) device to clear the fault. In this case the load feeder is downstream of the branch feeder which is downstream of the bus feeder. Otherwise, users between the upstream device and downstream devices will lose service unnecessarily. The time-current curve of the upstream device must be above the downstream device curve, with some time margin. Unfortunately, this level of selectivity requires a sacrifice in speed. Fault-clearing time increases as the fault moves to the line sections located closer to the source, where the fault current is higher. The undesirable result is longer clearing times for more severe faults.

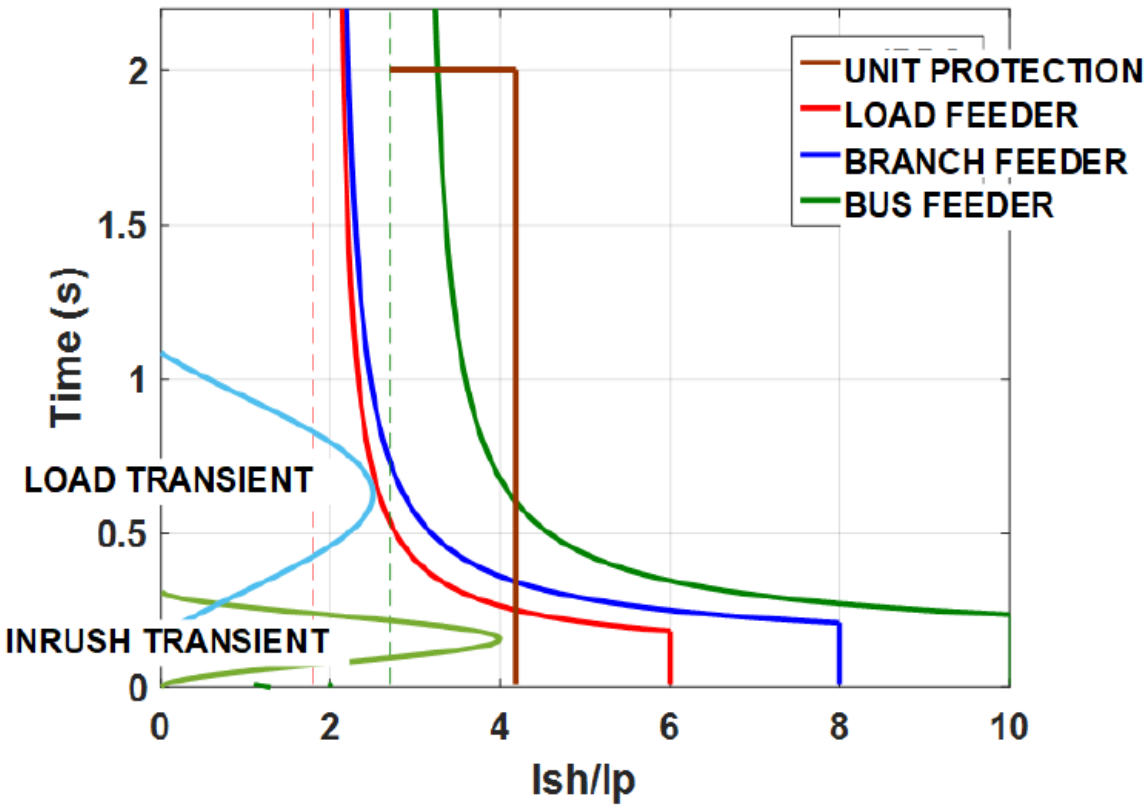

Figure 5-2 - Coordination of overcurrent protection in a radial AC system

Although instantaneous overcurrent elements provide faster tripping, they can be coordinated only when the feeder impedance creates substantial difference in fault current between close-in and remote faults. In tightly knit distribution systems, such as those in urban areas, in manufacturing plants, and aboard ships, these elements become difficult or impossible to coordinate, because the fault current may not change significantly from the source to the farthest load.

5.2.3 Time Trip Curves during a DC Fault

In order to solve the DC protection dilemma a complete paradigm shift away from how conventional AC systems are protected must be acknowledged.

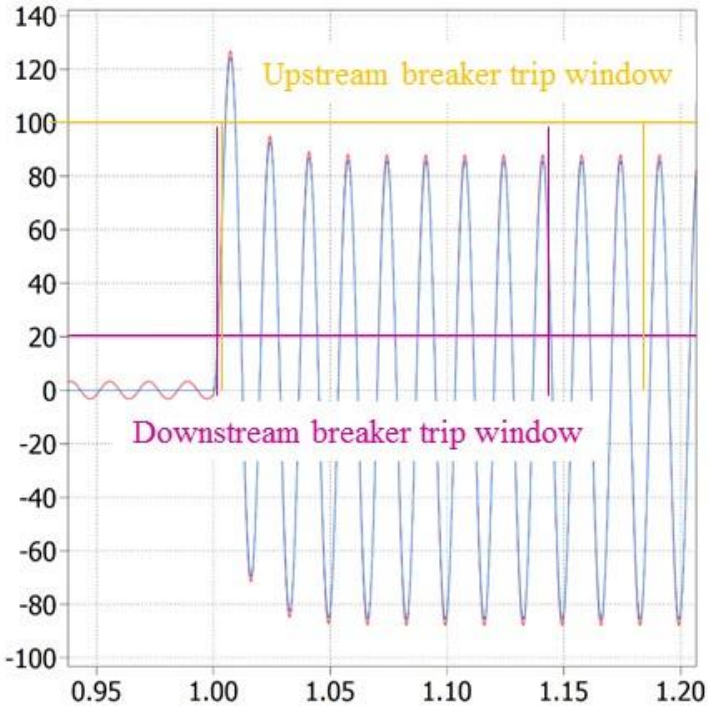

Figure 5-3 - Upstream and downstream circuit breaker currents with a fault downstream of the downstream breaker location in an AC system

The reason for this is illustrated by the simulation results shown in the graphs in this section of the chapter. Conventional AC distribution fault characterization is shown in Figure 5-3 for the conditions of a suddenly applied zero ohm fault applied downstream of a load feed. The superimposed current and time envelopes from the set time-trip characteristic of upstream and downstream breakers show that this current does not exceed the upstream breaker's time-current trip points. This means only the downstream will be tripped and the loads between upstream and downstream will not be cut off incorrectly. The upstream and downstream circuit breakers can achieve coordination because the AC reactance limits the increasing rate of fault current. On the

other hand, Figure 5-4 shows equivalent DC fault characterization. Because of sudden discharge of upstream power converter filter capacitor current, the peak currents for conditions of both a fault between the two breakers and downstream of the two breakers would exceed the breaker instantaneous trip levels and, because the upstream power conversion folds back its output on an overcurrent protection, the current surge associated with the fault is over well before either circuit breakers' time trip. This means that both upstream and downstream circuit breakers will trip. The reason for this characteristic in DC system is that sudden discharge of upstream power converter filter capacitor. It is impossible for two normal circuit breakers to coordinate with the current limitation of upstream source.

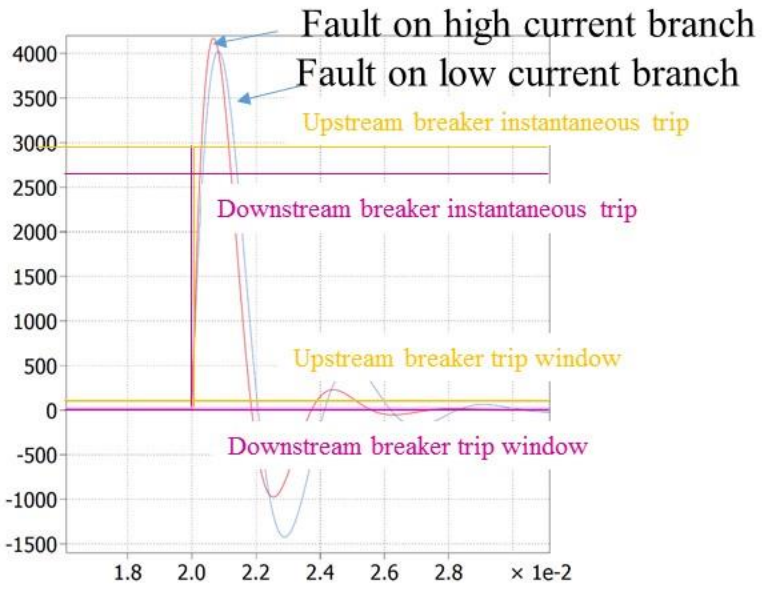

Figure 5-4 - Upstream and downstream circuit breaker currents with faults at two locations in a DC system

If, on the other hand, protective devices could trip within microseconds of fault inception it would be possible to coordinate upstream and downstream devices by simple trip levels. This is demonstrated by the zoomed in curves of Figure 5-5.

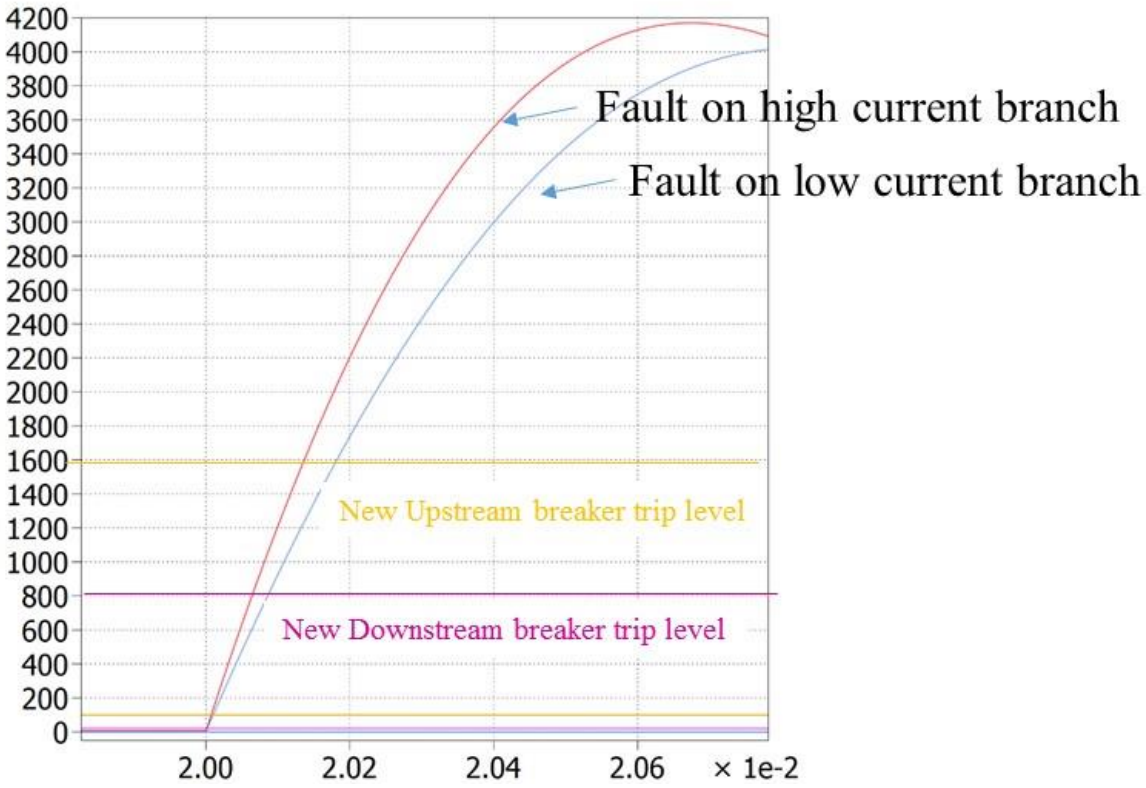

Figure 5-5 - Zoomed in upstream and downstream circuit breaker currents with faults at two locations in a DC system

In this case it can be seen that based on the trip level we can have the downstream trip before the upstream and vice versa depending on whichever is closer to the fault and we can have scenarios where we do not have to set the entire system off which is what happens if we do not have a fast acting solution.

5.3 SSCB as the Solution

A key enabler to viable DC distribution would be to have some kind of solid state trip device, or SSCB, that could reliably trip on fault currents within microseconds. If a SSCB were implemented using normally-off devices, such as an IGBT or IGCT, the device would need to be commanded on when connected to the load and utilize external current sensing circuitry to detect a high current fault so that the switch could be commanded to the off state and thus drive fault

current to zero, removing the fault from the circuit. No load isolating switches connected in series with the solid state portion of the SSCB would then need to open in order to isolate the fault. There can be two possible approaches for the DC Solid State Circuit Breakers.

5.2.1 Current Sensor Based

A notional current sensor based approach of a system would look like Figure 5-6. This system would have the following characteristics:

- Normally “Off” switches – They would need to be externally driven to turn on.
- Requires external power to connect and disconnect switches.
- Relies upon external current feedback to turn off devices.
- Current feedback signal chain limit ability to respond to sudden fault inception.
- Higher cost – It might be expensive as it depends on the types of sensors and precision costs money.

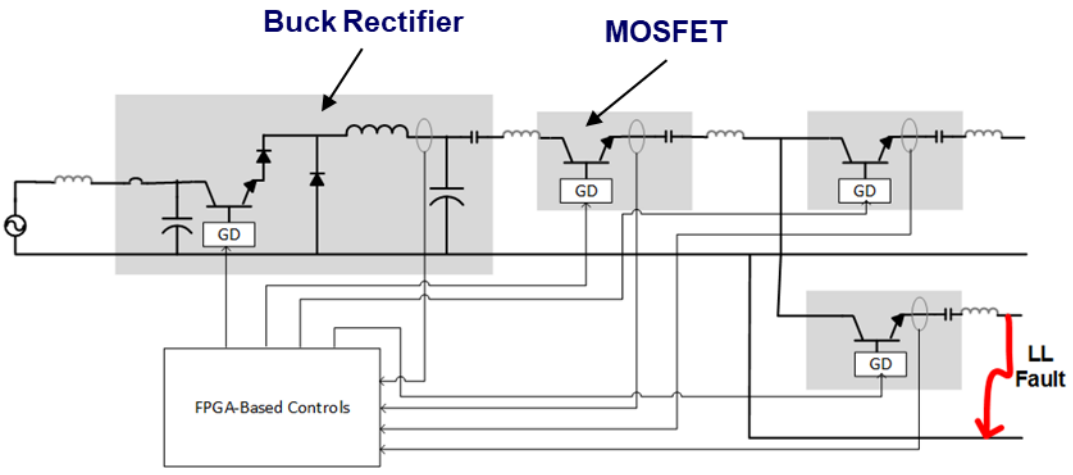

Figure 5-6 - Sensor Based

5.2.2 Self-Powered

A notional current sensor based approach of a system would look like Figure 5-7. This system would have the following characteristics:

- Normally “On” switches – They do not need an external supply for operation.
- Powered by the fault current itself to gate off the devices.
- Autonomous response to sudden fault inception and overload (like conventional AC breakers).
- Immediate response – They are faster than their counterparts as they are not waiting for a signal from elsewhere for their operation.
- Lower cost – It is less expensive than a system with sensors as there is no requirement for external accessories.

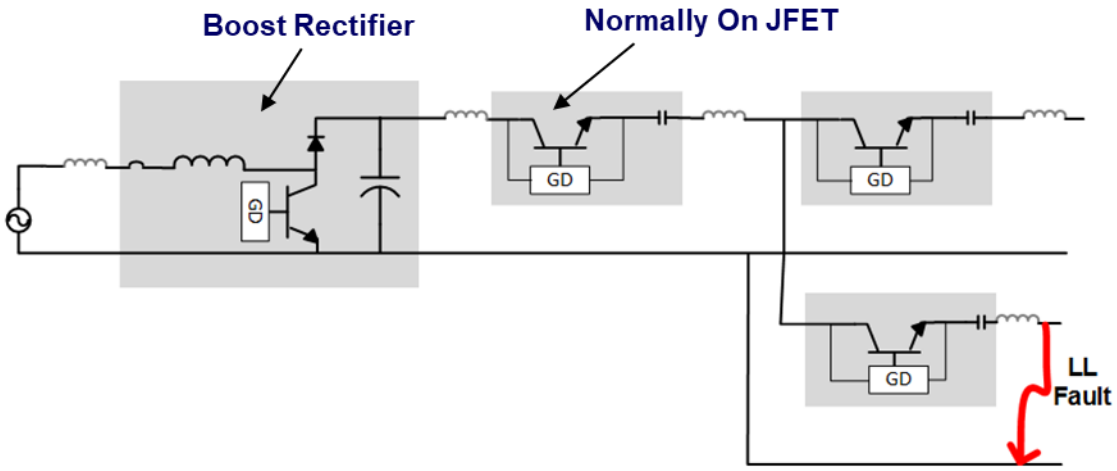

Figure 5-7 - Self-Powered

5.4 DC Microgrid Approach

5.4.1 Protection Device

The Self-Powered SSCB seemed the right approach for the DC Community Microgrid. The new SSCB is faster and it will be able to quickly act during a fault situation as it does not require an external trigger to act. It is the right direction to build the system off of due to some of the reasons discussed in this section.

The fault is Characterized by the system capacitance and cable inductance, so the device must be able to act very quickly to limit current during sudden fault inception current surge that is characterized by the connected bus capacitance and cable inductance to the fault as shown in the equations below:

$$i(t) = \frac{v_c(0)}{L * \omega_d} * e^{-\alpha t} * \sin(\omega_d t) \qquad \text{Equation 5-1}$$

Where, the damping frequency, time constant and the resonant frequency are given by

$$\omega_d = \sqrt{\omega_0^2 + \alpha^2} \qquad \text{Equation 5-2}$$

$$\alpha = \frac{R}{2 * L} \qquad \text{Equation 5-3}$$

$$\omega_0 = \frac{1}{\sqrt{L * C}} \qquad \text{Equation 5-4}$$

As demonstrated in Figure 5-8, the traditional electromechanical circuit breakers minimum response time to fault is around several tens of milliseconds but they can achieve very high current rating. Many SSCBs that have been proposed previously, exhibit a minimum response time about several milliseconds with a reasonable current rating. However, the typical self-protection response time of DC-AC power converter is in microsecond time scales, which means

both electromechanical and previously-proposed solid state circuit breakers cannot serve as a reliable overcurrent protection for the DC power converter or DC Microgrid.

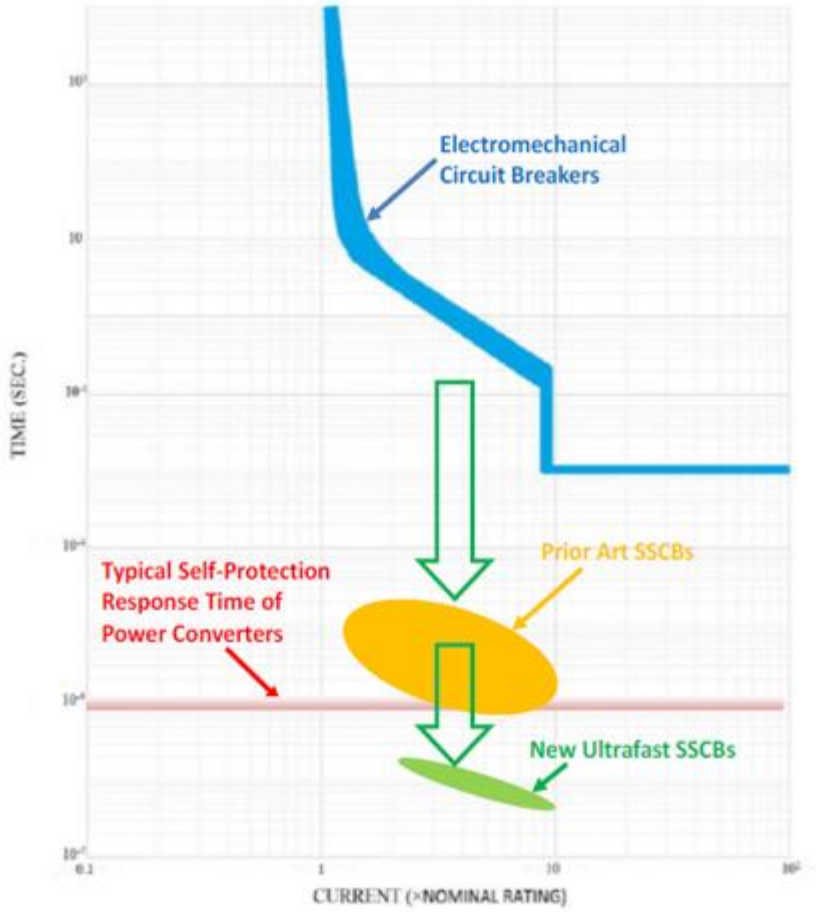

Figure 5-8 - Comparison of time-current characteristics of different circuit breaker technologies

A new SSCB using a normally-on SiC JFET has been presented in [97] to provide a feasible solution to DC short circuit faults. This new SSCB shows many excellent characteristics over previously-proposed circuit breakers, such as self-powered, ultra-fast response. It offers a reaction time of 1-2 microsecond, about 10 times faster than any previously reported SSCBs and 10,000 times faster than any mechanical circuit breakers, and is well within the overload

tolerance time window of a typical power converter. The working principal and the implementation of the new SSCB will be discussed in the next chapter.

5.4.2 System Design

The proposed system is a meshed/radial system as shown in Figure 5-9 - Protection System. The system is a combination of meshed and radial. It is meshed in the part that there might be connections within individual homes on the other side of the PCC within the community set up. It is radial in the aspect that it connects radially from the DC Source or AC source through the PCC to the individual houses and the loads in the house through PCC and custom panels.

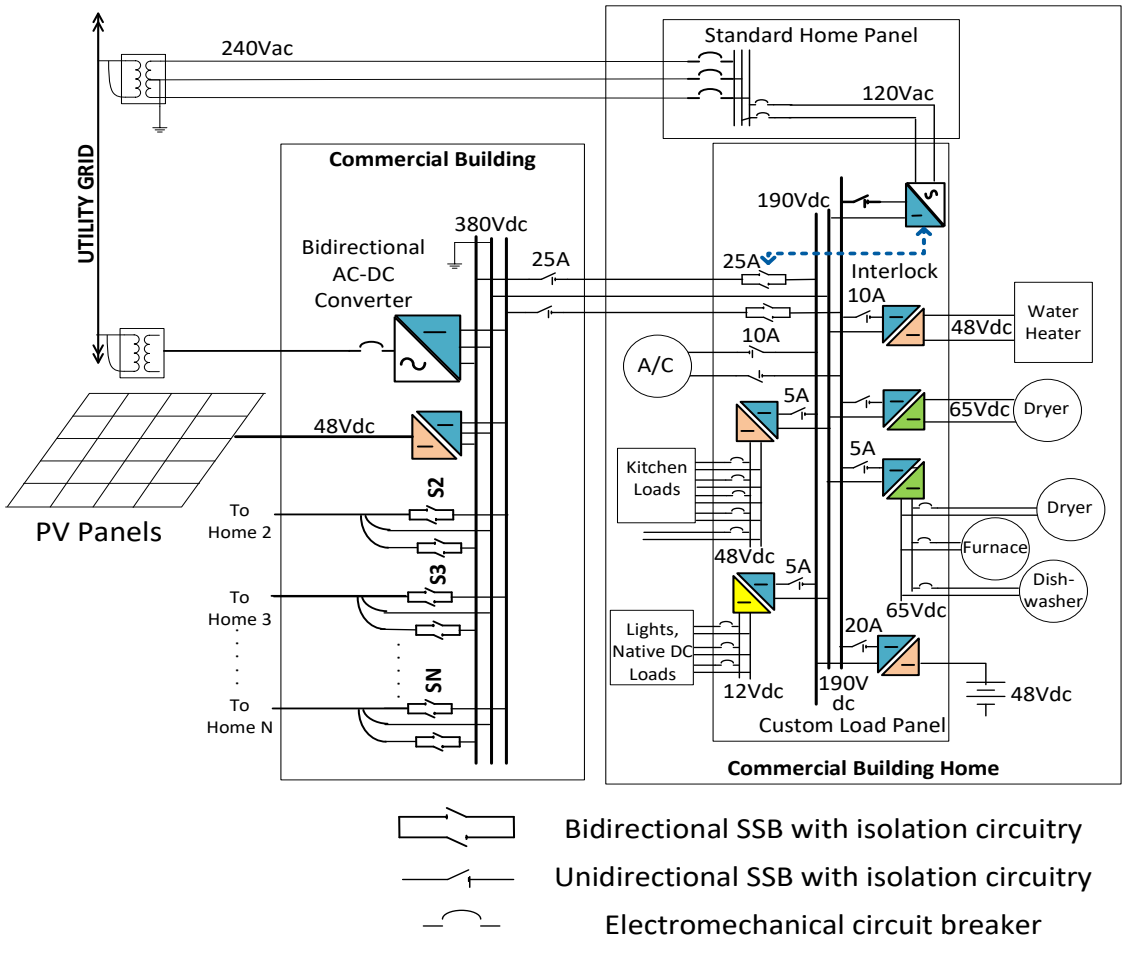

Figure 5-9 - Protection System

The SSCB is designed in a way that it should be able to be modified to fit in different parts of the distribution system in order to help with fault discrimination and coordination as will be discussed and analyzed in the next chapters (6 and 7).

5.5 Summary

In this chapter, the protection system framework was designed and the platform was set to be able to implement and see the results through simulation and experiments in the next chapter. The requirements and challenges around protection of DC systems were looked at in this chapter, then the appropriate approach between current sensor based and self-powered protection devices were chosen. Then a protection system for the DC Community microgrid in contention was designed.

Chapter 6 Protection System Implementation

The core of the protection system is implemented by a series of steps from the basic component to the system as a whole. The first and the most important piece of the design is the basic component, SiC JFET, that is firstly looked at and simulated to observe the behaviors. Then, we build the SSCB with the SiC JFET and make the switch which will be the component which will be the integral part of the design. The different components will be looked at in detail and a behavioral analysis with the current commutation will be presented as well. We will then look at the fault characterization capabilities of the device in the DC Microgrid setting through simulations in this chapter.

6.1 SiC JFET

With the development of microelectronics technology, the performance of conventional semiconductor such as Silicon (Si) and Gallium Arsenide (GaAs) has almost reached their peak due to the nature of the materials. And the opportunities for both power density and efficiency improvements of inverter have come with the development of commercially available wide bandgap (WBG) devices. "Wide-bandgap" refers to higher-energy electronic band gaps, the difference in energy levels that creates the semiconductor action as electrons switch between the two levels. Another advantage to the use of some WBG materials is that the thermal coefficient of expansion (TCE) is better suited to the ceramics used today in packaging technology.

SiC unipolar devices such as JFETs or MOSFETs exhibit a very low on-resistance and a large safe operating area (SOA) below a voltage rating of 4500 volts [116]. For the voltage rating of 1200V, SiC JFETs and MOSFETs exhibit a typical specific RDS(ON) of 2-4 mΩ-cm2, or 100X lower than silicon MOSFETs or 10X lower than silicon IGBTs. Furthermore, SiC devices can

sustain a much higher junction temperature under both static and transient conditions, making them suitable for SSCB applications where the energy burst during a short circuit event can drive the junction temperature beyond the silicon limit. A large turn-off current capability is needed for a given solid state device and Si MOSFET, Si CoolMOS, SiC MOSFET and Sic JFET were compared in [117] and SiC JFET had the highest maximum allowable turn-off current density and the highest peak power density amongst all thereby reiterating our choice of the same for our system. The SiC JFET lends itself to be a simple two terminal device which can operate without the need of an external gate like the others and that is what gives it the speed we desire.

6.1.1 SiC JFET Model

UJN1205K3 SiC JFET is used in our work. As JFETs are not readily available in any of the software's except PSIM and LT Spice, the model was built on LT Spice. This was done so because the SiC JFET can be built from scratch i.e., individual resistors and capacitors associated with the source, drain and gate, that is not possible in PSIM. The model is as shown in Figure 6-1 - LT Spice model of the SiC JFET. It can be seen on the top of the figure that we define the individual diodes and there is an intricate model for the connections between the Gate, Drain and Source and how they link to each other to be accurate to capture the current flow when operational. The other functions, dependencies and individual parameters of the components which make the JFET are clearly defined and modeled as accurately as possible.

6.1.2 SiC JFET Characteristics

The threshold characteristics of the JFET is shown in Figure 6-2. The threshold on the data sheet was about -7 and the simulation maps close to that.

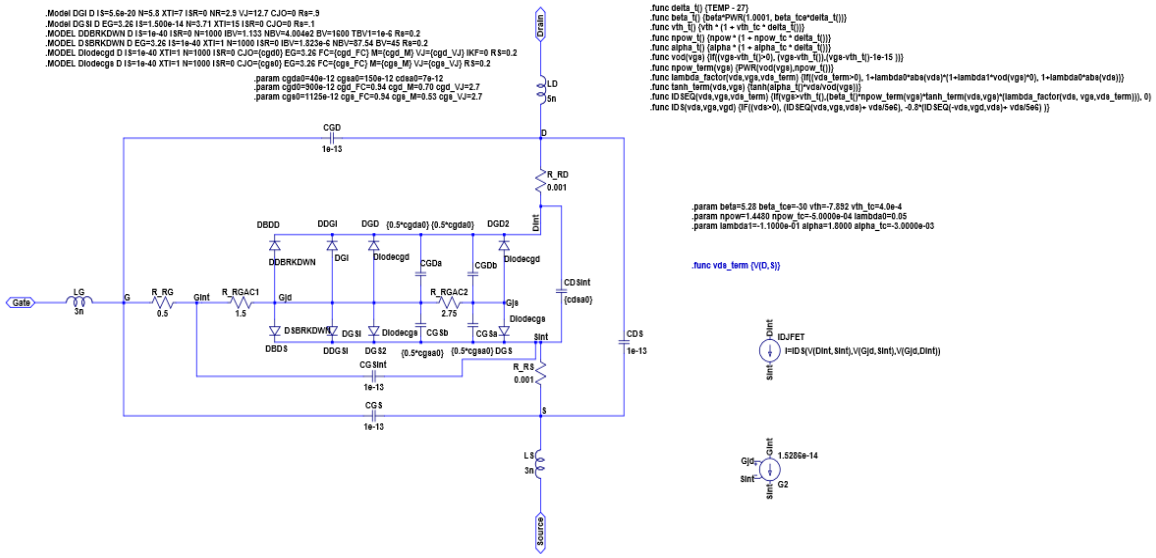

Figure 6-1 - LT Spice model of the SiC JFET

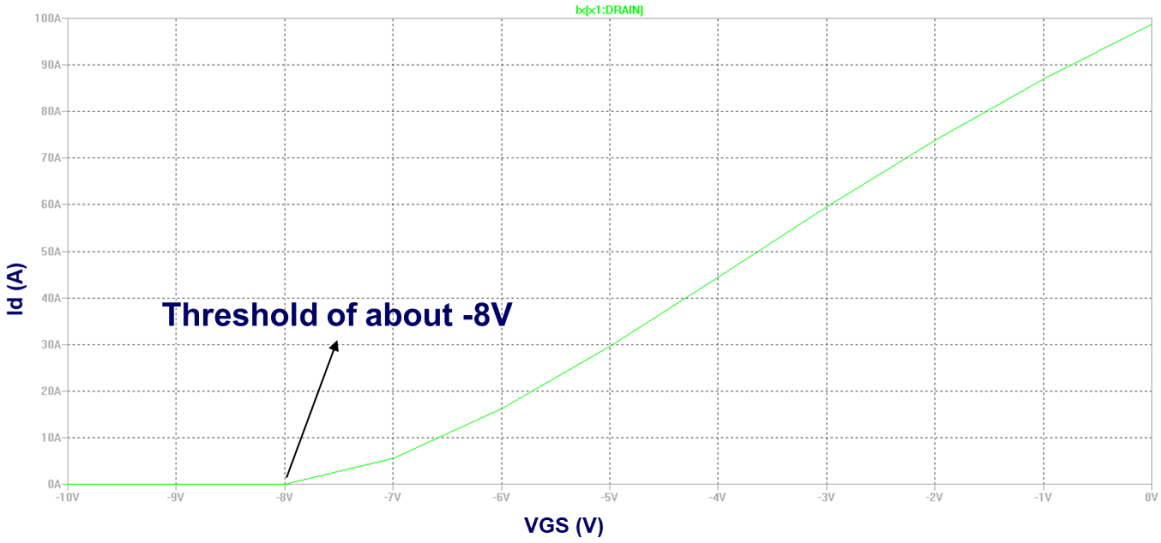

Figure 6-2 – Threshold Characteristics of the SiC JFET

The threshold characteristics of the JFET is shown in Figure 6-2. The threshold on the data sheet was about -7 and the simulation. The Id vs VDS at different VGS values as shown in Figure 6-4 matched the data sheet points as well. The SiC JFET was modeled into a submodule so it could

be used as an integral part of the SSCB and the schematic to capture the Id vs VDS characteristics is as shown in Figure 6-3.

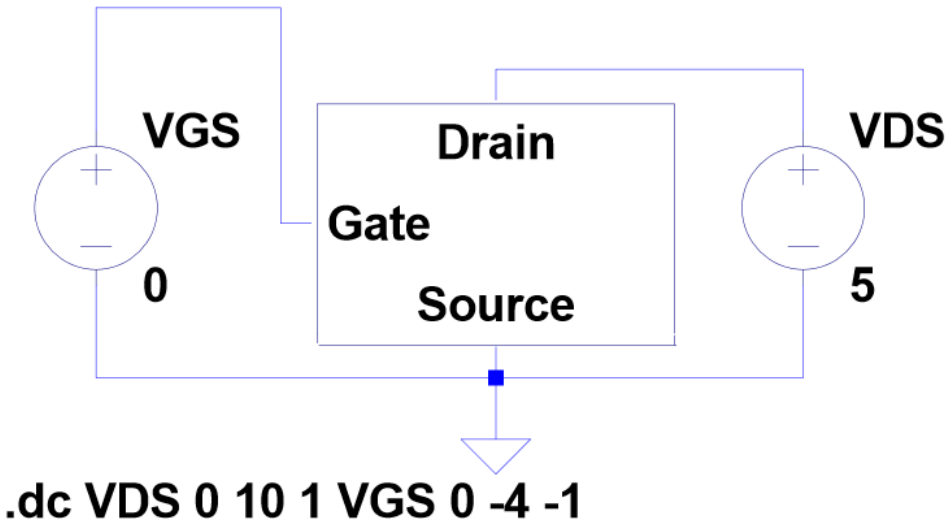

Figure 6-3 – LT Spice model to capture Id vs VDS Characteristics of the SiC JFET

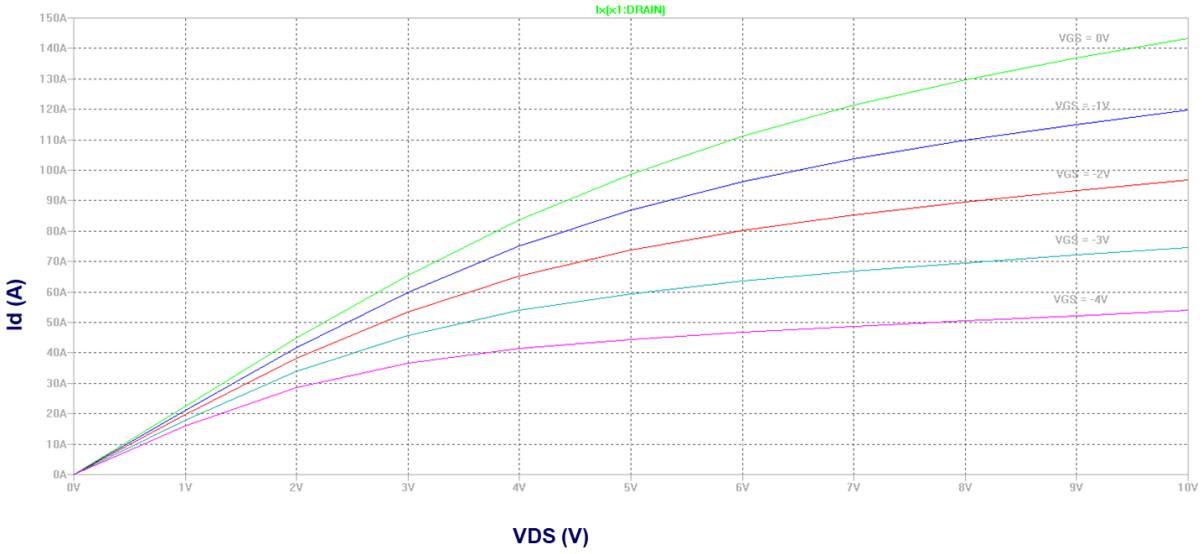

Figure 6-4 – Id vs VDS Characteristics of the SiC JFET

Table 6-1: UJN1205K3 Parameters

Parameter	Symbol	Test Conditions	Value	Units
Drain-Source Breakdown Voltage	BV_{DS}	V_{GS} = -20V, I_D = 1mA	1200	V
Total Drain Leakage Current	I_D	V_{DS} = 1200V, V_{GS} = -20V, T_j = 175°C	30	µA
Total Gate Leakage Current	I_G	V_{GS} = -20V, T_j = 175°C	10	µA
Drain-Source On-Resistance	$R_{DS(on)}$	V_{GS} = 2V, I_F = 30A, T_j = 175°C	105	mΩ
Gate Threshold Voltage	$V_{G(th)}$	V_{DS} = 5V, I_D = 70mA	-6	V
Gate Resistance	R_G	V_{GS} = 0V, f = 1MHz	5	Ω

6.2 SSCB

The Solid State Circuit breaker is a simple two terminal device with a faster response time than most. It is built to be suitable for 400V to 1000V, the SiC JFET being at 1200V lets the SSCB be operational and effective at that voltage with a high power density. a solution for a low cost SSCB acts with sufficient speed to limit fault currents in converter fed DC systems is proposed. The proposed SSCB utilizes a normally-on SiC JFET. Short circuit fault inception induces a drain to source voltage rise. A specially designed sensing circuit draws power from the fault condition to turn off and hold off the SiC JFET. Both unidirectional and bidirectional implementations of the SiC JFET based SSCB's are shown in Figure 6-5 and Figure 6-6 respectively.

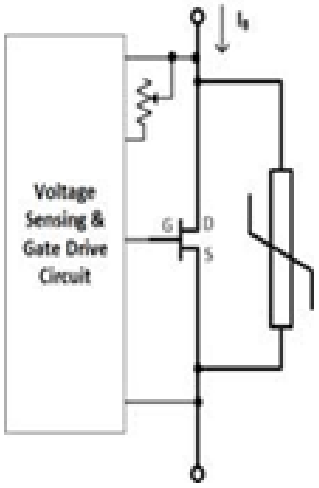

Figure 6-5 – Unidirectional SSCB

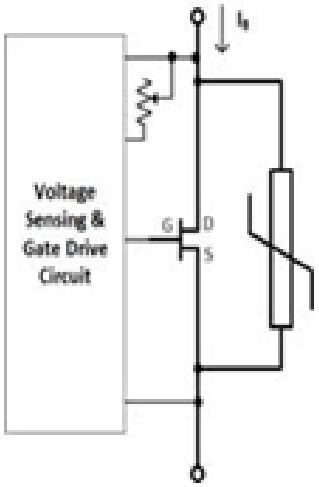

Figure 6-6 – Bidirectional SSCB

A detailed schematic of the unidirectional Solid State Circuit Breaker is as given in Figure 6-7. The core of the SSCB is Q1, a commercial normally-on 1200V SiC JFET (UJN1205K from USCi). The JFET exhibits a typical RDS(ON) of 45 mΩ at zero gate bias and a breakdown voltage of 1420 V at a gate reverse-bias of -16V. This normally-on characteristic, while undesirable for most power converter applications, is ideal for this SSCB design due to the extremely small conduction resistance. As shown in the schematic the SSCB is made up of three main components as we will see in this section.

6.2.1 Voltage Sensor

The voltage sensor network is an RC network as shown in Figure 6-8. The voltage sensing network acts like the probe which looks for potential differences across the leads of the capacitor C2. The voltage across the capacitor is as given by the equation below. The voltage between the drain and the source terminal is monitored and if that exceeds a value of about 3V to 5V then the PWM signal generator gets enough power to turn on and gets activated. This sensing network is what makes the SSCB a self-powered SSCB, it acquires the required current from the fault across the JFET and turns on the PWM if the threshold is breached.

$$v_{C2}(t) = \frac{C1}{C1+C2} v_{DS}(t) * (1 - e^{-\frac{t(C1+C2)}{R2C1C2}})$$

Equation 6-1

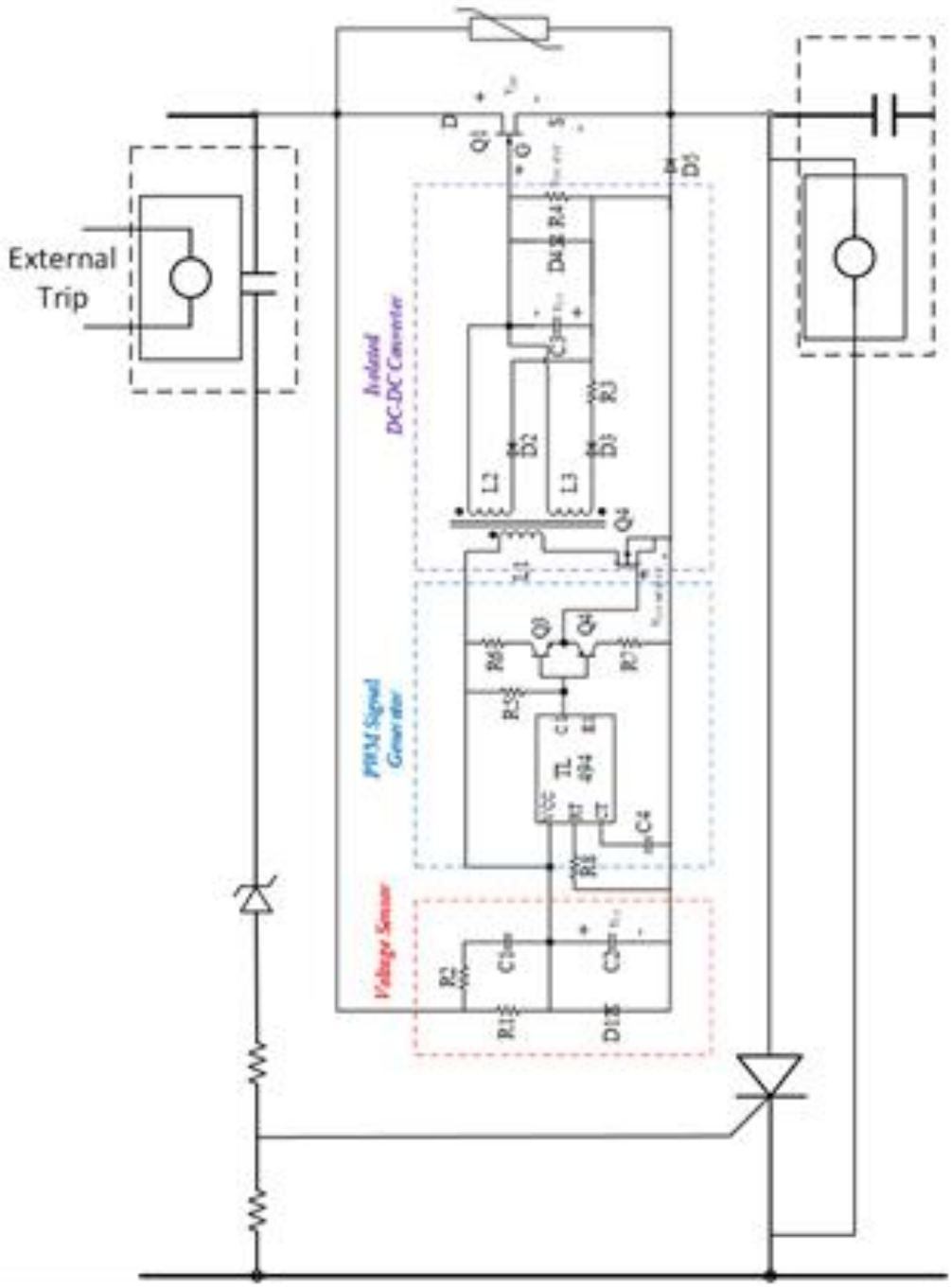

Figure 6-7 – Detailed Schematic of the unidirectional SSCB

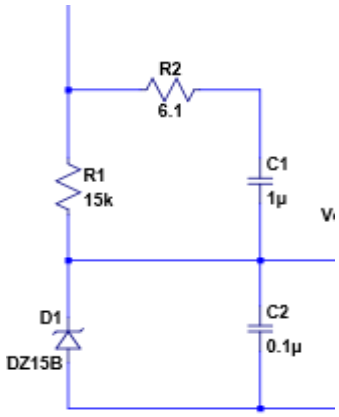

Figure 6-8 – Voltage Sensor

6.2.2 PWM Signal Generator

The role of the PWM generator is to generate PWM signals for the converter. It is as shown in Figure 6-9.When a short circuit fault occurs, the drain-source voltage of the JFET suddenly increases as a result of a large overcurrent through the JFET. For example, an overcurrent of 200A will yield a drain-source voltage of 9V assuming the 45mΩ JFET does not enter its quasi-saturation regime yet. Capacitors C1 and C2 are charged through resistor R2 in the voltage sensor network. When the current continues to charge C2 and the voltage across C2 hits the threshold value around 3-4 volts, PWM signal generator will be activated. The PWM generator will provide the gate signal of MOSFET Q2 through a simple amplifier circuit made up with two transistors and turn Q2 on and off to transfer energy from primary winding to secondary windings of the transformer. To generate the signal, PWM control IC (Texas Instruments TL494 [118]) with a fixed frequency PWM control scheme. The PWM IC is configured to provide a pulse width of 2 µs and a PWM frequency of 60 kHz during steady state operation.

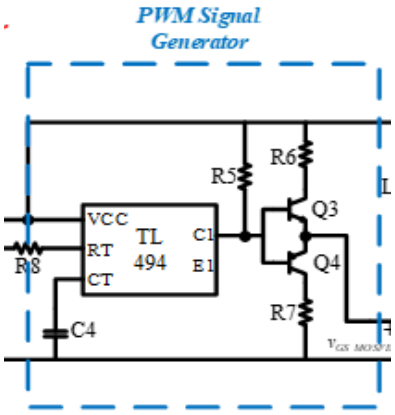

Figure 6-9 – PWM Signal Generator

6.2.3 Isolated DC/DC Converter

The isolated DC/DC converter is a combined Forward and Flyback converter to achieve a faster response time. When Q2 turns on during the initial cycle, charge from C2 is quickly transferred to the output capacitor C3 via the forward secondary winding L3 of the transformer. The negative C3 voltage is quickly established between the gate and source of the JFET. At the end of the first PWM cycle, the Flyback secondary winding L2 starts to charge C3 and contributes to the negative gate biasing of the JFET. After around 2-3 duty cycles, the voltage on C2 accumulates to the threshold value of -16V and the JFET will turn off.

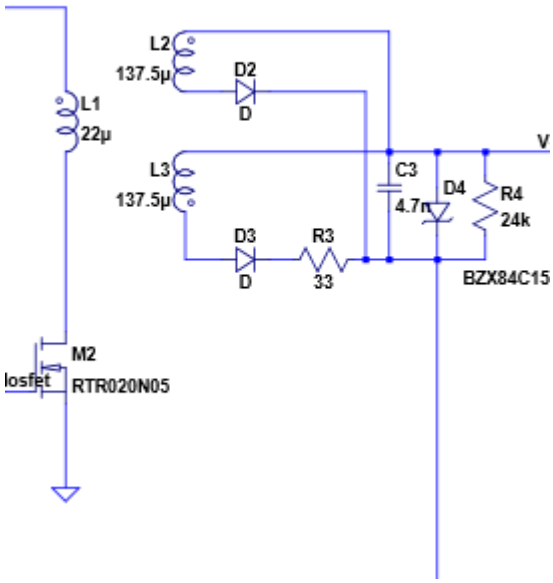

Figure 6-10 – Isolated DC-DC Converter

To eliminate the fault current and isolate the short circuit fault physically, a relay controlled no load contactor is added to SSCB as shown in Figure 6-7. The contactor isolates the faulted branch following turn-off of the SiC JFET and can be reset manually when the fault is cleared. The implementation also includes a thyristor-based crow-bar circuit to induce short circuits during a manual trip or a trip that may be induced by coordinated controls of the MEMS/HEMS units in order to handle ground faults, arcing faults and other fault types that do not sufficiently power the SiC JFET gate circuit. Since the SiC JFET operates autonomously at very high speeds to discriminate faults, it will be necessary to ensure that false trips do not occur.

6.3 Protection Driver Operation

There are two modes of operation of the protection drives namely Flyback and Forward-Flyback. The time it takes to activate the protection driver circuit from standby directly determines how fast the SSCB reacts to a short circuit event, and therefore is the single most important design parameter. The goal is to achieve an SSCB response time within a few microseconds. On the other hand, high efficiency or accurate output regulation is not as a high design priority for the

protection driver as for common DC/DC converters. The protection driver does not operate at all under normal conditions, and is activated only during a short circuit event with a power rating of tens of milliWatts The design considerations of these two modes (Flyback and Forward-Flyback) are discussed in this part.

6.3.1 SSCB with Flyback

The DC/DC converter in Figure 6-10 can be reduced to a simple Flyback topology if L3, D3 and R3 are removed. The switching waveforms of the SSCB implemented with the simple Flyback topology are shown in Figure 6-11, and are explained as the following.

At t0 a short circuit event occurs. The current through the JFET iDS increases immediately and the drain-source voltage of the JFET vDS also increases proportionally, due to the on-resistance of the JFET. Both iDS and vDS reach a plateau at t1 given by

$$i_{DS}(t) = \frac{V_{DC}}{R_{DS(ON)} + R_{SC}} \qquad \text{Equation 6-2}$$

$$v_{DS}(t) = i_{DS} * R_{DS(ON)} \qquad \text{Equation 6-3}$$

where VDC is the DC bus voltage, RDS(ON) is the on-resistance of the JFET, and RSC is the short circuit loop resistance. Strictly speaking, the rate of rise of iDS is also limited by the parasitic inductance in the short circuit loop.

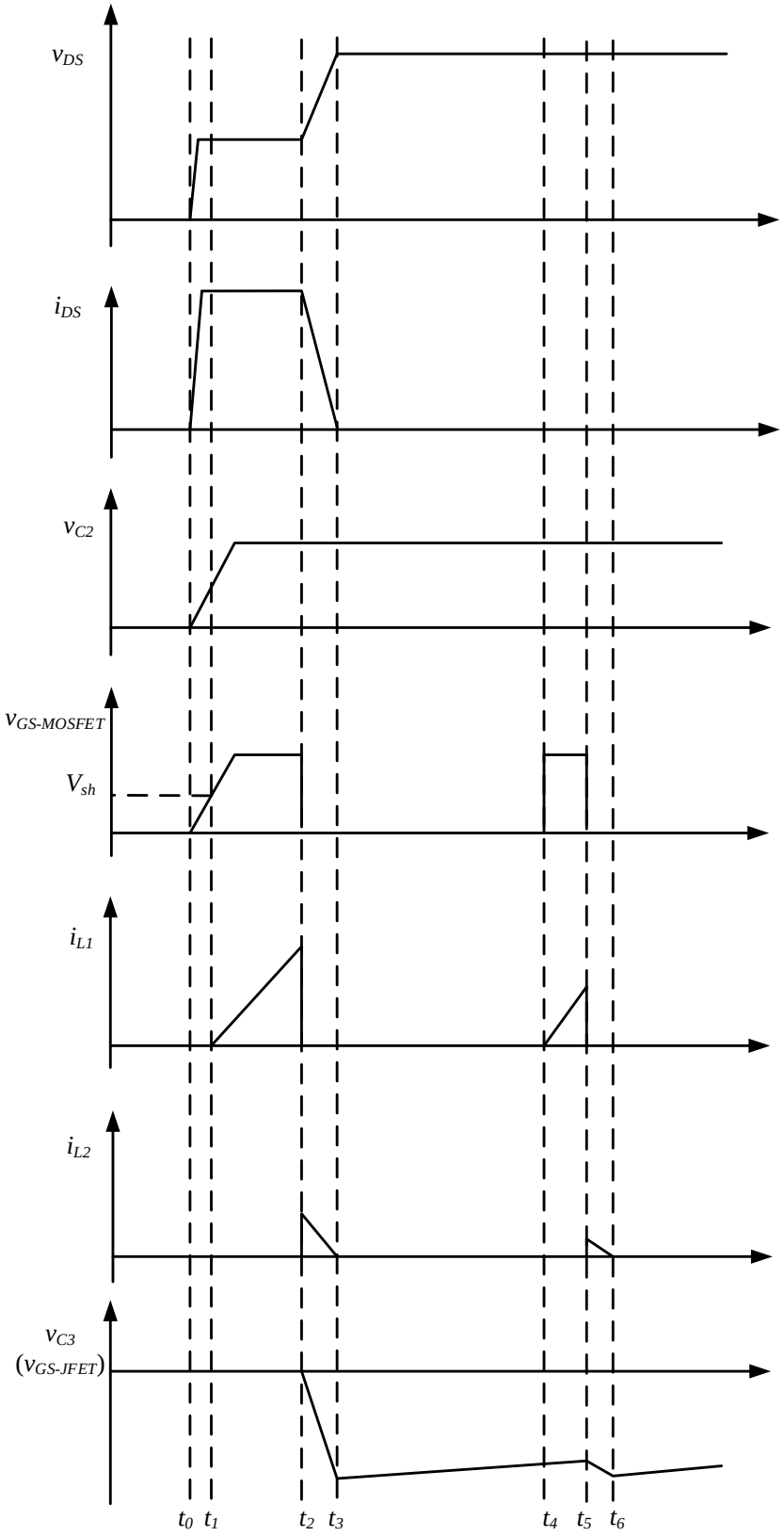

Figure 6-11 – Flyback DC-DC Converter

C1 and C2 are charged by drain and source current vDS via R2 during the short circuit fault. The voltage on C2 is derived by

$$v_{C2}(t) = \frac{C1}{C1+C2} v_{DS}(t) * (1 - e^{-\frac{t(C1+C2)}{R2C1C2}})$$

Equation 6-4

The voltage of C2 is applied between the gate and source of the MOSFET Q2 through R6 and Q3. The gate-source voltage of Q2 vGS_MOSFET is the same as vC2 during this time period.

At t1, the C2 voltage vC2 first exceeds the threshold voltage (roughly 3 V) of the MOSFET Q2 and then the minimum supply voltage of the PWM control IC (roughly 4.5 V). Q2 is turned on through R5, R6, and Q3. Current of L1 begins to flow through the primary side of the transformer

$$i_{L1} = \frac{V_{C2}}{L_1}(t - t_1)$$

Equation 6-5

At t2, Q2 is turned off by the PWM control IC. The energy stored in the transformer is transferred to the Flyback secondary winding L2 and to charge C3. The L2 current iL2 decreases as vC3 increases, until iL2 becomes zero at t3. The energy stored in C3 at t3 is approximately given by

$$\frac{1}{2} v_{C3}^2(t_3) = \frac{1}{2} i_{L1}^2(t_2)$$

Equation 6-6

The JFET is turned off by the negative voltage between its gate and source. The fall time is estimated by

$$t_3 - t_2 = \frac{1}{2}\pi\sqrt{L_2 * C_3}$$

Equation 6-7

At t3, the SSCB is completely turned off, and the responsibility of protection driver from this point on, is only to maintain the negative voltage of C3. Between t3 and t4, C3 is partially

discharged through R4 until the falling edge of the next PWM pulse at t5. The Flyback DC/DC converter charges C3 again from t5 to t6 during the second switching cycle. It repeats this operation until the short circuit fault is cleared. R4 serves the purpose of maintaining a zero-biasing voltage on the JFET gate in absence of short circuit faults.

6.3.2 SSCB with Forward-Flyback

The switching waveforms of the SSCB implemented with a combined Forward-Flyback topology are shown in Figure 6-12. The operation of the combined Forward-Flyback DC/DC converter during the period of t0 to t1 is the same as the previously-mentioned Flyback-only topology.

At t1, the C2 voltage vC2 first exceeds the threshold voltage (roughly 3V) of the gate drive chip TL494 and will activate MOSFET Q2. Q2 is turned on and the energy passes through R5, R6, and Q3. Voltage vC2 is directly dropped across the primary winding of the transformer and immediately transferred to the forward secondary winding L3. Current from L3 flows through D3 and R3 to charge C3 to provide a negative voltage between gate and source of SiC JFET. The voltage of C3 vC3 is given by

$$v_{C3}(t) = nV_{C2} * (1 - e^{-\frac{t}{R3C3}}) \qquad \text{Equation 6-8}$$

where n is the transformer turn ratio of L3/L1. At t2, C3 is charged to the induced voltage of L3 which is derived by

$$v_{C3}(t_2) = V_{L3} = n * V_{L1} = n * V_{C2} \qquad \text{Equation 6-9}$$

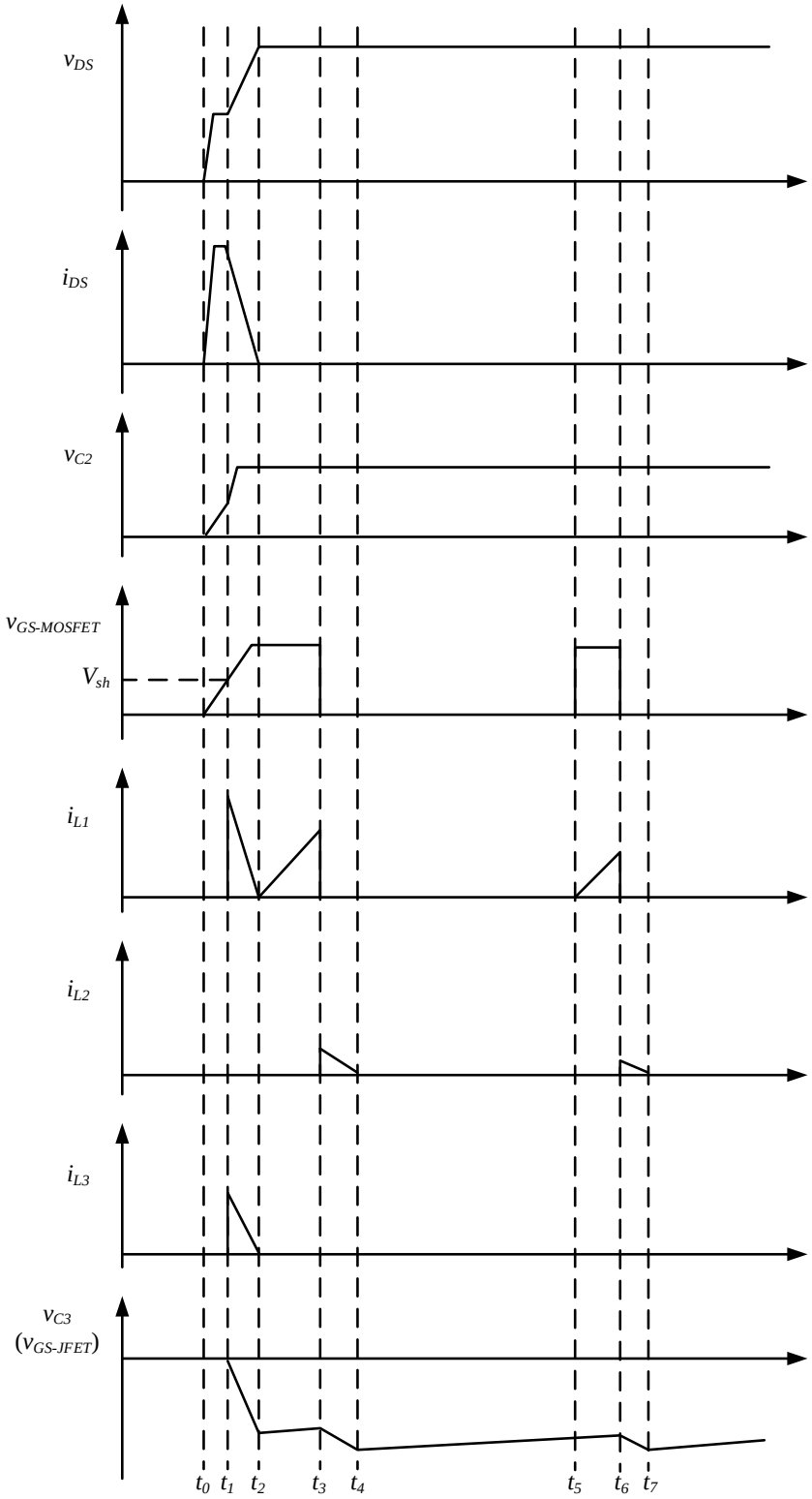

Figure 6-12 – Forward-Flyback DC-DC Converter

At t2, iL3 decreases to zero, and diode D3 turns off. The JFET is turned off by the negative voltage between its gate and source. During the period of t2 to t3, primary current iL1 of the transformer continues to ramp up like in a typical Flyback transformer.

At t3, Q2 is turned off and the energy stored in the primary winding of transformer during the period of t2 to t3 will be transferred to secondary part through Flyback secondary winding L3 and charge C3 to a voltage level more negative than the previous value established by the forward mode charging between t1 and t2. After t3, D3 will remain reversely biased and the forward winding L3 is no longer active. The Flyback converter is now solely responsible for maintaining the negative JFET gate voltage, and repeatedly charges C3 until the short circuit fault is cleared.

6.3.3 Performance Comparison of the Two Designs

The dynamic responses of the two SSCB designs are compared. The schematic of the test setup is as shown in Figure 6-13. An external 15 V power source with a ramping rate of 5 V/μs is supplied to the capacitor C2 for the two SSCB designs respectively. This performance test is done to show the difference in the startup time between both the topologies. A model of the schematic of the 15V source with the SSCB was built in LT Spice for this purpose. The schematic shown is for the Forward-Flyback version and if we remove L3, D3 and R3 (circled green in the schematic), that makes this SSCB operate as a Flyback only driver.

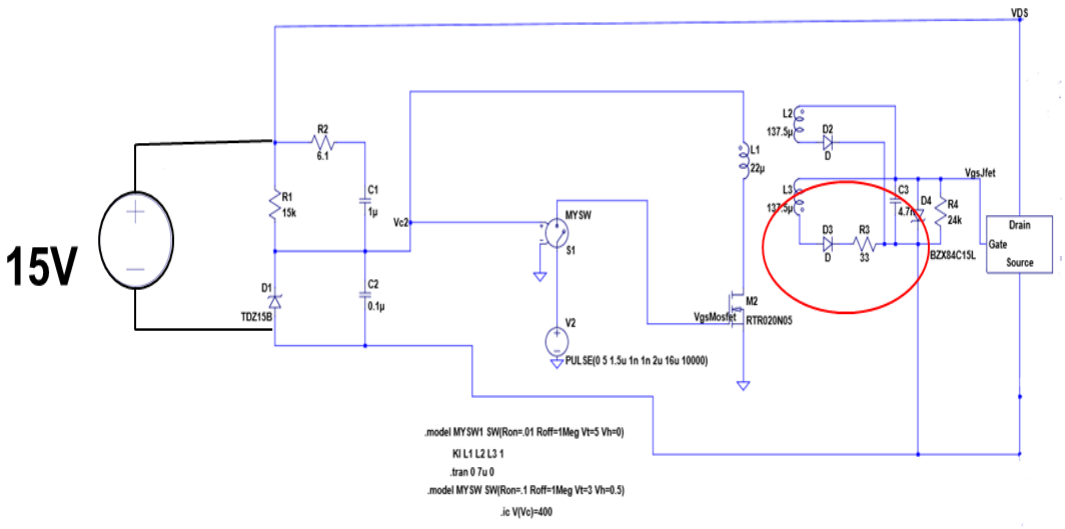

Figure 6-13 – Test Setup Schematic

The waveforms of the external voltage vC2, the power MOSFET Q1 gate-source voltage vGS_MOSFET, and the SiC JFET gate-source voltage vGS_JFET for both SSCB types are shown in the following figures. For the Flyback-only SSCB design, vGS_JFET changes from 0 to -20 V only after Q2 is completely switched off with a delay time of about 2.7 µs as shown in Figure 6-14. For the Forward-Flyback SSCB design, vGS_JFET changes from 0 to -20 V long before Q2 is completely switched off and therefore with a much smaller delay time of only 0.8 µs as shown in Figure 6-15.

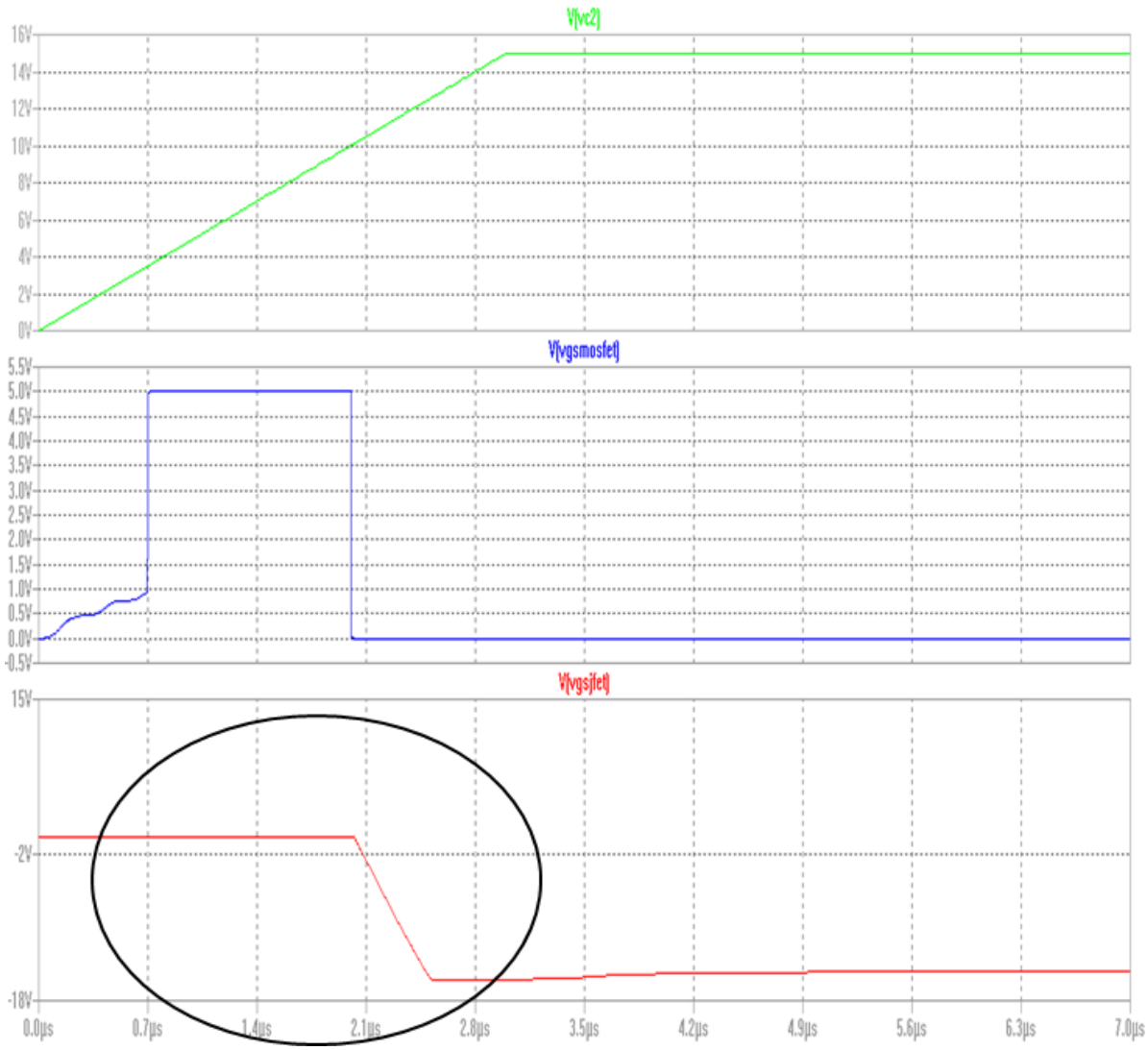

Figure 6-14 – Flyback Design Start Up

This significant difference in startup time for the two DC/DC converter designs have a major impact on the performance of the SSCB. This will determine how quickly a fault can be discriminated and the time it is going to take to completely shut off from the circuit. The Forward-Flyback option is chosen for the rest of the work unless otherwise mentioned ads that give the best results and all the analysis and results are based on the SSDCB operating with that topology.

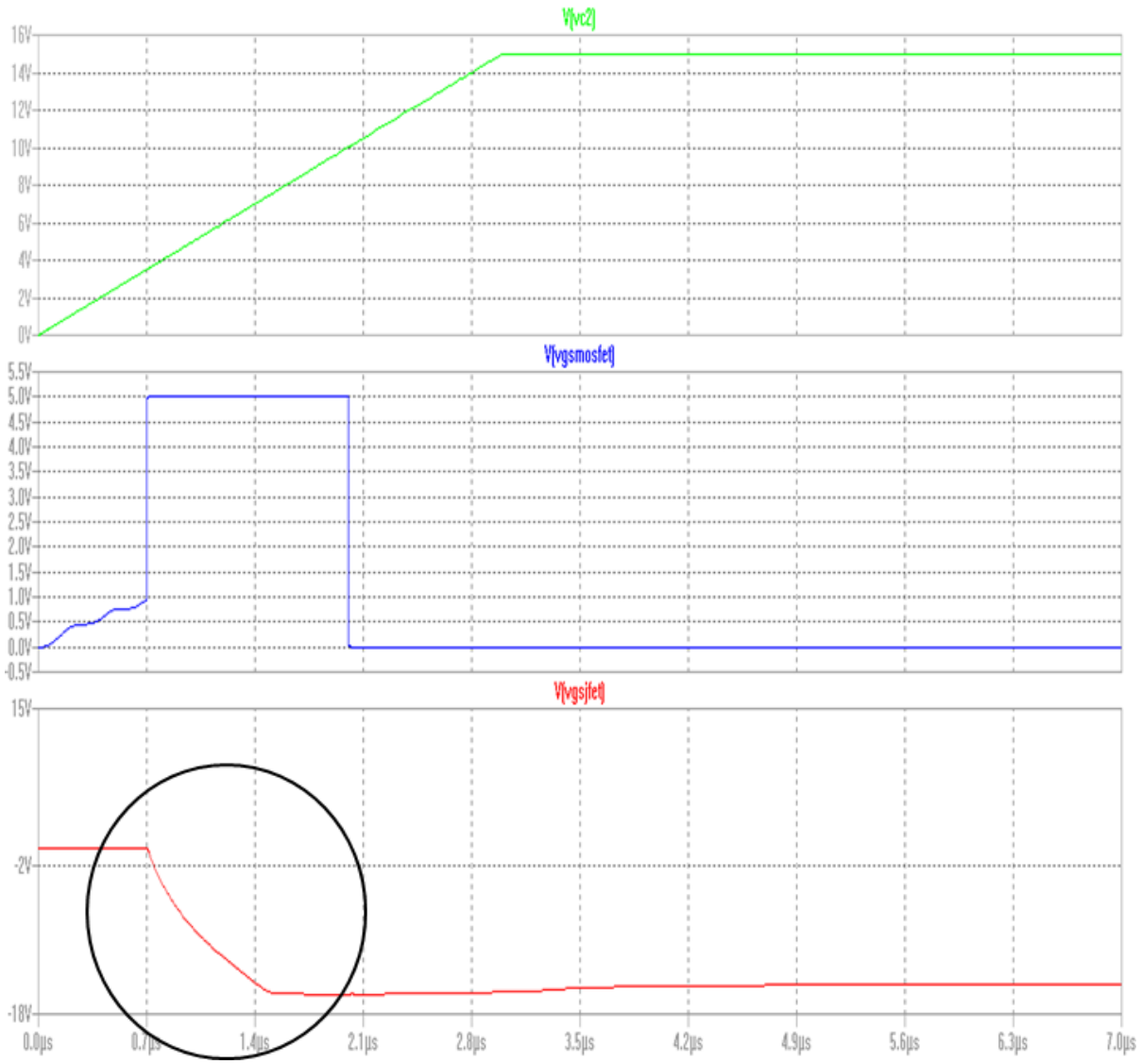

Figure 6-15 – Forward-Flyback Design Start Up

6.3 Unidirectional SSCB Behavioral Analysis

The proposed SiC JFET-based SSCB exhibits both fast and autonomous response to sudden short circuit fault inception. The SiC JFET under consideration has the best maximum turn off capability i.e., the maximum current that a switch can interrupt and has the highest peak power

density compared to alternative power semiconductor choices. Figure 6-16 shows the simulated behavior of the unidirectional device with a Forward-Flyback converter when a short circuit current is induced by discharging a capacitor charged up to 400V into a short circuit.. It is safe o assume that the Forward-Flyback converter will be used in this chapter and next, unless otherwise mentioned, because that has a better response time. The details of the SSCB with the voltage sensing and gate drive circuit are shown in the following figures.

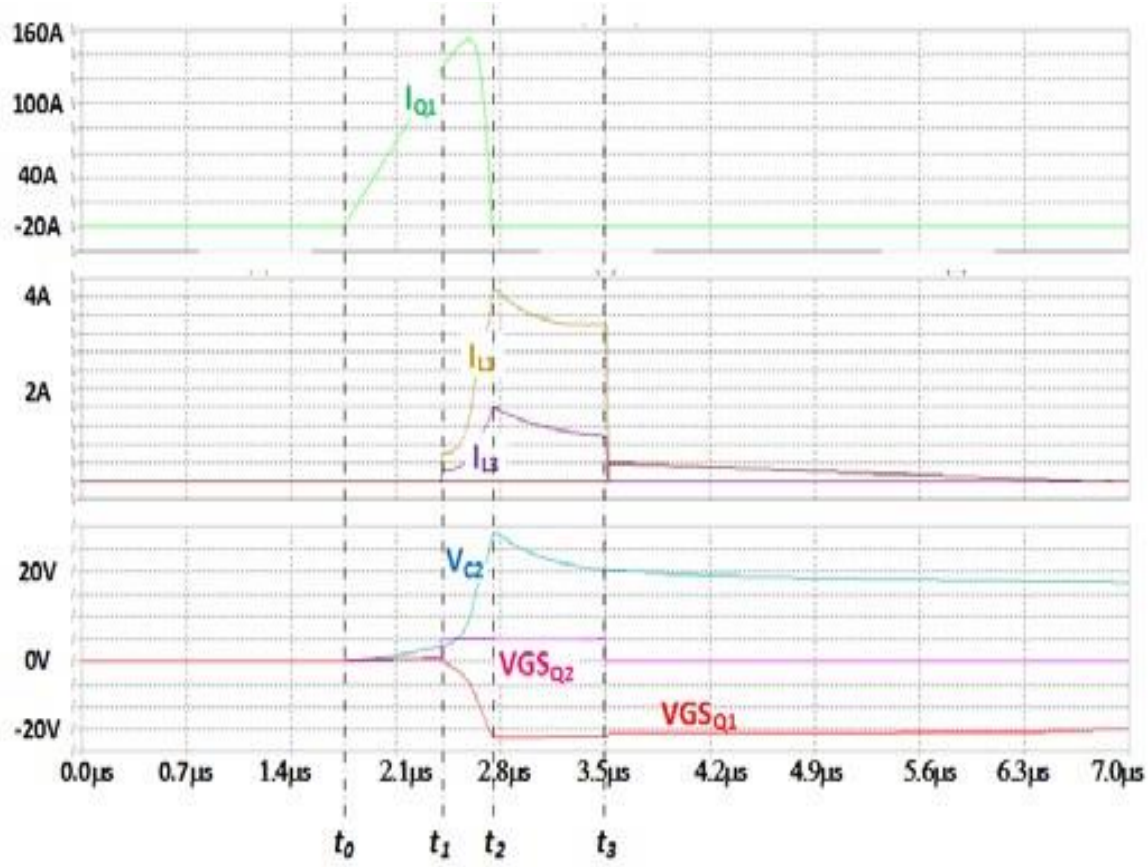

Figure 6-16 – Unidirectional SiC JFET based SSCB switch current (top), inductor currents (middle), sensing and driving voltages (bottom)

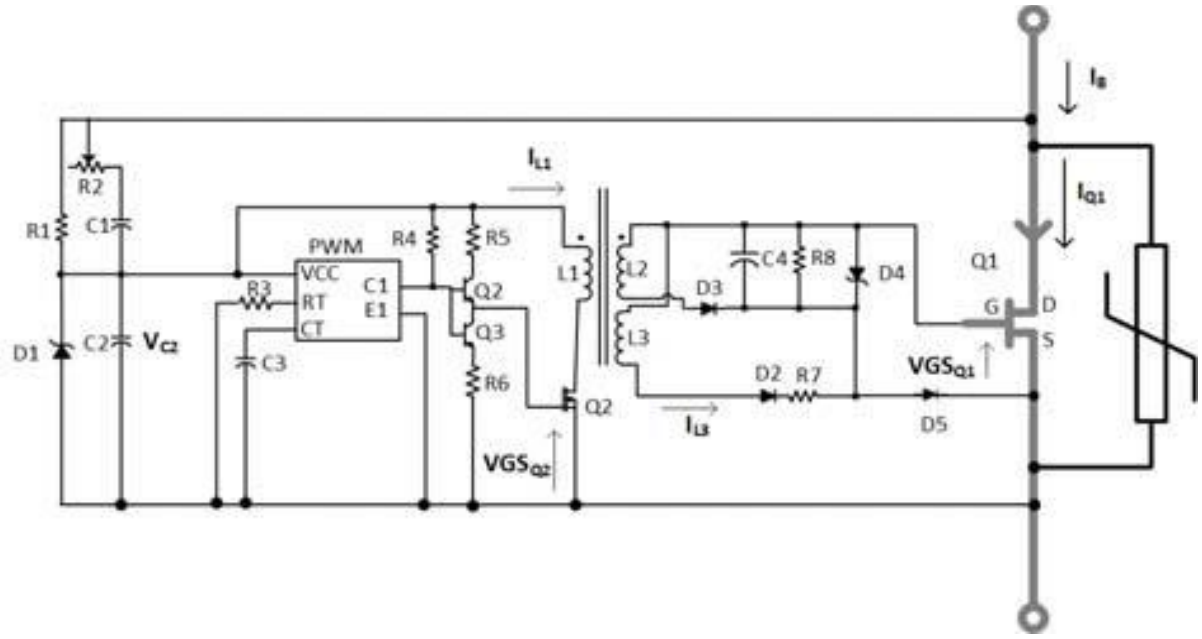

Figure 6-17 – $t0 \leq t < t1$

During initial fault inception, between times t0 and t1, the JFET, Q1, is conducting and voltage begins to build up across C2.

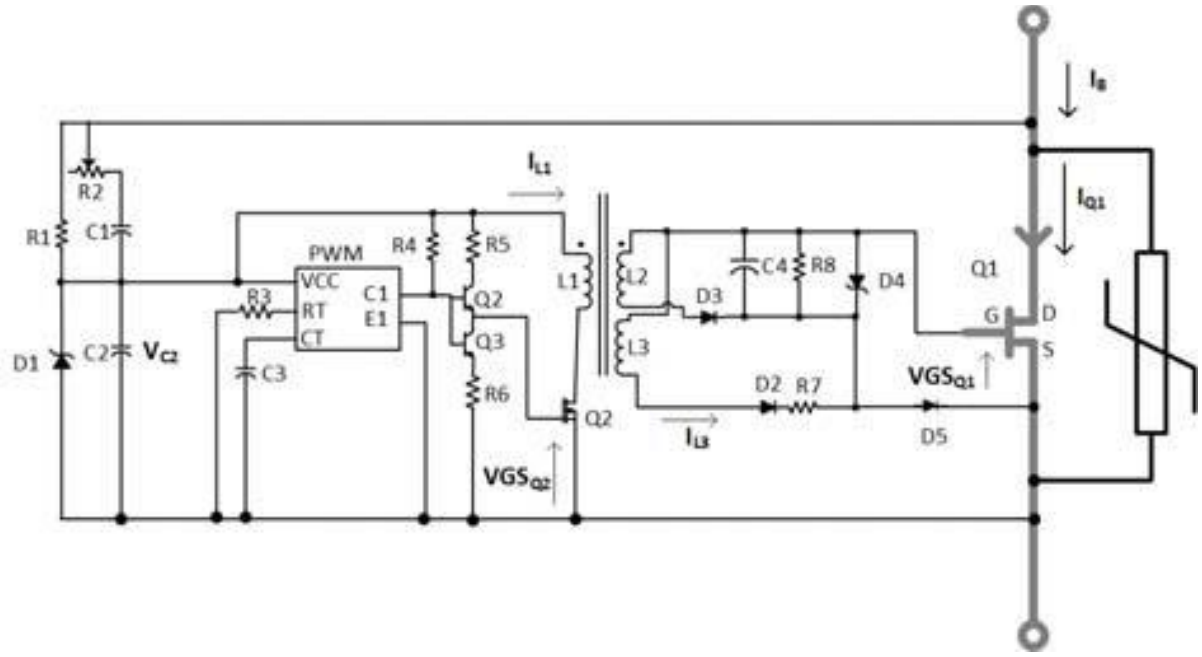

Figure 6-18 – $t1 \leq t < t2$

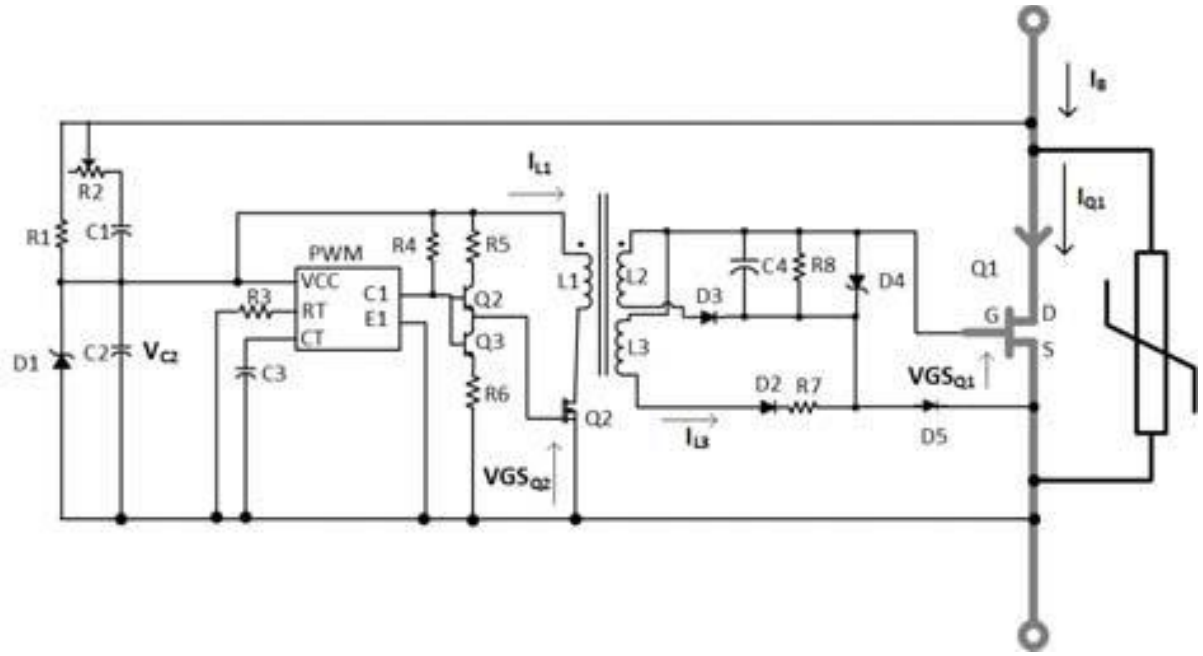

Figure 6-19 – $t_2 \leq t < t_3$

The main path for fault current is through the JFET as shown in Figure 6-17. At time t1, VC2 reaches a sufficient level for the MOSFET Q2 to be gated on and VC2 continues to rise while Q2 provides a path for current build-up through the inductors L1 and L3. The inductors which together with Q2 and D2 comprise an isolated forward converter which builds up a negative voltage from the gate to source of Q1 as shown by the highlighted current paths in Figure 6-18. During this time current through Q1 is dropping. At time t2 the Q1 gate voltage reaches -18V, which is sufficient to turn off JFET Q1. From t2 to t3, VC2 is clamped at the D1 Zener diode voltage. When energy build up into the gate drive circuit stops, L1 and L3 currents drop inducing currents into L2 which provides further hold-up of the Q1 gate voltage shown by the current paths in Figure 6-19. After t3 all remaining fault energy is dissipated through the MOV, which at some point in the commutation sequence, depending upon the amount inductive energy that is stored in the fault path, conducts in order to clamp the voltage across Q1 to safe levels as shown by the highlighted current path in Figure 6-20.

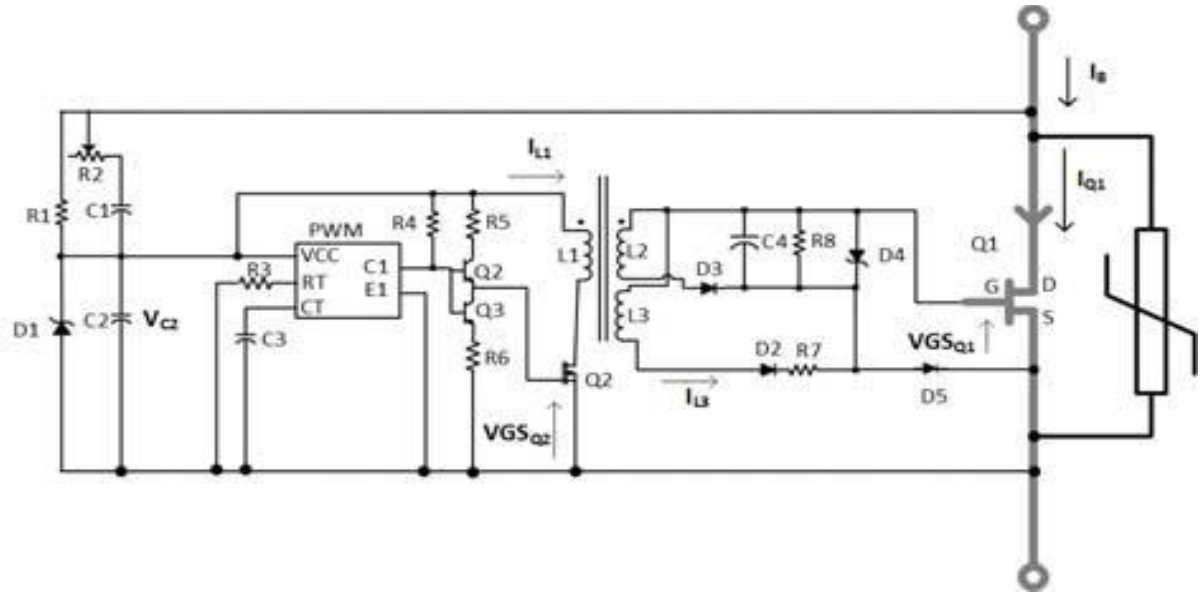

Figure 6-20 – $t>t_3$

6.4 SSCBs in the DC Microgrid

The final stage of the implementation is to integrate the SSCBs into the community DC MG structure. The SSCBs are arranged in a cascaded arrangement, fanning out from a common hub point that makes a shared interface to the utility grid with introduction of solar PV plus battery sources of energy at each home's garage interface to the microgrid as shown in Figure 6-21. The upstream and downstream SSCBs should be coordinated to ensure circuit protection during a short circuit fault power continuity to non-faulted loads.

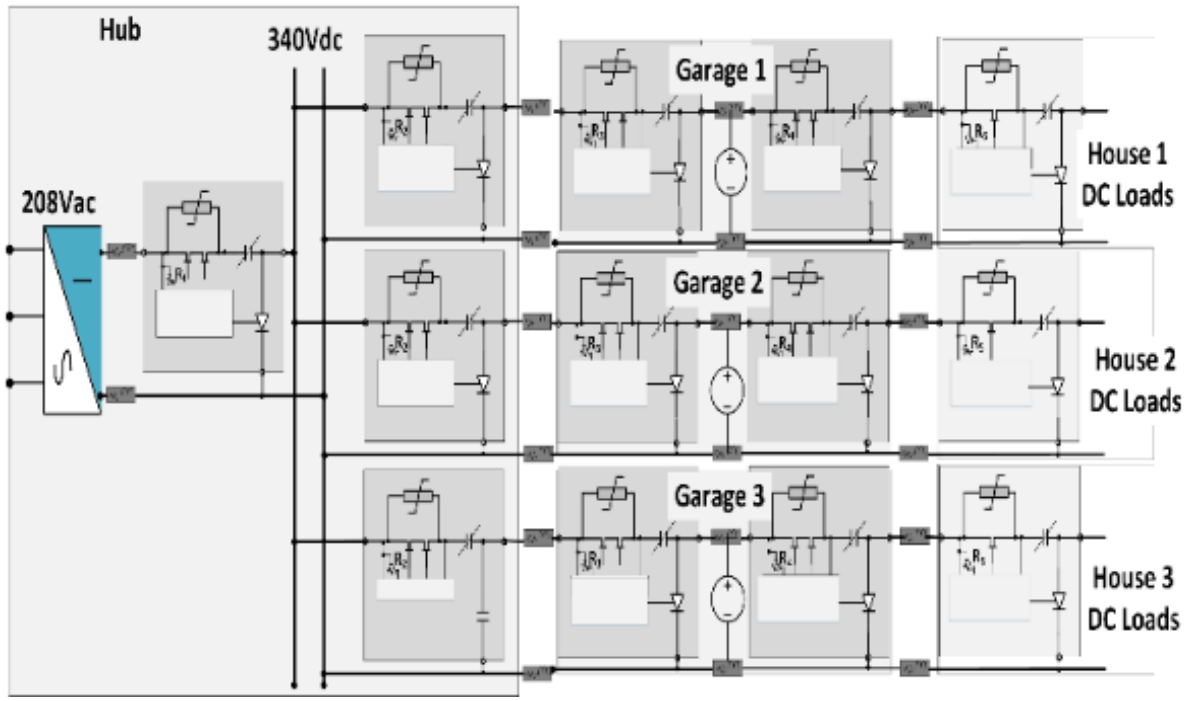

Figure 6-21 – Radially distributed residential DC microgrid structure

Fault coordination is accomplished through a simple variable resistor adjustment. This is done by maneuvering the R2 resistor on the voltage sensor network of the SSCB shown in Figure 6-8. To fulfill coordination, the fault clearing time among the SSCBs in different locations should be different, so the design of the SSCBs need to be modified. During the starting stage, the fault current will charge C2 through the RC network and different parameters for RC network will lead to different charging time. In order to find how does the voltage sensor network affect the charging time, the transfer function for RC network is given by

$$\frac{v_{C2}}{v_{DS}} = \frac{(R1+R2)C1\cdot s+1}{C1C2R1R2\cdot s^2+(C1R1+C1R2+C2R1)\cdot s+1} \qquad \text{Equation 6-10}$$

where VC2 is the voltage across C2, and VDS is the voltage dropped between JFET drain and source terminals. Through this transfer function and aforementioned Equation 6-4, it clearly shows that the value of R2 has significant influence on the charging time. So, different values of

R2 has been applied to test which one can achieve the best coordination. Fault coordination was verified using Matlab/Simulink and LT Spice as shown below.

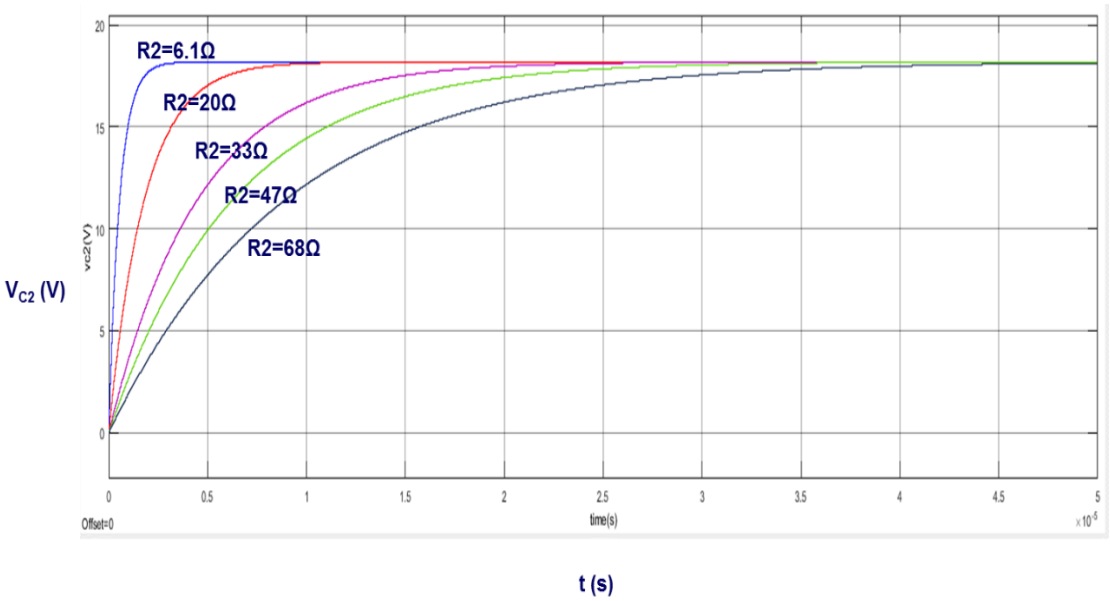

Figure 6-22 – Simulation Results in Matlab

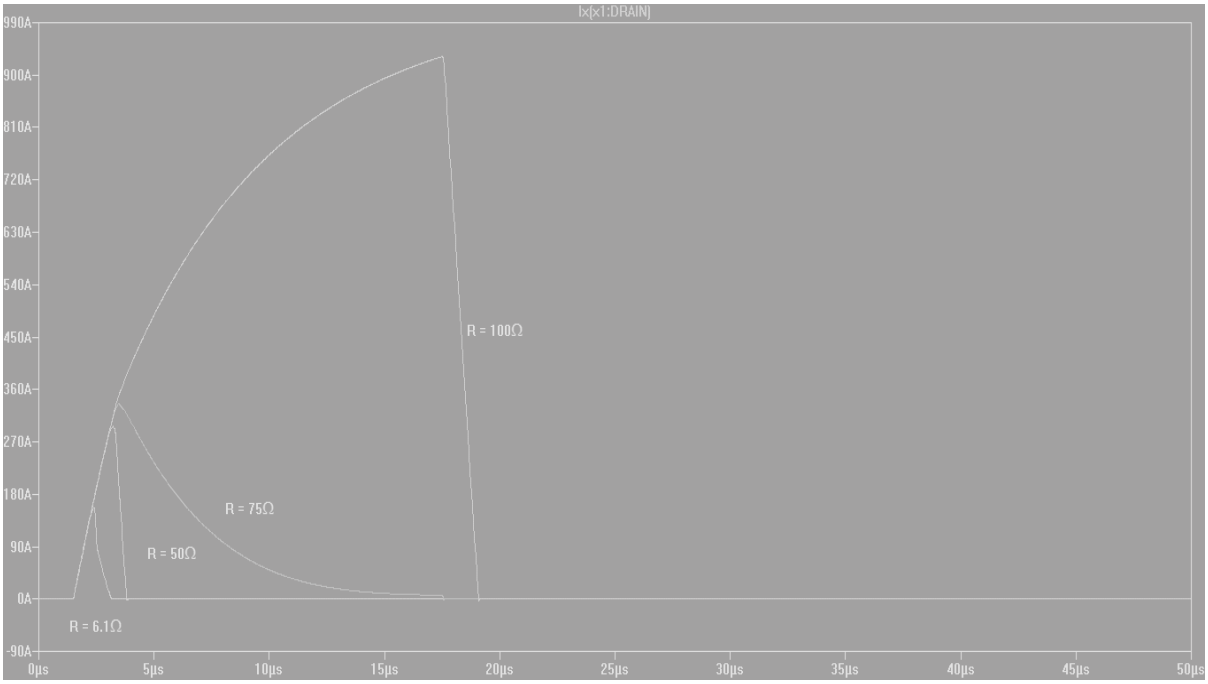

Figure 6-23 – Simulation Results in LT Spice

A real network was built together with a transfer function based network. According to the transfer function and experiences, different values for the R2 have been chosen which are 6.1 Ω, 20 Ω, 33 Ω, 47 Ω and 68 Ω respectively. The simulation results are shown in Figure 6-22. The charging time of VC2 is increasing when the value of R2 is bigger.

The LT Spice model of the SSCB was built and replaced by resistors with values of 6.1 Ω, 50 Ω, 75 Ω and 100 Ω. It can be seen from Figure 6-23 that as the resistance gets higher the time it takes for the current to come down gets longer. This means that if we have the SSCB with the faster response near the fault and the rest elsewhere in the system, we may be able to coordinate the SSCBs to discriminate the faults in our radially distributed network. The graph depicts the time It takes foe the current to get to zero meaning the SSCB to completely be on and not allow any current anymore.

6.5 Fault Characterization

In order to properly design the protective system, it will be important to understand how the SSCB behaves in a realistic large scale simulation of the entire microgrid so that time-trip requirements of protective devices can be established. The results of this fault characterization are then used a criterion against which the proposed SSCB can be tested. The feasibility of the approach is then determined through hardware tests both to establish the time-trip response of the SSCB and to verify the ability of cascaded SSCBs to discriminate faults. Figure 6-24 shows the applied fault locations to be characterized.

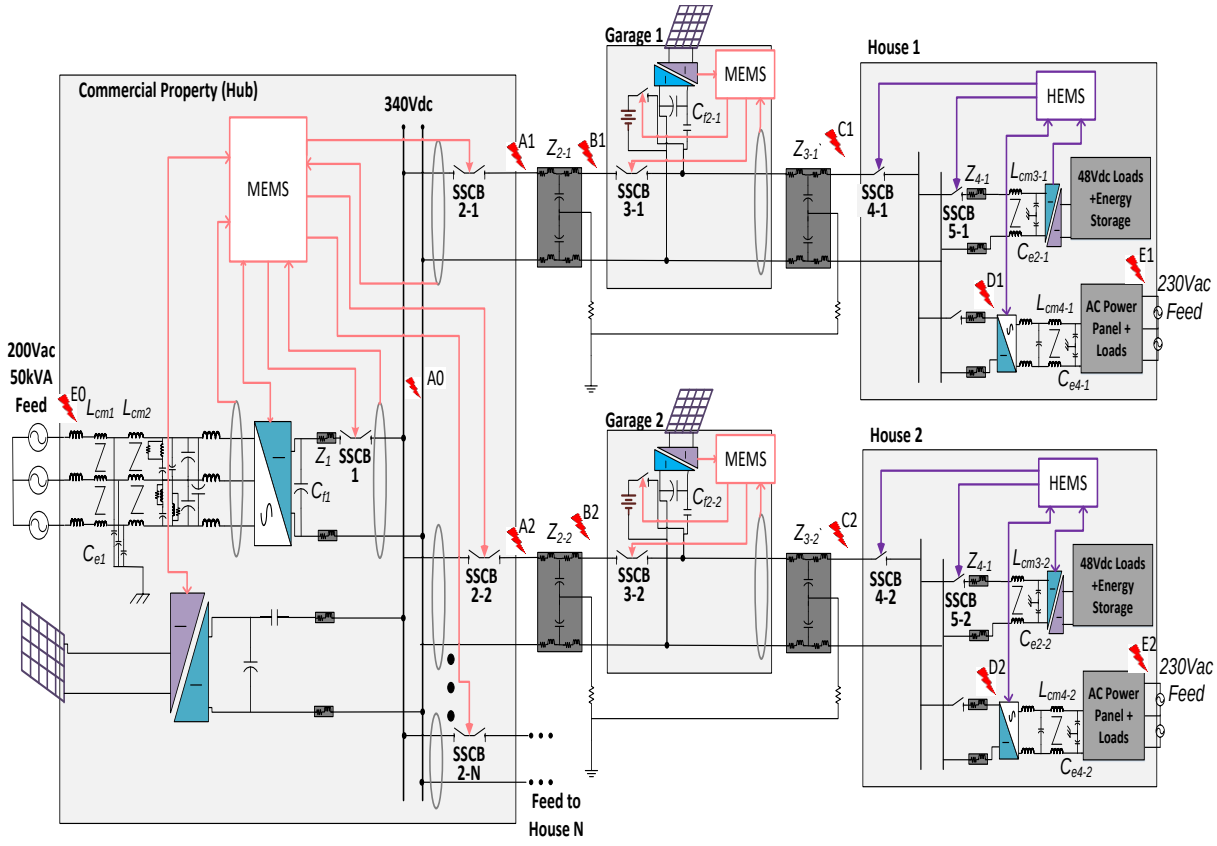

Figure 6-24 – Residential DC microgrid block diagram, with fault locations to be studied

Fault locations A1-D1 represent likely fault scenarios along the longest length of cabling between the hub and a property that is connected to the microgrid. Fault locations A2-D2 represent likely fault scenarios along the shortest length of cabling between the hub and a property. The cable lengths assumed are realistic based on the actual installation described in [4] and cable impedances were calculated based on cable trays within the commercial property (location of the hub) and buried cables from the hub to the associated feed garage and from the garage to the house.

A simulation was implemented using PLECS that includes detailed switching models of the AC to DC converter interfacing the hub to the utility and the DC to DC converters interfacing the microgrid feeds in each house to the DC loads within the houses. As a first step, this paper

establishes the fault characteristics of the radial system feeding out from the hub without the solar PV interfacing DC to DC converters and batteries connected to the microgrid at the hub and the garages. The batteries would establish long term fault clearing capability if the ultra-fast SSCBs do not intervene. However, as will be shown, it will be necessary for the SSCBs to intervene very quickly in order to avoid damage to the equipment. Therefore, the impact of the batteries to the fault characterization will be negligible because their impacts are not seen within the time-frames considered. The PV interfacing DC to DC converters may cause fault current to be sourced from unexpected directions. However, as will be shown, bi-directional and unidirectional SSCBs are applied to the system in order to effectively mitigate these effects. The impact of the PV interfacing converters will be more important when the microgrid is islanded from the grid, i.e. the AC-DC converter inputs are disconnected from the grid or under the E0 fault condition. Also, since power distribution within the houses is both DC and AC, there may be impacts of faults at locations E1 and E2 but these are not considered in this paper. Presently, the intention is to not allow power flow from the microgrid into the household AC loads in order to avoid charges from the utility associated with mixing of PV power with utility power at each home. Therefore, E1 and E2 fault locations are only relevant under conditions when the microgrid is isolated from the house, in which case fault protection within the house will operate using conventional household AC circuit breakers. The only consideration would be the impacts to DC loads (which would then be fed by the AC supplied utility). This last scenario is a special case and will be considered later.

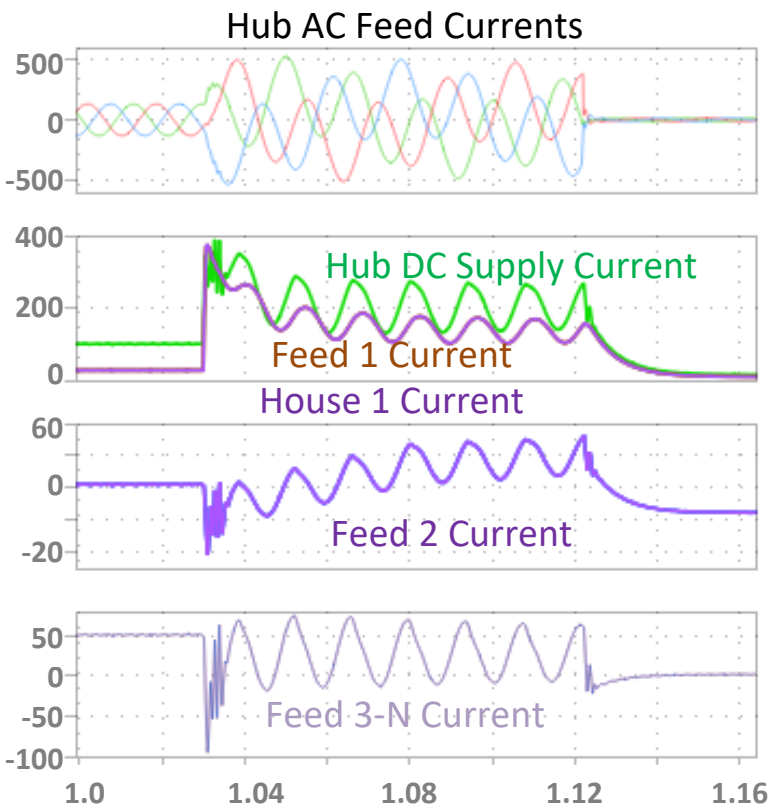

Figure 6-25 – Response to fault at the feed to House 1 (D1)

The AC to DC converter includes input EMI filtering and only a conventional Silicon IGBT-based converter is assumed. Figure 6-25 shows the AC and DC feeder current responses to sudden application of a zero ohm line to line fault applied to the DC bus within House 1. The initial fault current surge comes from the combined impacts of the AC to DC converter output DC filter capacitance, Cf1 and the internal DC link capacitance(s) of the load DC to DC converter(s) within the home. For the purposes of simulation, all DC loads within the Houses are assumed to be applied through a 320V to 48V DC to DC converter. Once the capacitors are discharged into the fault (which occurs in less than 10ms) the AC to DC Converter attempts to limit current into the DC bus unsuccessfully because IGBT forward diodes are commutated on by the incoming AC voltages. After a period of 50ms the AC to DC converter trips off and the

remaining let-through current from the AC fault is through the IGBT forward diodes. Because of the high AC impedances associated with the filter the let-through currents are limited. Therefore, it would be necessary to shunt trip the AC feeder circuit breakers to the AC to AC converter if the fault were not mitigated by some downstream means on the DC bus.

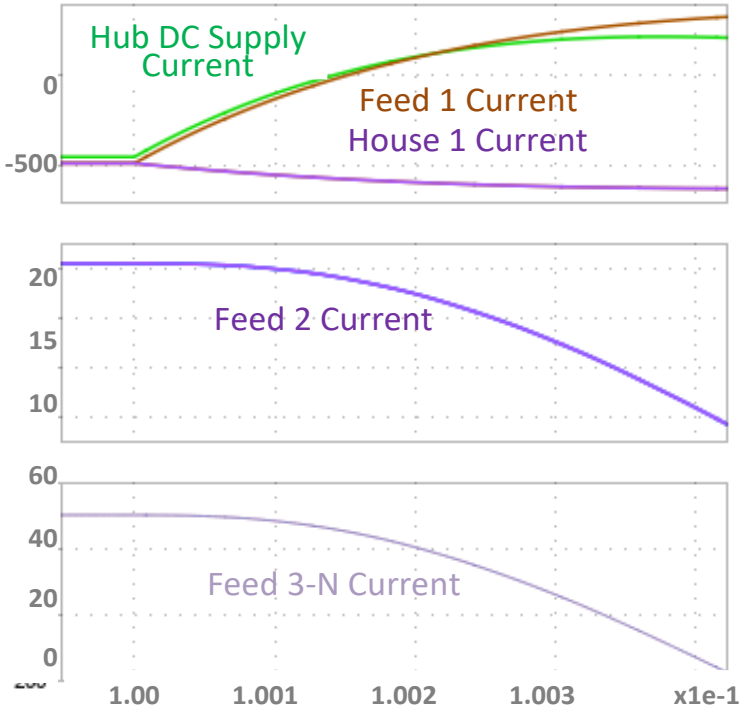

Figure 6-26 – Fault close to the hub building (A1)

The remaining focus is on the first several milliseconds following fault application as described in Figure 6-26 - Figure 6-37. Figure 6-26 - Figure 6-29 shows the DC currents in the system for fault locations A1-D1 and Figure 6-30 - Figure 6-33 for fault locations A2-D2. Faults are only considered on the feeds having the longest and shortest cable lengths of the system, assuming that faults on any other feeds will exhibit characteristics that lie between these two extremes. The impacts of the remaining feeds are simulated as the parallel equivalent of 7 remaining dwellings. As described earlier, 3 of these dwellings are apartments within the commercial property and the remaining are 3 houses clustered around the commercial property and 1 in

between this cluster of properties and the property at the furthest extremity of the neighborhood. In the simulation, the equivalent stored energy of these dwellings back-feeds the fault on either the House 1 or House 2 feed via the feed shown in Figure 6-24 as “Feed to House N”. Prior to fault application, the microgrid is assumed to be drawing nominal power from the hub AC to DC converter (40kW) with that power evenly distributed between the dwellings.

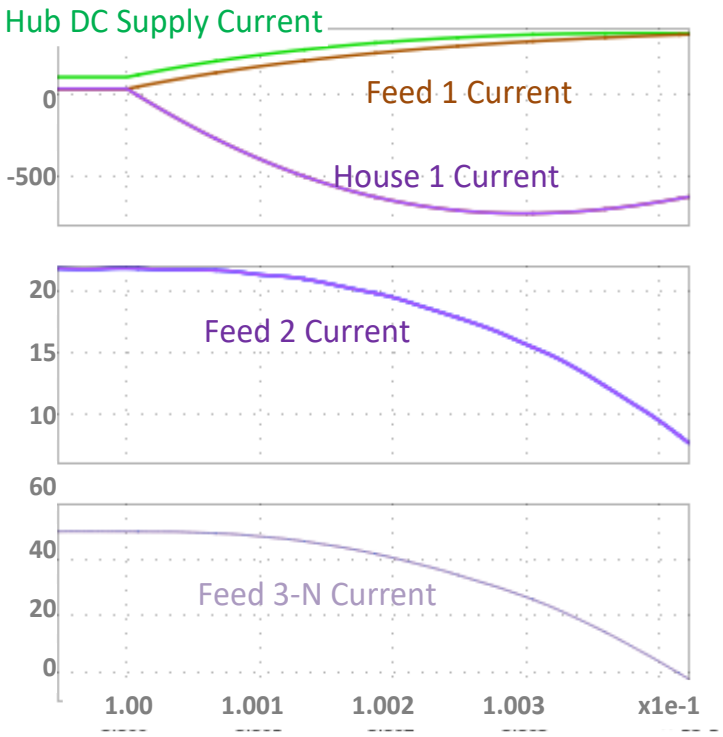

Figure 6-27 – Fault close to the Garage 1 (B1)

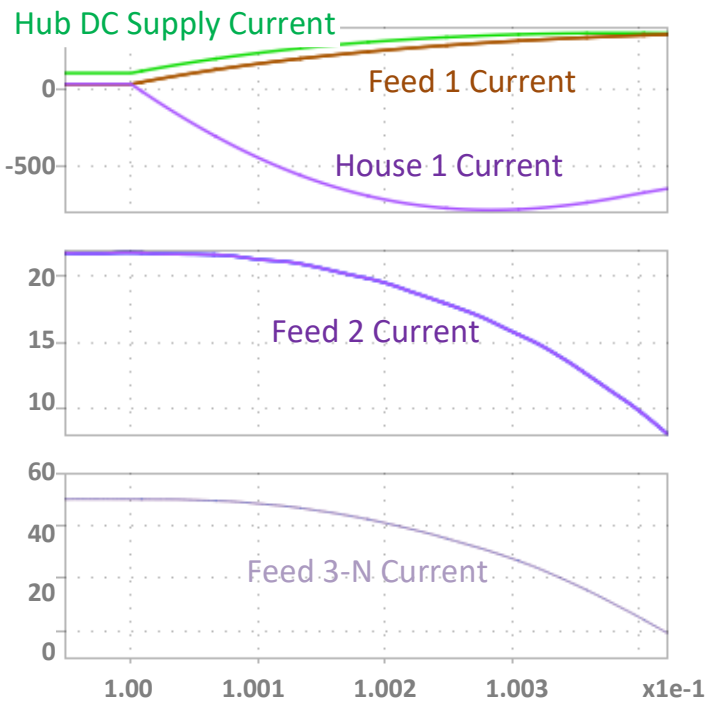

Figure 6-28 – Fault between Garage 1 and House 1 (C1)

The most straightforward behavior is associated with the faults in House 1 (D1) or House 2 (D2) as shown in Figure 6-29(long cable length to House 1) and Figure 6-33 (short cable length to House 2) respectively. The fault current is fed from the hub House 1/2 feed, discharged from the AC to DC converter. The currents shown are the currents that would be measured at the locations of SSCB 1 (Hub DC Supply Current), SSCB 2-1/2 (Feed 1/2 Current), SSCB 4-1/2 (House 1/2 Current). For the D1 fault of Figure 6-29, currents in all House 1 Feed DC SSCBs, except for SSCB 5-1, will be identical, all feeding into the fault at location D1. The fault current will be reduced by current supplied through SSCB 5-1 in the opposite direction being discharged from the House 1 DC to DC Converter input capacitor(s). The currents being supplied from the House 2 Current will add to the House 1 Fault Current, being discharged from the House 2 DC to DC Converter input capacitor(s) into fault D1. For the D2 fault of Figure 6-33, currents in all House 2 Feed DC SSCBs, except for SSCB 5-2, will be identical, all feeding into the fault at

location D1. The fault current will be reduced by current supplied through SSCB 5-2 in the opposite direction being discharged from the House 2 DC to DC Converter input capacitor(s). The currents being supplied from the House 1 Current will add to the House 2 Fault Current, being discharged from the House 1 DC to DC Converter input capacitor(s) into fault D2. Because of the short cable length, the surge current into the fault is significantly higher with an associated higher di/dt. This represents the worst case scenario driving the SSCB requirements.

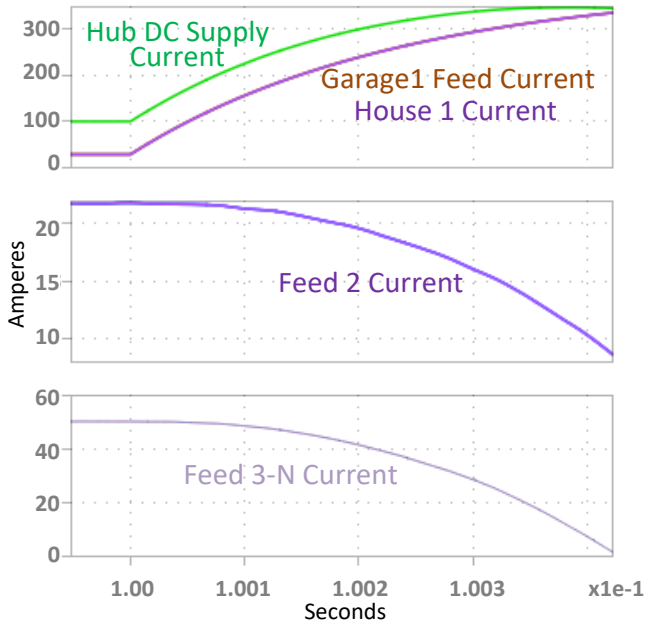

Figure 6-29 – Fault inside of House 2 (D1)

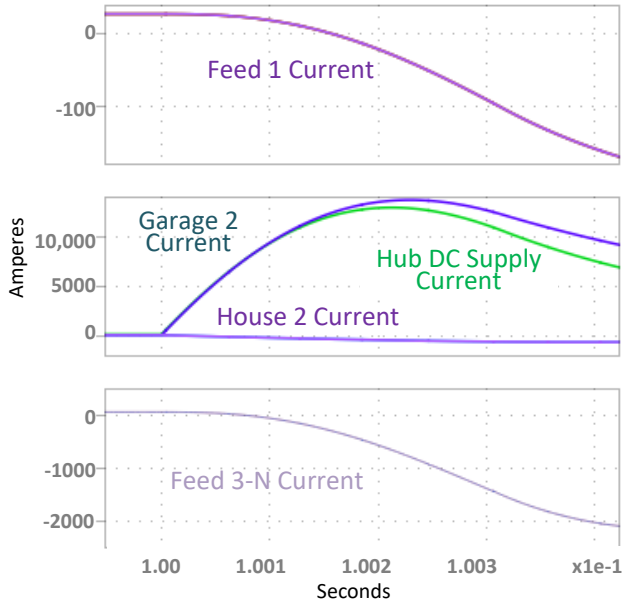

Figure 6-30 – Fault close to the hub building (A2)

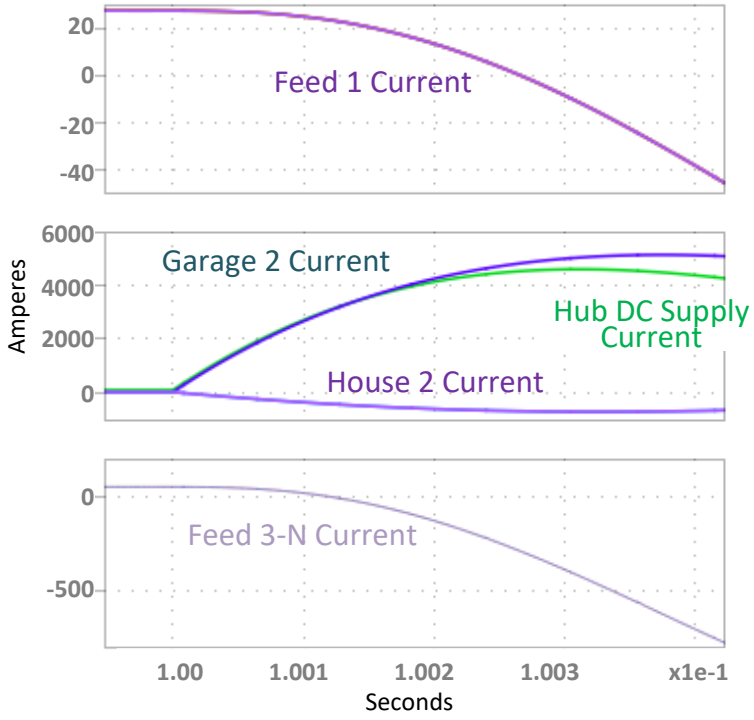

Figure 6-31 – Fault close to the Garage 2 (B2)

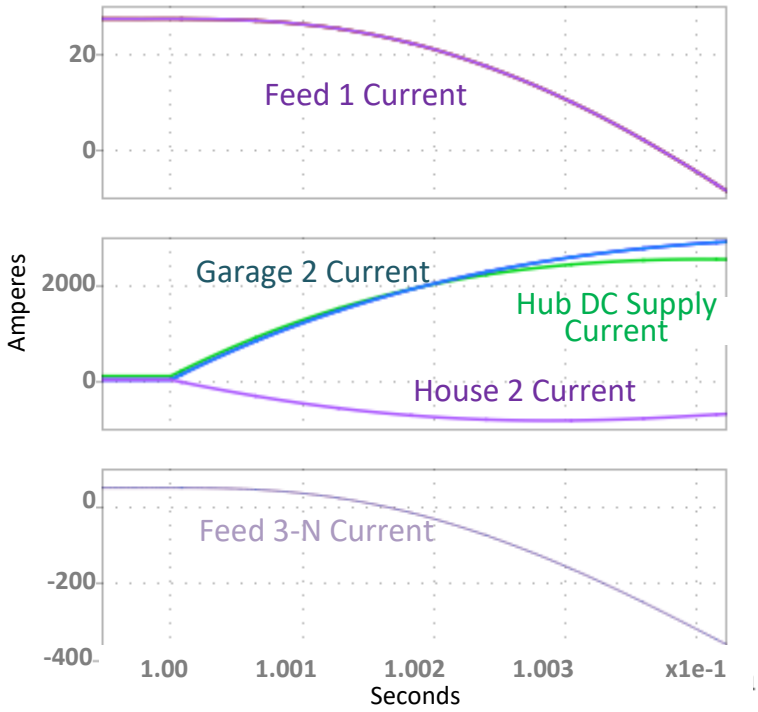

Figure 6-32 – Fault between Garage 2 and House 2 (C2)

Figure 6-34 shows the entire time span for the fault currents going through the House 1 Feed for two fault scenarios, C1 and D1. Similarly, Figure 6-35 shows fault currents going through the House 2 Feed for C2 and D2 faults. The required behavior for fault discrimination will be tripping of the circuit breakers in series with the main feed to the house trip for faults D1 and D2, leaving the status of all circuit breakers upstream unchanged. The required behavior for faults C1 and C2 will be tripping of circuit breakers in the associated garage feeds to the house. The time trip curves of appropriately sized mechanical molded case circuit breakers superimposed on these curves for upstream (i.e. at Garage 1/2) and downstream (i.e. at the main feed inside House 1/2) are superimposed on these curves. For the C1 and D1 faults in Figure 6-34, neither circuit breaker will trip. On the other hand, for the D2 fault of Figure 6-35 it is likely that both circuit breakers will trip due to the instantaneous magnetic trip mechanisms. From the expanded views of Figure 6-34 and Figure 6-35 fault currents for both fault scenarios cannot be distinguished.

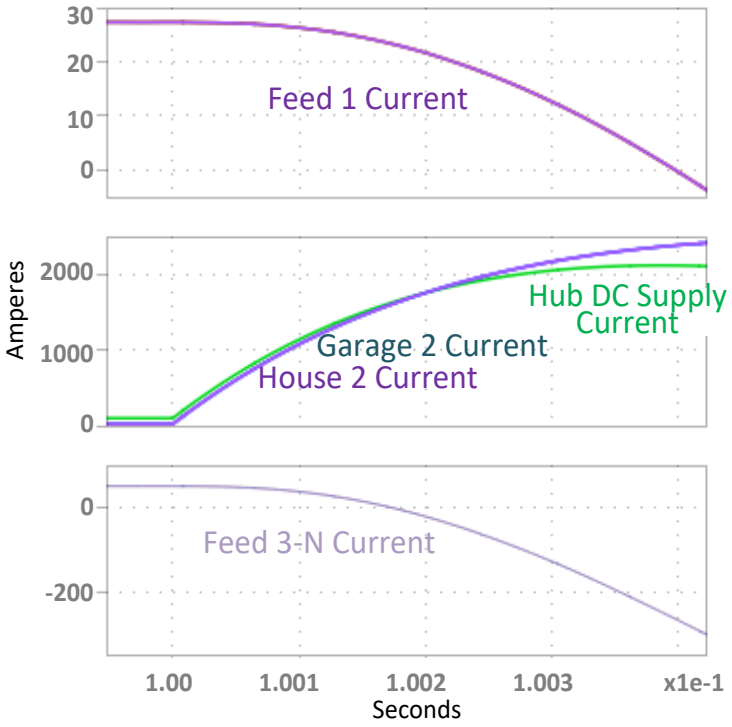

Figure 6-33 – Fault inside of House 2 (D2)

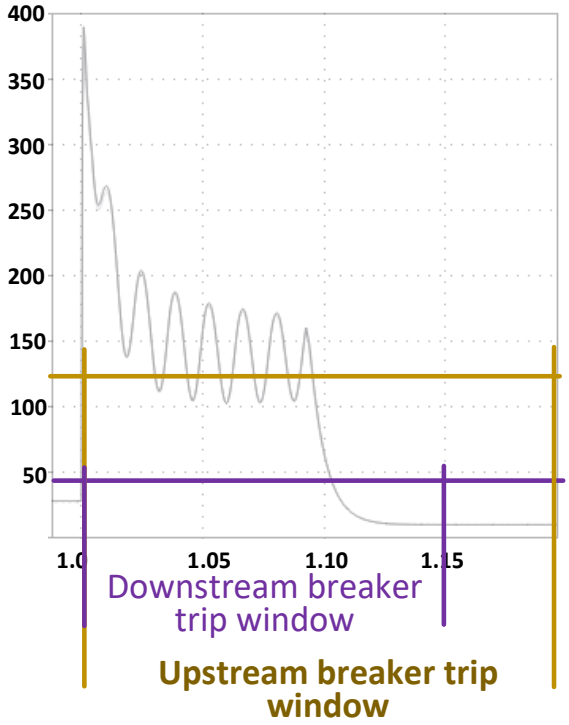

Figure 6-34 – Long cable length to fault location (C1, D1)

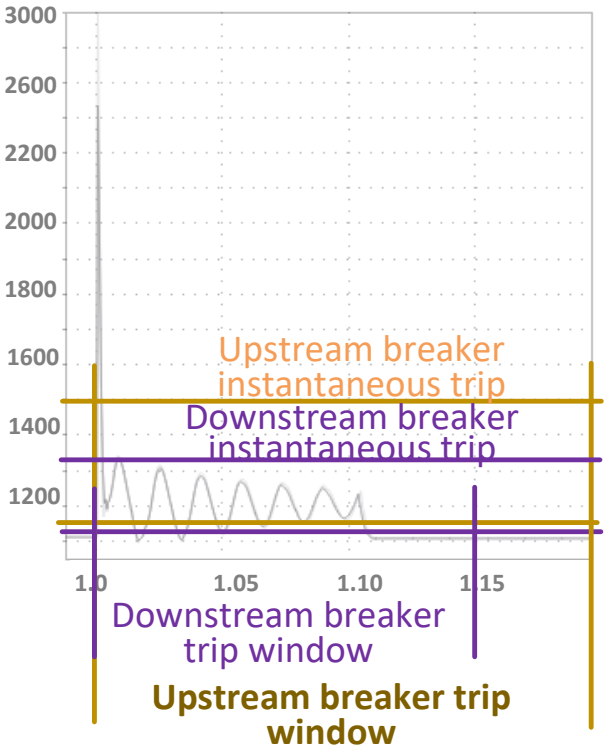

Figure 6-35 – Short cable length to fault location (C2, D2)

The possibility for fault discrimination is only understood by zooming into currents over the first 1-5ms as shown in Figure 6-36 and Figure 6-37. A viable approach is to utilize identical circuit breakers at corresponding positions in each feed, i.e. SSCB 2-x, SSCB 3-x, SSCB 4-x, SSCB 5-x. Therefore, the requirements for the SSCBs should be derived from the highest di/dt scenario of House 2 feeds shown in Figure 6-37. A feasible approach will be to set an instantaneous trip level for the downstream circuit breaker that is lower than a trip level for the upstream circuit breaker. If, for example, the downstream trip level is set to 150A and the downstream trip level is set to 250A, a SSCB with the capability of taking action to drive fault current to zero with a latency of $\Delta T<10\mu$seconds.

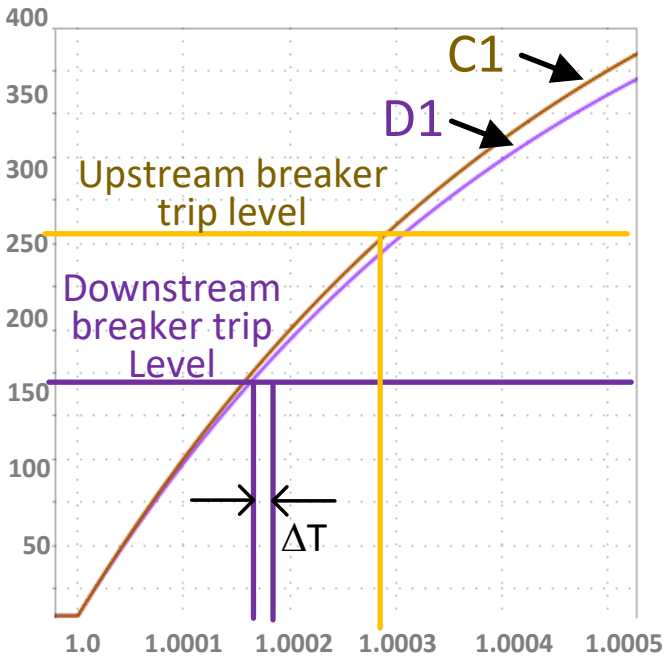

Figure 6-36 – Long cable length to fault location (D1)

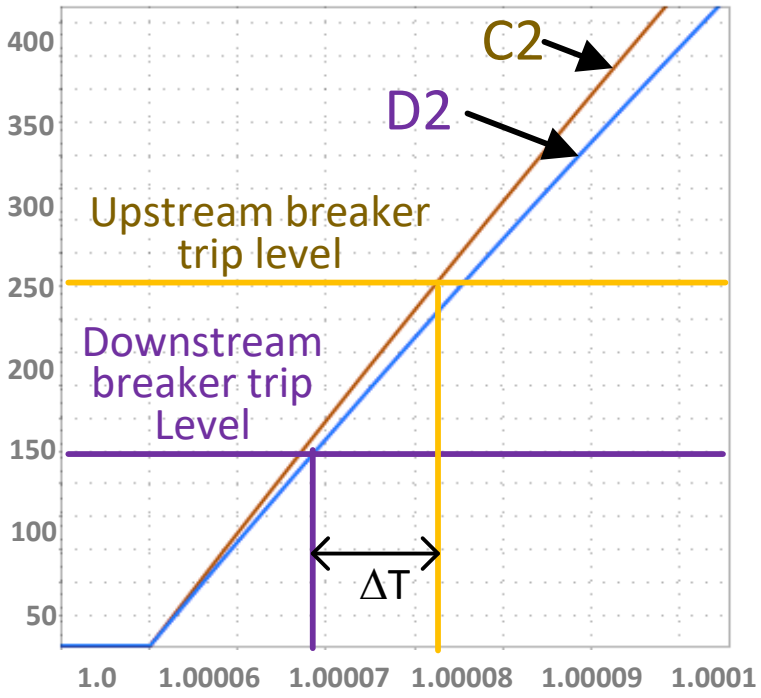

Figure 6-37 – Short cable length to fault location (D2)

A bi-directional version of the JFET-based SSCB is described in [71]. So far, the unidirectional SSCB described blocks current in only one direction. This means that for the cases of faults A1-C1 and A2-C2 of Figure 6-26 - Figure 6-28 and Figure 6-30 - Figure 6-32 let-through current from the house feeding a fault occurring between house and garage or between garage and hub in the direction of fault location outside of the house will not cause the SSCB(s) inside the houses to trip. For SSCBs in the garage and hub, it is desirable to allow tripping in either direction in order to fully isolate the fault. Therefore, bi-directional SSCBs are installed in these locations as indicated in Figure 6-21. The only concern is that tripping may occur in adjacent branches, however the results of Figure 6-26 - Figure 6-33 indicate that di/dt is lower in the branches adjacent to the fault.

6.5 Summary

In this chapter the protection system was implemented in a bottoms up approach. The details about the SiC JFET was presented and the protection system implementation was built off of that as it scaled up. The SSCB was defined and its various modes and topologies were discussed. The behavioral analysis of the SSCB with the most used topology i.e., Forward-Flyback was conducted and presented. The whole protective design of the DC Microgrid structure with the SSCBs integrated was shown and finally, a fault characterization simulation to bring it all together was discussed and explained.

Chapter 7 Simulation and Experimental Validation

This chapter describes the operation of the SSCB during sudden inception of a line to line short circuit, validated by both simulation and experimental results, and the capabilities of the SSCB to perform coordination to discriminate faults in a radially distributed network. The Single SSCB case is first presented followed by multiple ones to show and validate the discrimination abilities.

7.1 Single SSCB Operation

The schematic for studying and verifying the short circuit operation of the SSCB is as given in Figure 7-1. This setup will be used to validate the SSCB. The Variable DC Supply will charge the capacitor initially and then the solid state switch is flipped to apply a sudden fault to test the SSCB. The simulation is done in LT Spice and the experimental validation is done and the results are presented in this section. Li and L2 are cable inductances to try to model for the wires.

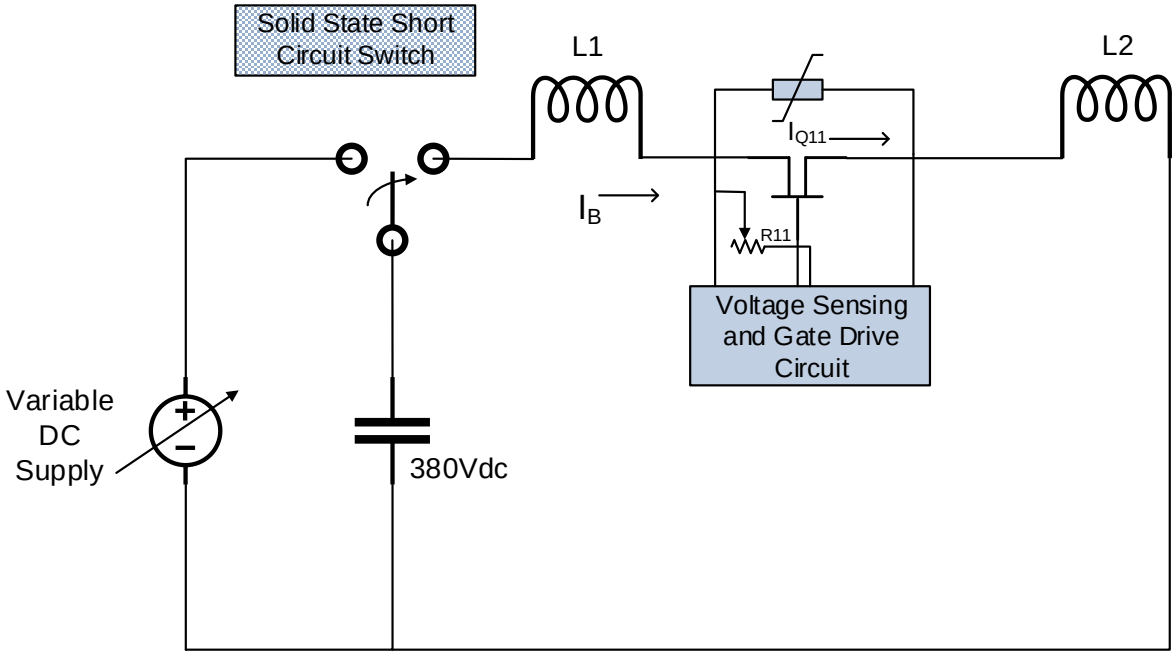

Figure 7-1 – Single SSCB Schematic

7.1.1 Simulation

The SSCB is built from the SiC JFET as mentioned in the previous chapter. The schematic of the SSCB was introduced in Figure 6-7. The simulations and the tests in this section will be done on a unidirectional SSCB with the Forward-Flyback configuration. The LT Spice model for the SSCB schematic given in the previous diagram is as given in Figure 7-2.

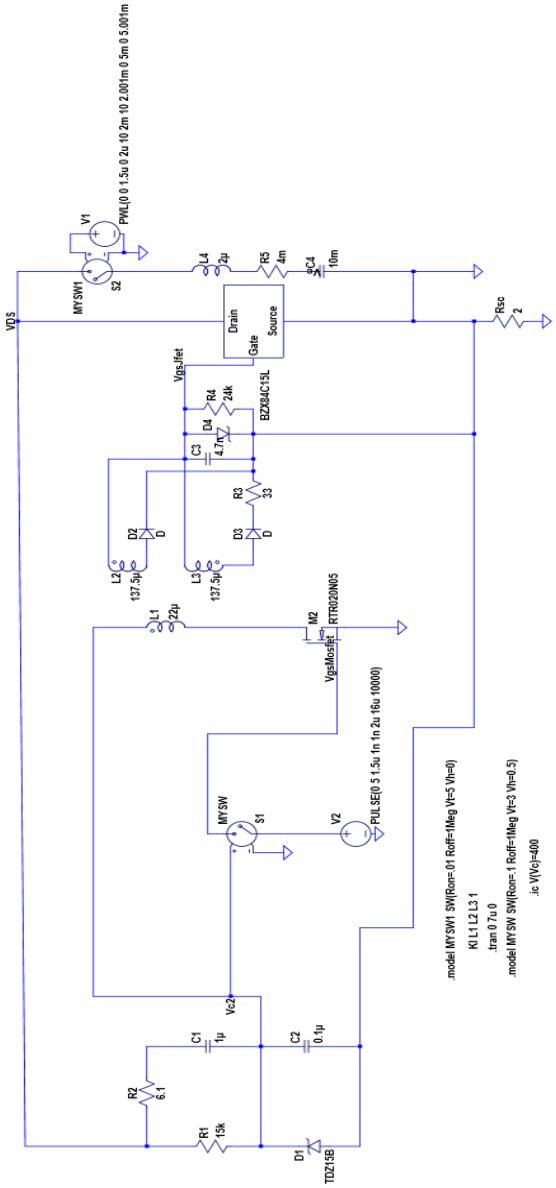

Figure 7-2 – Single SSCB Simulation

There is a disclaimer needed to be made about the LT Spice simulation methods used in this chapter. The SSCB has a TL494 chip to provide the PWM when the threshold voltage of the capacitor C2 goes over 3V and an MOV to suppress the voltage across the JFET so we are able to keep the SiC JFET safe in terms of the voltage across the device albeit the limit being 1200V. These two components are not available on LT Spice and could not be modeled exactly like the SSCB operation. The alternative used was a voltage controlled pulse generator which generates pulses at the frequency of the PWM and the MOV was completely ignored because the mathematical model tried during the simulation was not able to handle such rapid changes in the voltage with respect to time.

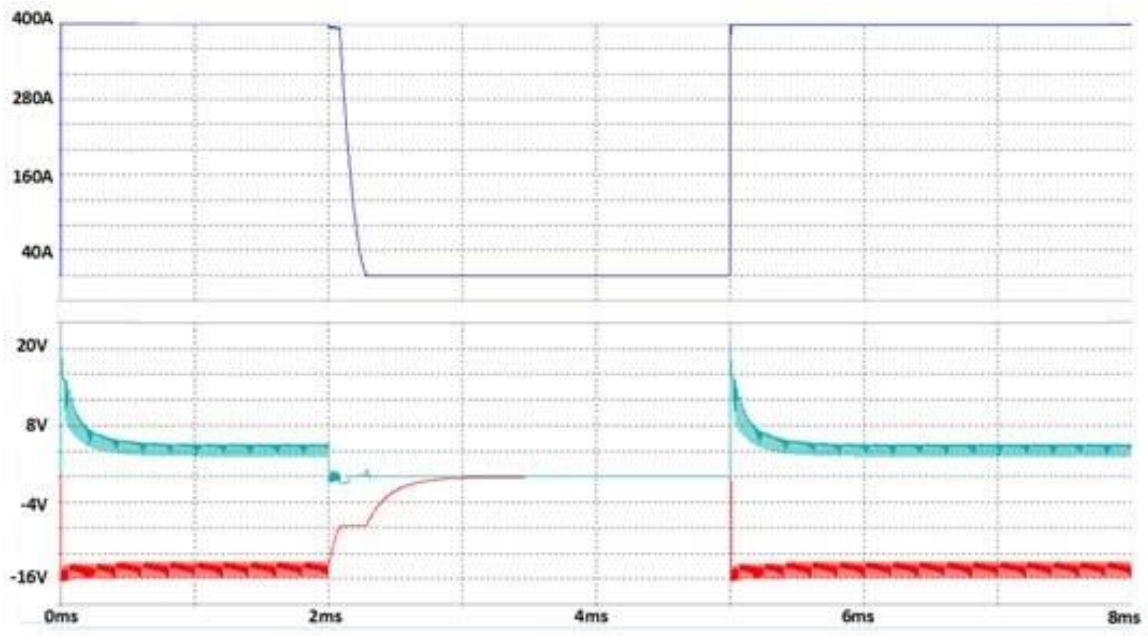

Figure 7-3 –Simulation of repetitive fault application and removal

The simulation results for the single SSCB is as shown in Figure 7-3 –Simulation of repetitive fault application and removal.The blue graph represents the short circuit voltage across the Drain and Source of the SiC JFET. The DC voltage through the capacitor was set to be 400V and hence the maximum value in the graph is as such. The green waveform represents the gate voltage of the

MOSFET feeding the isolated DC/DC converter. The waveform of interest is the one in the red, that is the Gate to Source Voltage across the SiC JFET, that value should be less that about -7V or so for the JFET to act and turn off as that is the threshold voltage value for the JFET. As seen in the figure, the red waveform is very close to -16V which means that the fault current was seen and that made sure the PWM turned on the isolated DC/DC converter to activate the JFET. The simulation shows that when the fault was removed the JFET goes back to zero and when the fault is applied again after sometime the JFET once again turns off.

7.1.2 Experimental Validation

The hardware implementation is shown in Figure 7-4 –Experimental Hardware Setup for Single SSCB, where only one solid state short circuit switch was implemented. The AC line was used to generate a DC bus through a rectifier and it was fed to the Capacitor through relay switched as indicated in the figure. The capacitor is connected to the SSCB switch through relays. The flipping of the switch then indicates the short circuit being applied to the switch through a Rheostat. The rheostat is used to limit the current through to the SSCB switch once the capacitor is connected. Rheostat resistance will be progressively reduced through subsequent tests in order to present a near zero-ohm fault to the system. Figure 7-5 shows the close up of the SSCB switch used in the experiment.

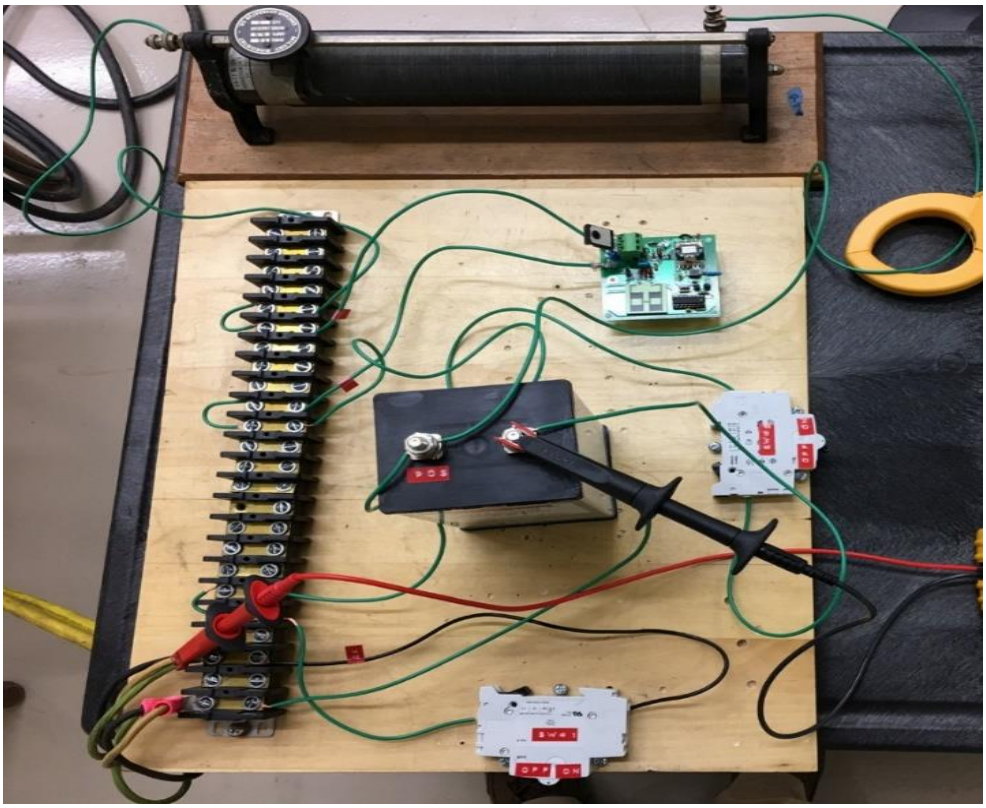

Figure 7-4 –Experimental Hardware Setup for Single SSCB

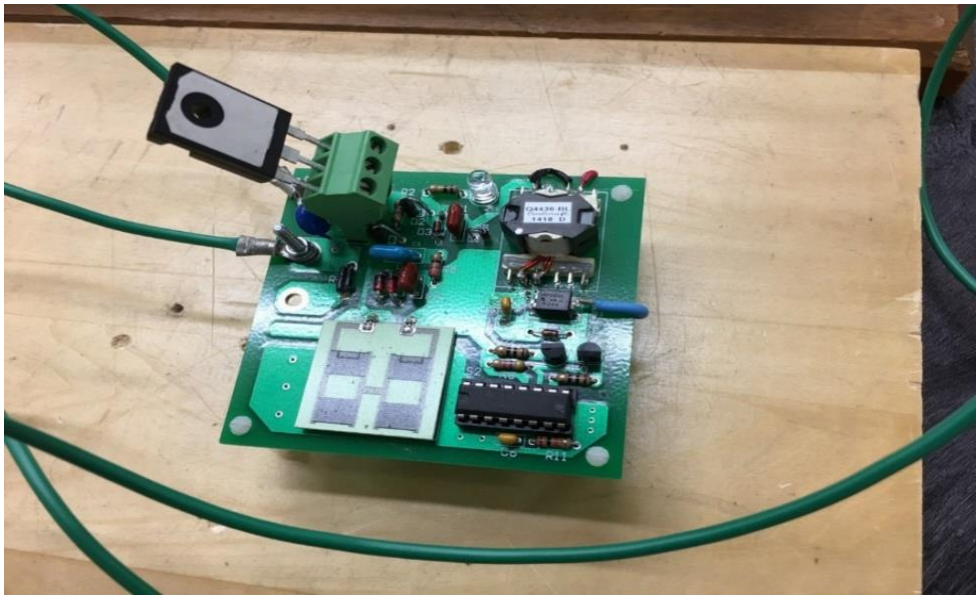

Figure 7-5 –Single SSCB Board

The result of the hardware tests are presented in Figure 7-6 and Figure 7-7. There were two tests which were conducted, first one was a 100Vdc short circuit which was applied to the Switch and next up 200Vdc short circuit fault was applied to the SSCB switch. Figure 7-6 shows the waveforms in the scope for the 100Vdc test. The blue line in the graph is the capacitor voltage, yellow line is the voltage across the Drain to Source of the JFET, green line is the Drain current flowing from the drain to source when the fault is present and the pink line is the gate to source voltage of the JFET. As seen, the fault is applied by changing the position of the switch on the capacitor from charging to discharging. The moment the capacitor starts to discharge the SSCB device feeds off of the charge and works to turn the JFET off by applying a high negative bias to the Gate to Source Voltage of the JFET. The rheostat was set to about 1.3□ while this test was conducted and hence the current measures to about 100A on the scope. It should be noted that once the current reaches a high level the SSCB biases the JFET driving down the drain current in order to mitigate the fault. This occurs within a couple of microseconds, which is significantly faster than what is possible with conventional electromechanical circuit breakers and SSCBs which rely upon current feedback to detect a fault and turn off the gate voltage to normally off devices. Figure 7-7 presents the results of the same tests conducted at about 200Vdc and results seem to be consistent and they match the simulations thereby providing validation of the simulated circuit performance.

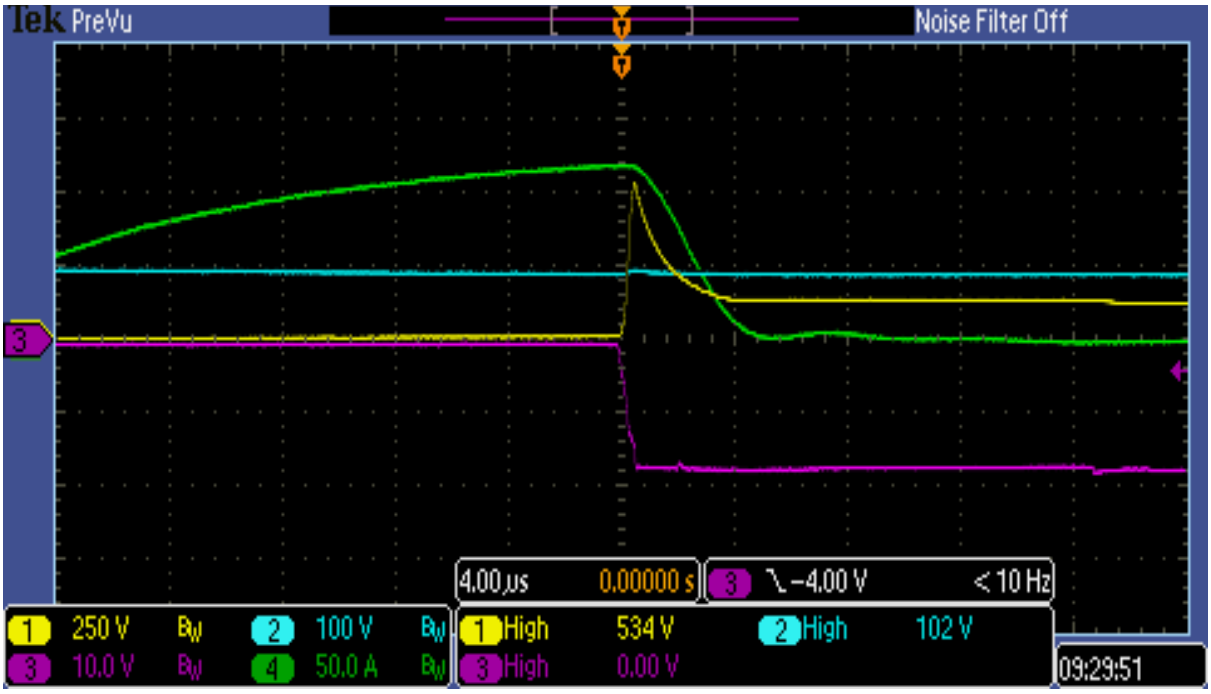

Figure 7-6 – 100VDC on the Capacitor. Ch 1(VDS) - 250V/Div, Ch 2(Vdc) – 100V/Div, Ch 3(VGS) – 10V/Div and Ch 4(IDS) 50A/Div

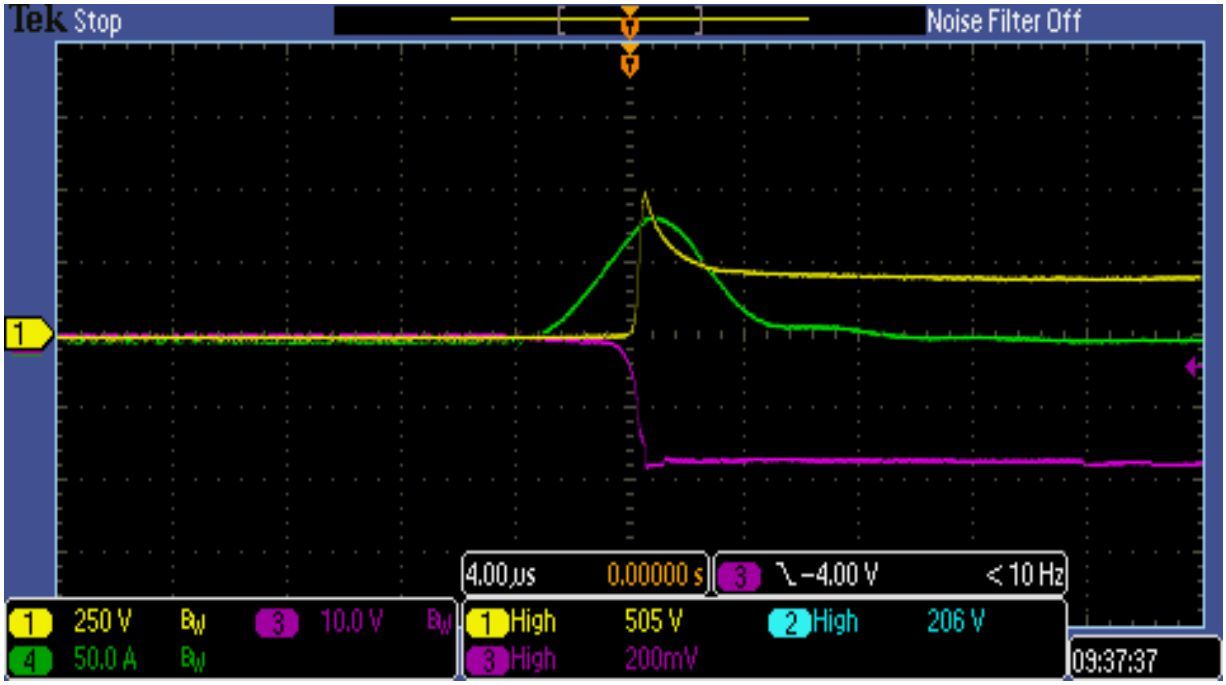

Figure 7-7 – 200VDC on the Capacitor. Ch 1(VDS) - 250V/Div, Ch 2(VGS) – 10V/Div and Ch 3(IDS) 50A/Div.

For the single JFET case, thermal effects on the JFET during operation were considered. An FLIR thermal camera was used to capture the thermal image of the JFET (circled in red) as shown in Figure 7-8. The JFET is in the center of the picture with a little hole in it, the JFET was initially heated before the fault was injected in the system and the temperature data of the JFET at that time was captured and is show in Figure 7-9 . The little blip at about 750 on the x-axis is when the fault was applied. It can be seen that there was no significant impact on the temperature variation across the JFET body and case while the fault was applied to the system and high amount of current was flowing through the JFET itself. This behavior can be attributed to the fact that the JFET had such a large amount of current go through it in a very short span of time before it opened and forced the current to zero, it is in the order of microseconds and hence it was not enough time to develop a significant level of heat spreading It is impossible to determine from this result the impact of the transient change in temperature from case to junction. However, this result does show that a sudden overcurrent transient does not contribute to average heating of the device.

Figure 7-8 – Single JFET Thermal Image

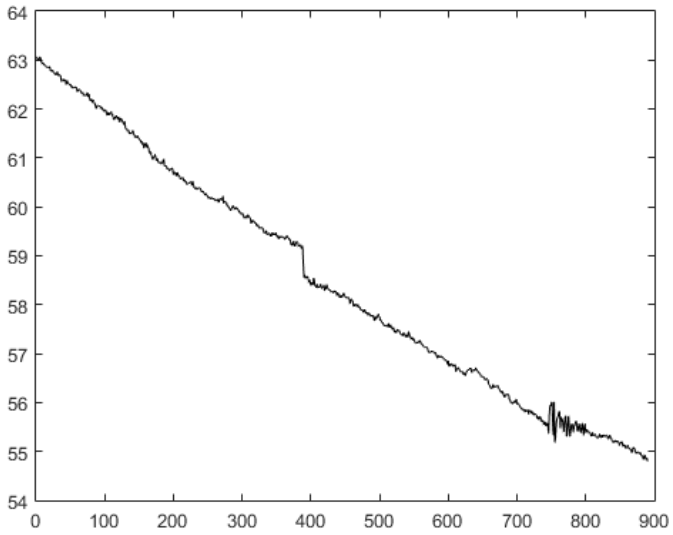

Figure 7-9 – Single JFET Thermal Data.

7.2 Fault Discrimination – Two SSCB Case

The schematic for the simulation with two SSCBs in series is as given in Figure 7-10. The additional L3 in the diagram is again the cable inductance. The same SSCB from the previous section is used and the difference in this case will be that each of the SSCBs will have a different resistor. The first one shows R11 and the other R12, this is done to be able to coordinate so the faults can be discriminated. The higher the value of the resistance the more time it will take to shut off so we want the device with a small constant i.e., less resistance to be closer to the fault so the others in the circuit do not have to turn off.

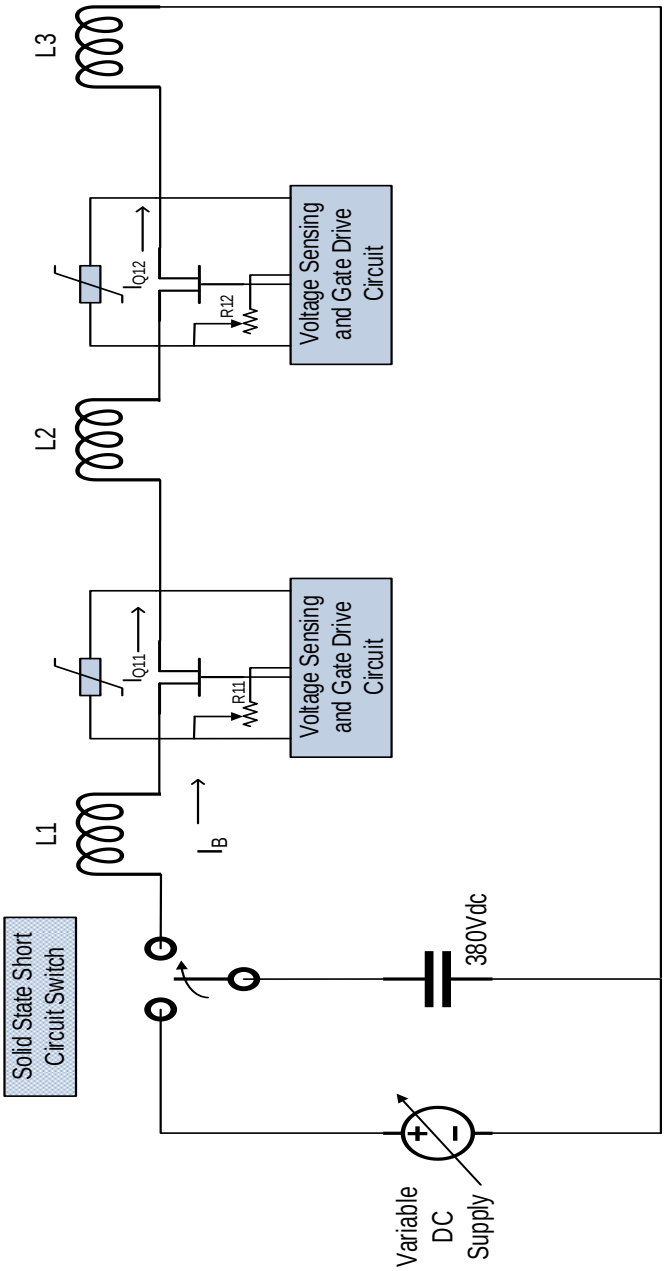

Figure 7-10 – Double SSCB Schematic

7.2.1 Simulation

The LT Spice simulation for this part is as given in Figure 7-11. The same set up and approach like the first case is followed. This time though the interest is to see which JFET turns off and which does not. The results of the simulation are given in Figure 7-12.

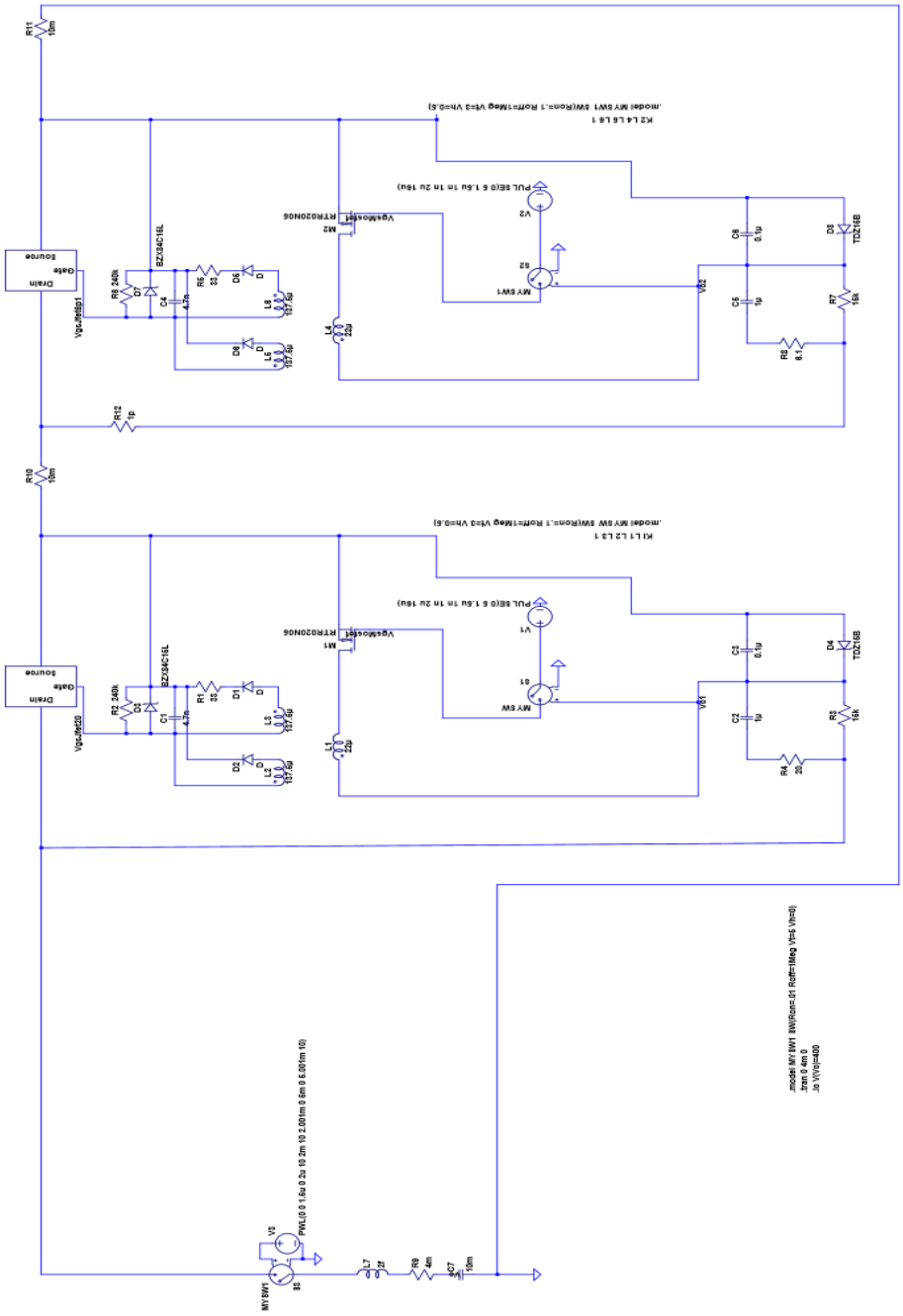

Figure 7-11 – Double SSCB Simulation

The operation of two cascaded unidirectional devices was simulated in LT Spice using a validated model of the system where the tuning resistor values R11 and R12 are 20 □ and 8 □ respectively. Simulated results in Figure 7-12 show that the currents in the cascaded devices,

IQ11 and IQ12, are essentially indistinguishable. However, the gate voltage of the upstream device, VGS11, (furthest away from the simulated fault location) never reaches a value sufficient enough to gate off the associated device Q11 while gate voltage, VGS12, associated with Q12 closest to the short circuit location reaches the threshold voltage of -18V thereby fully gating off Q12. These results indicate that the SSCBs can successfully discriminate between such that the SSCB closest to the fault removes current from the fault while the upstream SSCB remains gated on.

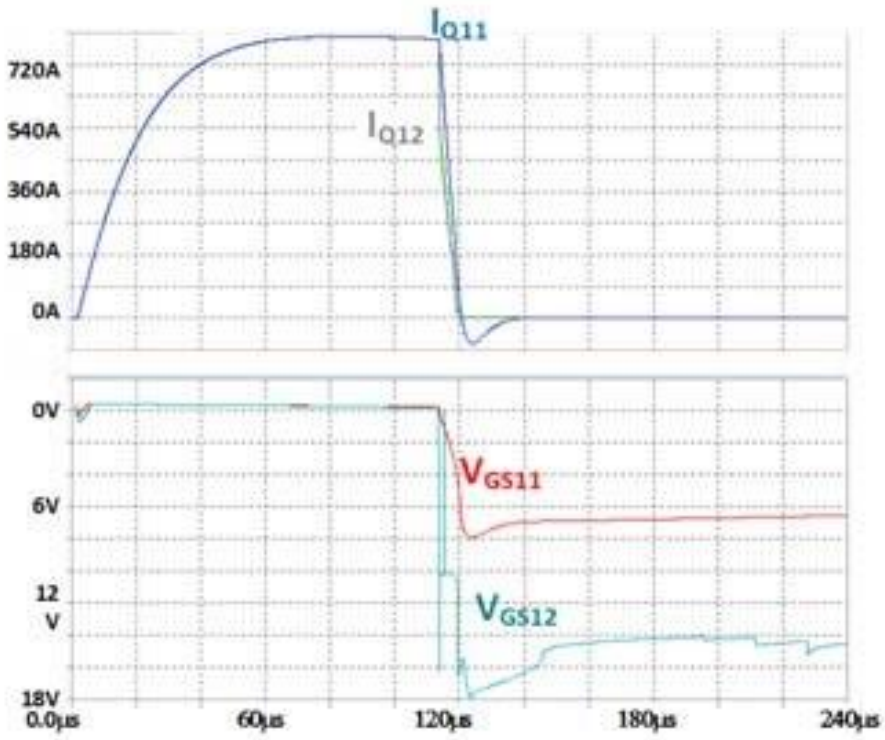

Figure 7-12 – Simulation of JFET currents and gate voltages for two cascaded devices

7.2.2 Experimental Validation

The experimental results for the cascaded two SSCB test are as given in Figure 7-13 and Figure 7-14. The outputs are captured in two scopes as each of the scopes could only take up to four channels and there was a necessity to capture the VGS and VDS of both the JFETs and the IDS values of them so the observation of discrimination and the coordination is possible.

In order to verify that the required timing and discrimination can be achieved in hardware with the proposed solution, two of the JFETs plus voltage sensing and drivers were connected in series and tested in the lab. A capacitor was charged up while not connected to the series arrangement. Then the capacitor was discharged into the two series SSCBs into a short circuit. So far, initial tests were performed without heat sinking the JFETs, so it was necessary to limit the fault current through a small series resistance of one ohm and the test was performed with a reduced voltage of 100V. The SSCB closest to fault was had R2=6.1Ω, while the SSCB furthest from the fault had R2=1kΩ. The experimental results are shown in Figure 7-13 and Figure 7-14. These results demonstrate successfully two important features. First of all, the SSCB is capable of driving current of 150A to zero in 6μs. Secondly, the V_{GS} of the upstream SSCB, with R2=1kΩ, did not reach the level of -16V required for turn-off and, therefore, continued to conduct current while the downstream SSCB drove the current to zero. These tests were performed with approximately 3 m of cable between the charged capacitor and the devices under test. This amount of inductance is significantly lower than is expected in the final applications.

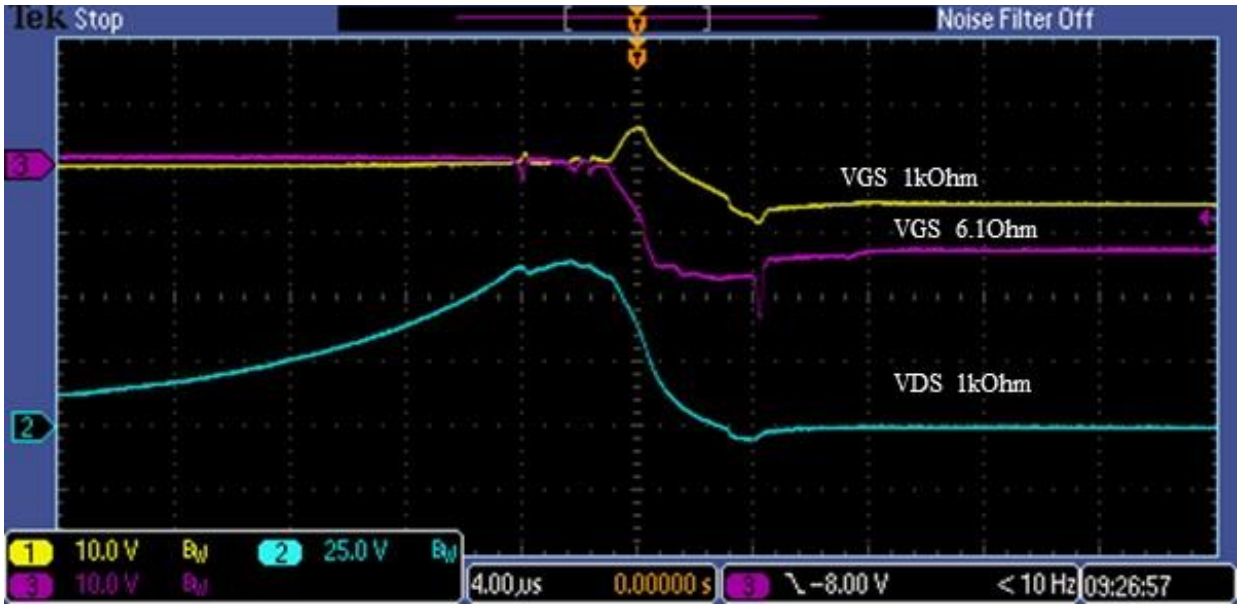

Figure 7-13 – Upstream device with trigger voltage of VGS from the downstream device with 4us/div; VGS, 10V/div; VDS, 25V/div; IDS, 50A/div

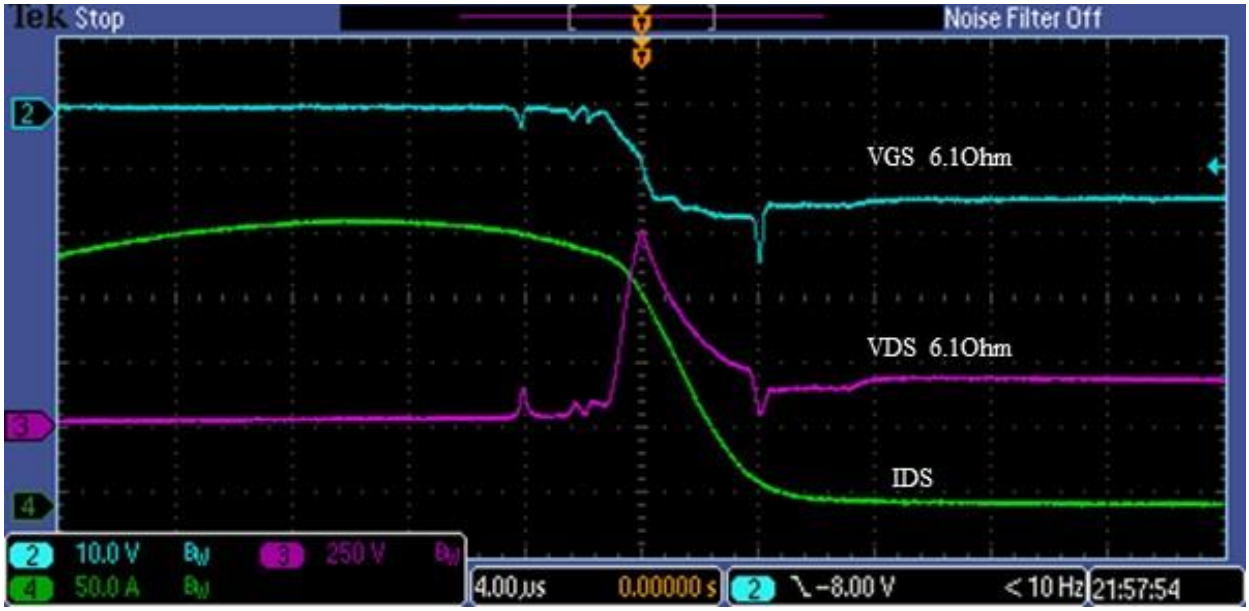

Figure 7-14 – Downstream device with 4us/div; VGS, 10V/div; VDS, 25V/div; IDS, 50A/div

7.3 Fault Discrimination – Three SSCB Case

The schematic for the simulation with three SSCBs in series is as given in Figure 7-15. The additional L4 in the diagram from the previous version is again the cable inductance.

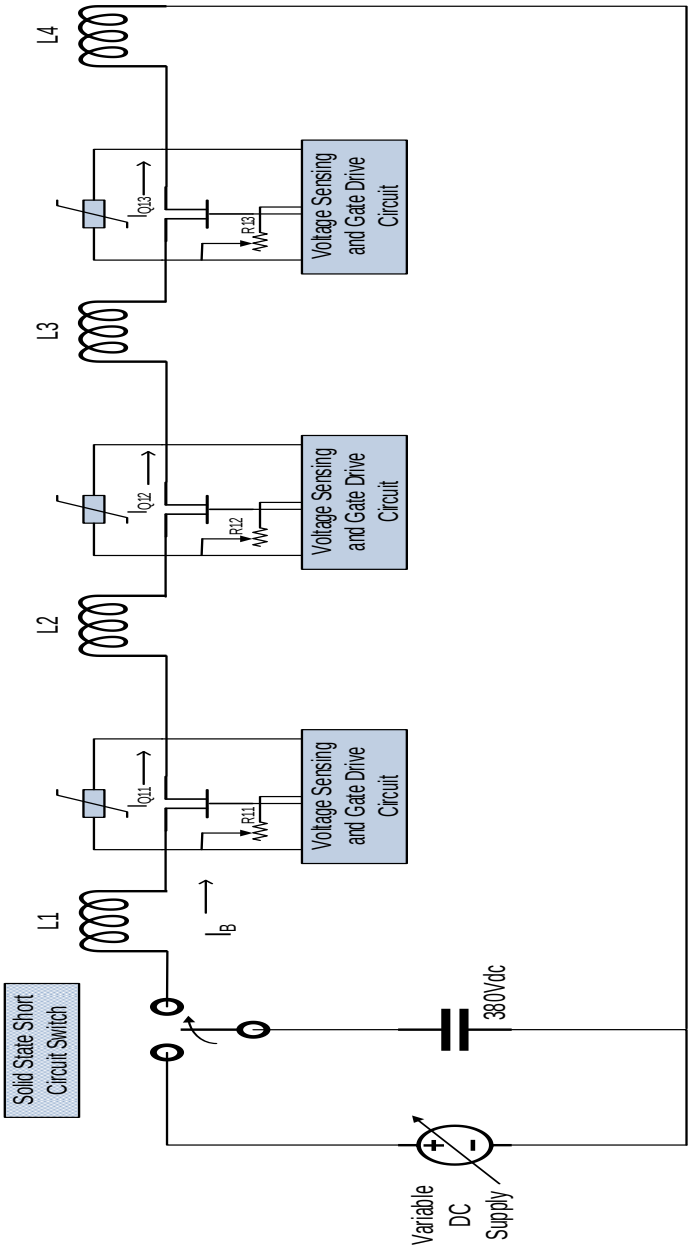

Figure 7-15 – Triple SSCB Schematic

7.3.1 Simulation

Figure 7-16 and Figure 7-17 show the LT Spice simulation of the three SSCB and multiple SSCB, in this case four SSCB models Figure 7-11. The same set up and approach like the first case is followed. This time though the interest is to see which JFET turns off and which does not. The results of the four SSCBs simulation are given in Figure 7-18. This was chosen to depict the fact that the coordination and discrimination does give us the expected results. 6.1, 20, 40 and 70 Ohms of resistance are used in each of the SSCBs in the model. When a fault is applied we except the 6.2 SSCB to go and the rest to stay. The black waveform in the simulated result graph is the VGD, Gate to Source voltage of the 6.1 Ohm SSCB. This means that, it will turn off. The rest of the values of the Gate to Source voltages of the other three SSCBS does not go beyond about -7.5V, which is the threshold for the JFET to turn off thereby rendering the SSCB non effective. The results show that we are able to discriminate based on the resistance even in case of multiple SSCBs.

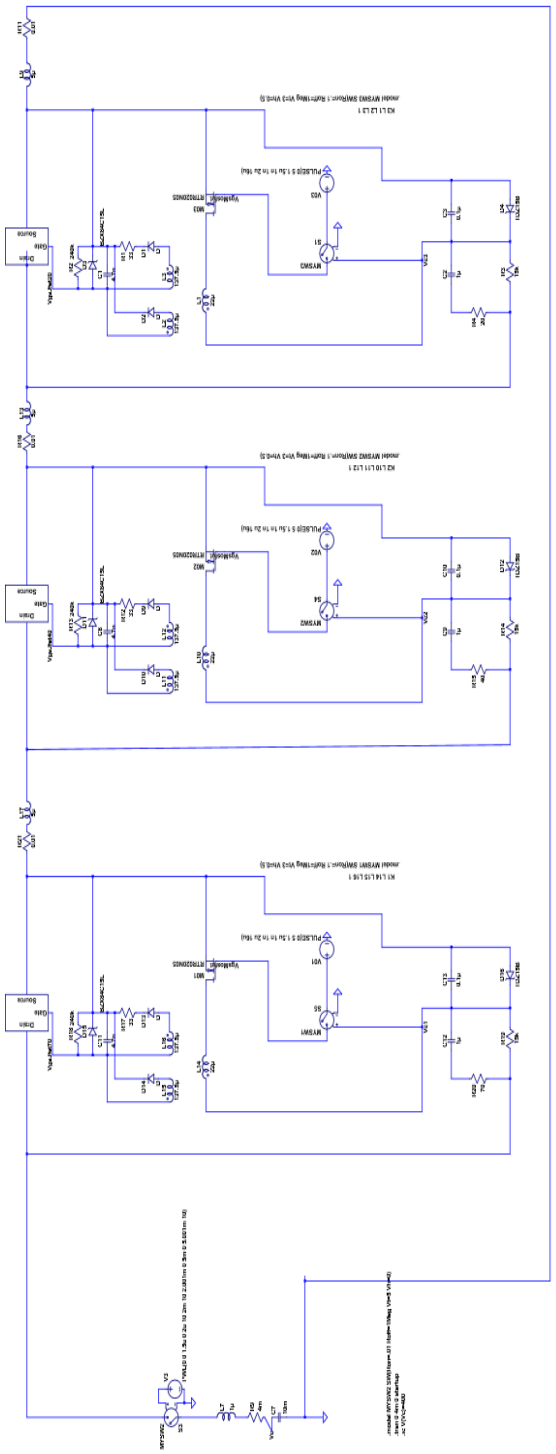

Figure 7-16 - Triple SSCB Simulation

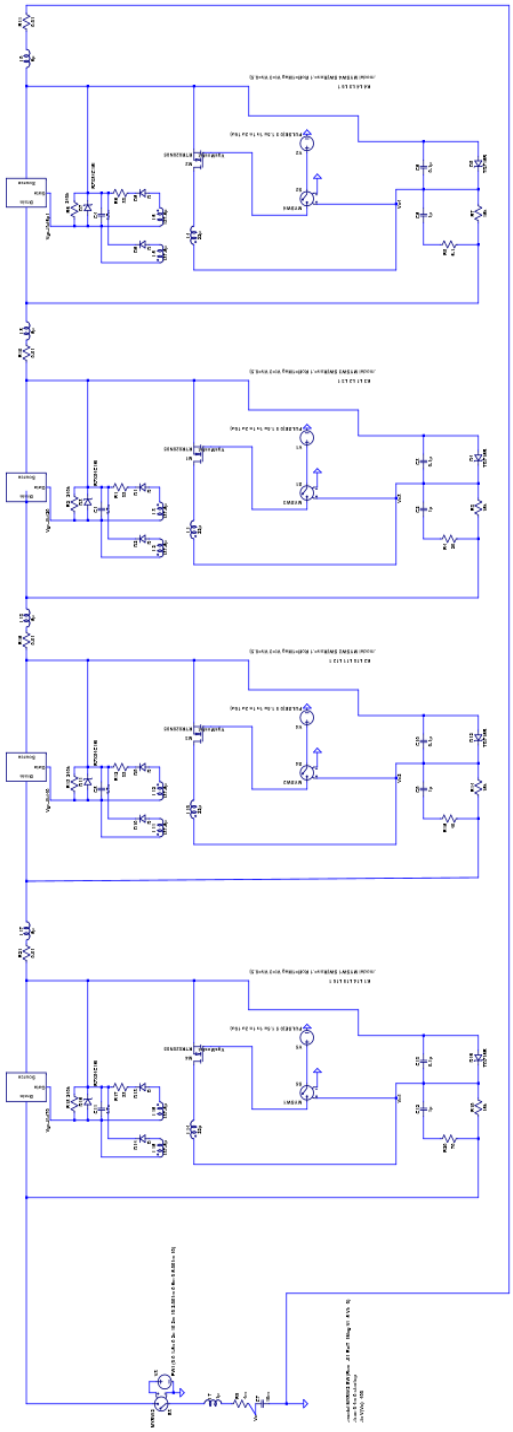

Figure 7-17 - Multiple SSCB Simulation

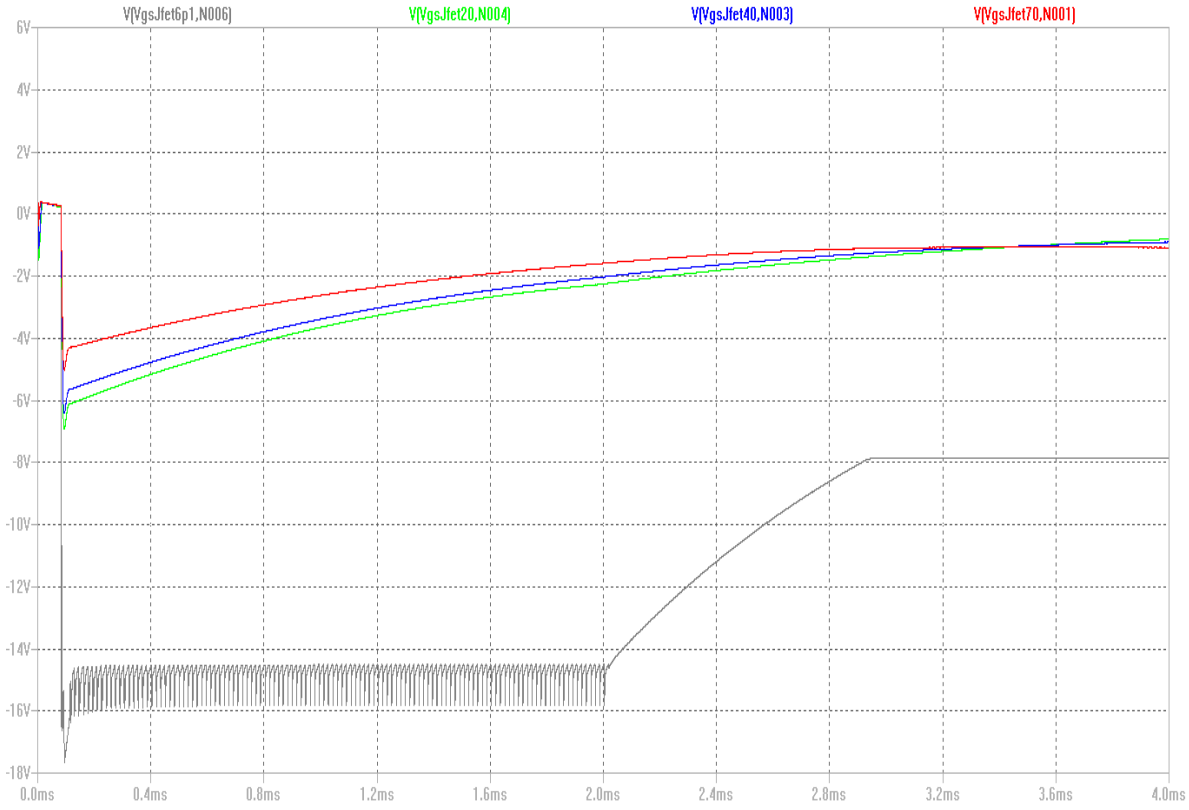

Figure 7-18 – Four SSCBs Simulation

7.3.2 Experimental Validation

The experimental setup for the cascaded JFET configuration is as shown in Figure 7-19.The setup consists of three JFETs in series with wires of short length in between them since due to the laboratory setting. It should be noted that this represents a worst case scenario. Long lengths of wires between JFETs in a more realistic scenario would tend to reduce the compressed time response demands on the SSCB implementation and provide a wider range of adjustment for fault discrimination. The first SSCB has a resistance of R2=6 Ω.. The second SSCB has a R2=200 Ω and the third one has a resistance of R3=470 Ω.. The setup is as such that the third SSCB is close to the Capacitor and the first SSCB is close to the rheostat. The expectation is to see the SSCB with R2=6 Ω resistance trip and the other two remain intact as the time constant for the same is lesser than the

other two. The test was conducted, was with the capacitor charged to around 100Vdc and that was applied as short circuit fault on the Switch.

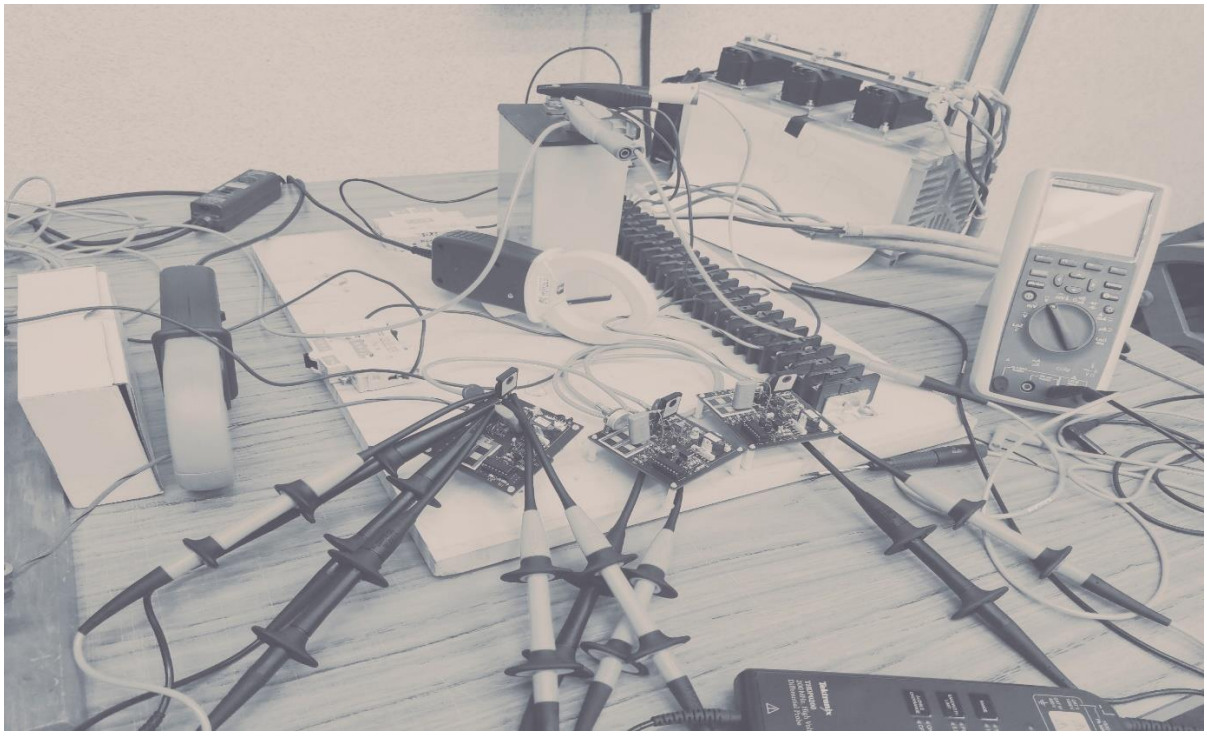

Figure 7-19 – Cascaded JFET experimental set-up

As there are three SSCBs and more data to capture, two scopes are used. Figure 7-20 shows the first scope picture recording the gate to source voltage of the R2=6 Ω SSCB with significantly more negative gate to source voltage compared to that of the R2=200 Ω SSCB. The gate to source voltage of the R2=200 ΩSSCB is negative but with a lower amplitude than the R2 = 6 ΩSSCB. The drain to source voltage across the SSCB with R2=6 Ω resistance shoots up before it steadies down at about 100Vdc. Figure 7-21 is a clearer plot of the data as obtained from the scope. Figure 7-22 shows the second scope picture. This records the gate to source voltage of the R2=6 Ω SSCB, which is going in the negative direction with a large amplitude and the gate to source Voltage of the R2=470 Ω SSCB, which is going negative but with a much lesser amplitude. The drain to source

current across the circuit is also shown. Figure is, again, a clearer plot of the scope data. The rheostat was set to about 0.5Ω while this test was conducted and hence the current measures to about 210A on the scope. The scopes were both triggered on the R2=6 Ω SSCB gate to source voltage. Figure 7-24 shows just the gate to source voltage of the three SSCBs alone and it can be seen that the 6 Ω SSCB gate to source voltage is the only one to go below the threshold of -7.5V, the other two do not even get close to the threshold of the JFET.

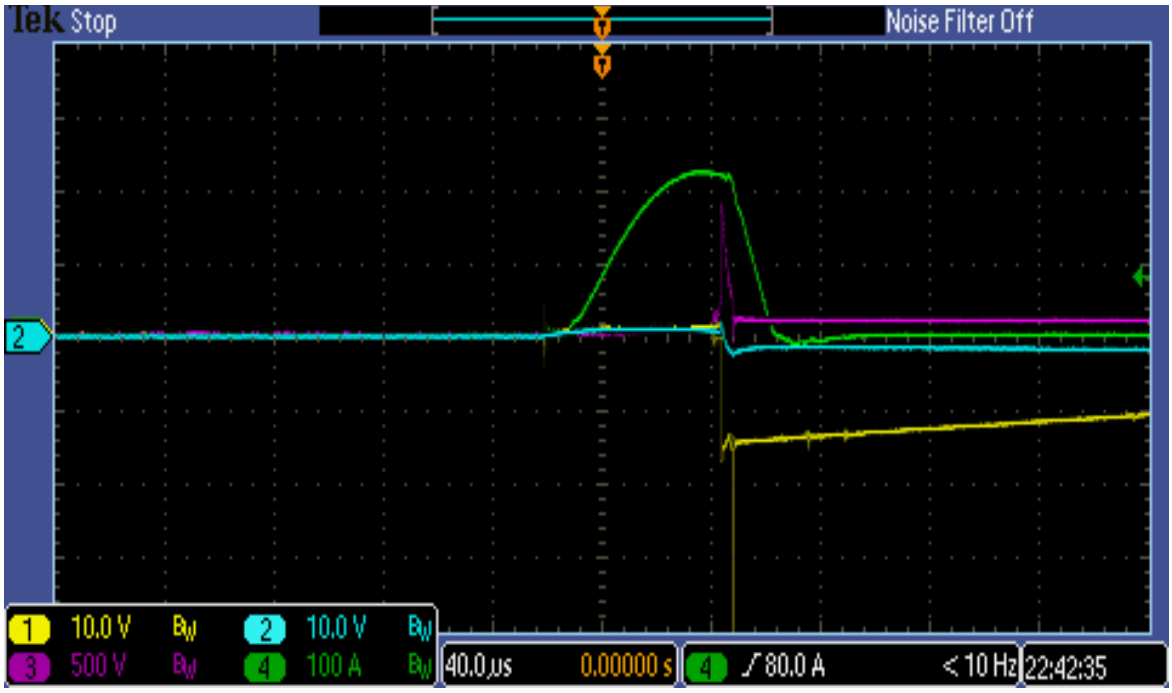

Figure 7-20 – Cascaded SSCB Scope 1 Plot in the Lab. Ch 1(VGS1) - 10V/Div, Ch 2(VGS2) – 10V/Div, Ch 3(VDS1) – 500V/Div and Ch 4(IDS) 100A/Div.

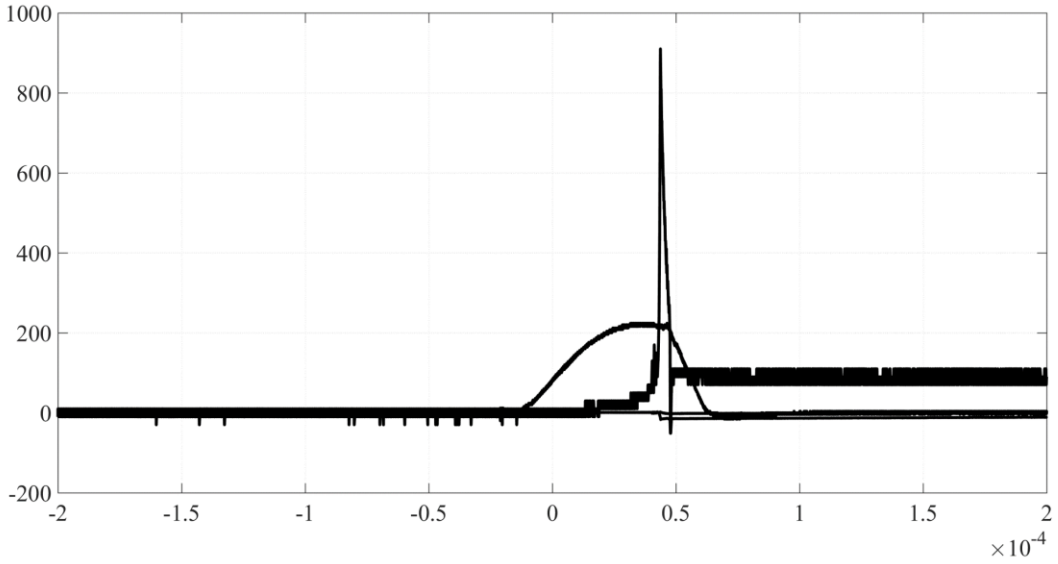

Figure 7-21 – Cascaded SSCB Scope 1 Data Points

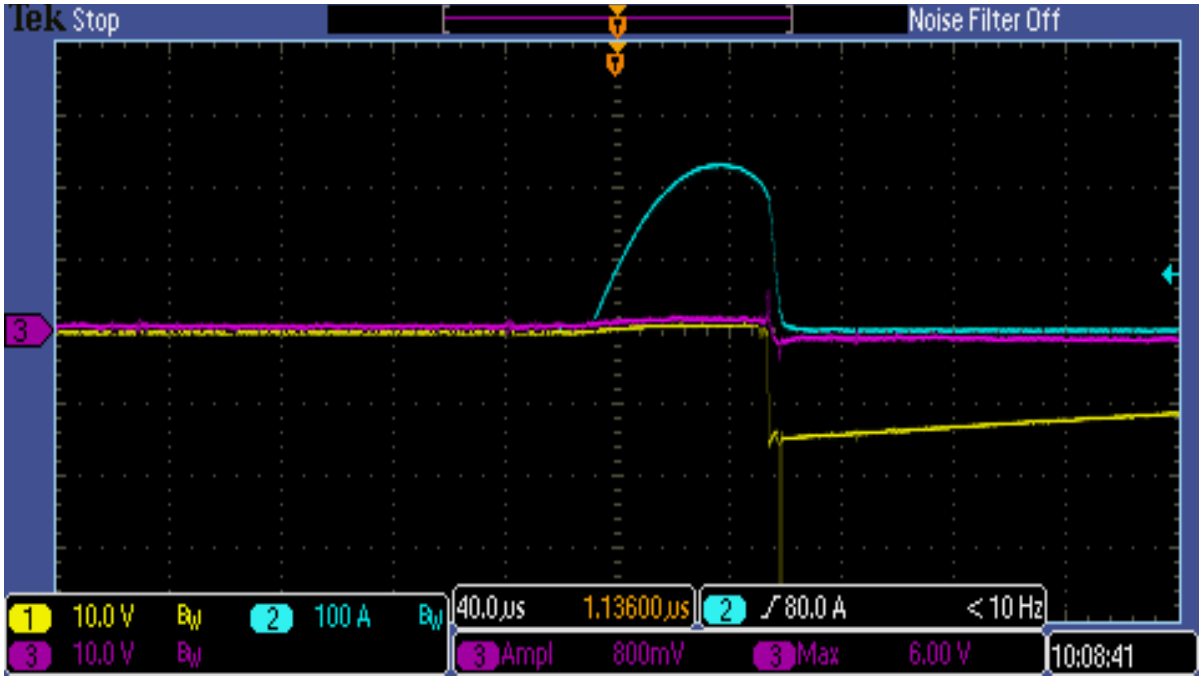

Figure 7-22 – Cascaded SSCB Scope 2 Plot in the Lab. Ch 1(VGS1) - 10V/Div, Ch 2(IDS) 100A/Div and Ch 3(VGS3) – 10V/Div.

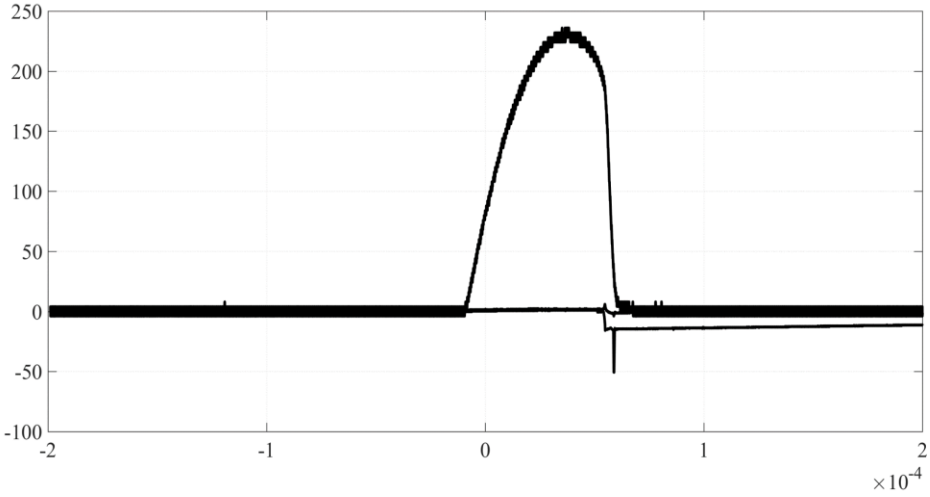

Figure 7-23 – Cascaded SSCB Scope 2 Data Points

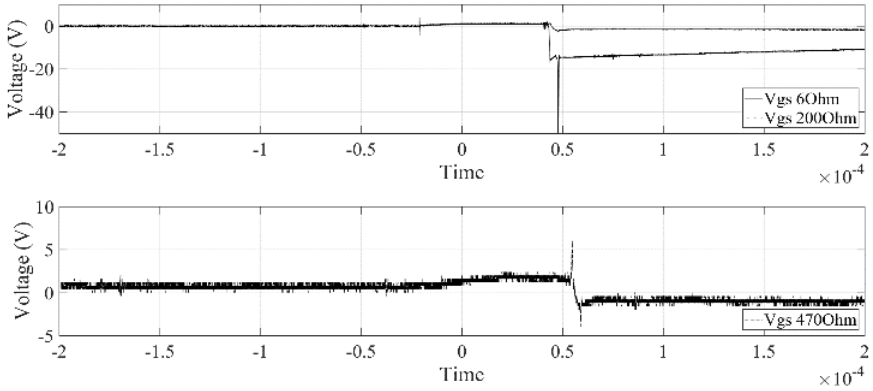

Figure 7-24 – Cascaded SSCB VGS Data Points

7.4 Summary

The SSCB was simulated and the results were validated with the experimental results in this chapter. Fault discrimination and coordination capabilities were presented and through simulations and experimental setups they were validated as well.

Chapter 8 Hardware in the Loop

Hardware in the loop systems as the name suggest is a hybrid of virtual and real components in a system. This allows for the development and testing of the real part of the system as the project chugs along. This chapter describes the basics of the HIL platform and presents an HIL system which was used to obtain some real time results for a part of the DC Microgrid system and compares it with the traditional Matlab simulation. A full blown Novel HIL implementation system is described as well.

8.1 Why HIL?

As the systems get complex, the methods to test and get quantifiable results becomes a challenge with traditional simulation methods. Some of the advantages of using real time systems is as given in Figure 8-1. The biggest impediment is the time it takes to run some of the simulations faster due to the sheer size of the model. HIL systems are developed across various domains to address these issues [132] - [133]. HIL can be used to test the electrical system or the power system, if a the controller is real, then you are testing the controller and that type of emulation is called the Controller HIL and if you have a system with real power components then that is called a Power HIL [134]. HIL systems are used to emulate the system in real time and play an important part in the development phase. An HIL system is used to test a controller in [135]. In [136], an HIL system is used to test fault conditions of HVDC using MMC. In [137] and [138], HIL systems are used to simulate medium voltage converters with hundreds of semiconductors using FPGA-CPU based simulators and in [139], it is used for automated testing.

Figure 8-1 – Real Time System Advantages

HIL systems operate at real time when needed, meaning a 2 second simulation time is actually done in 2 seconds instead of longer, like the regular simulation models take usually. This is helpful when the systems get complex, as it takes a lot more time to simulate the models. The definition of real time in the Opal system used here is as shown in Figure 8-2. In the real time system, embedded devices are given a predetermined amount of time to read input signals, such as sensors, to perform necessary calculations, such as control algorithms and to write all outputs such as actuators. Fixed step solvers solve the model at regular time intervals (50us in Figure 8-2) from the beginning to the end of the simulation.

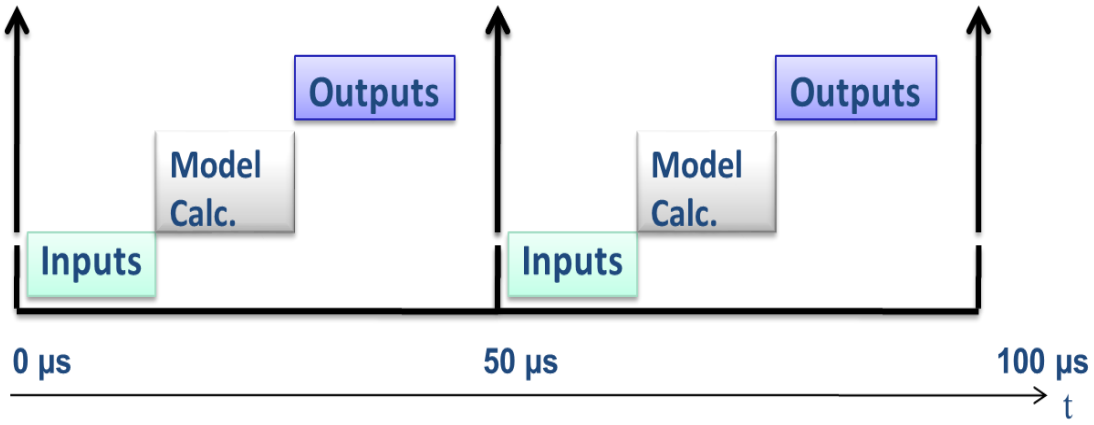

Figure 8-2 – Real Time - Definition

8.2 HIL Emulation

The DC Microgrid emulation diagram is as shown in Figure 8-3. The converters in the homes, panels and the utility are all listed. These maybe dual active bridge and point of load converters depending on their location. The DC to DC converters are shown as well.

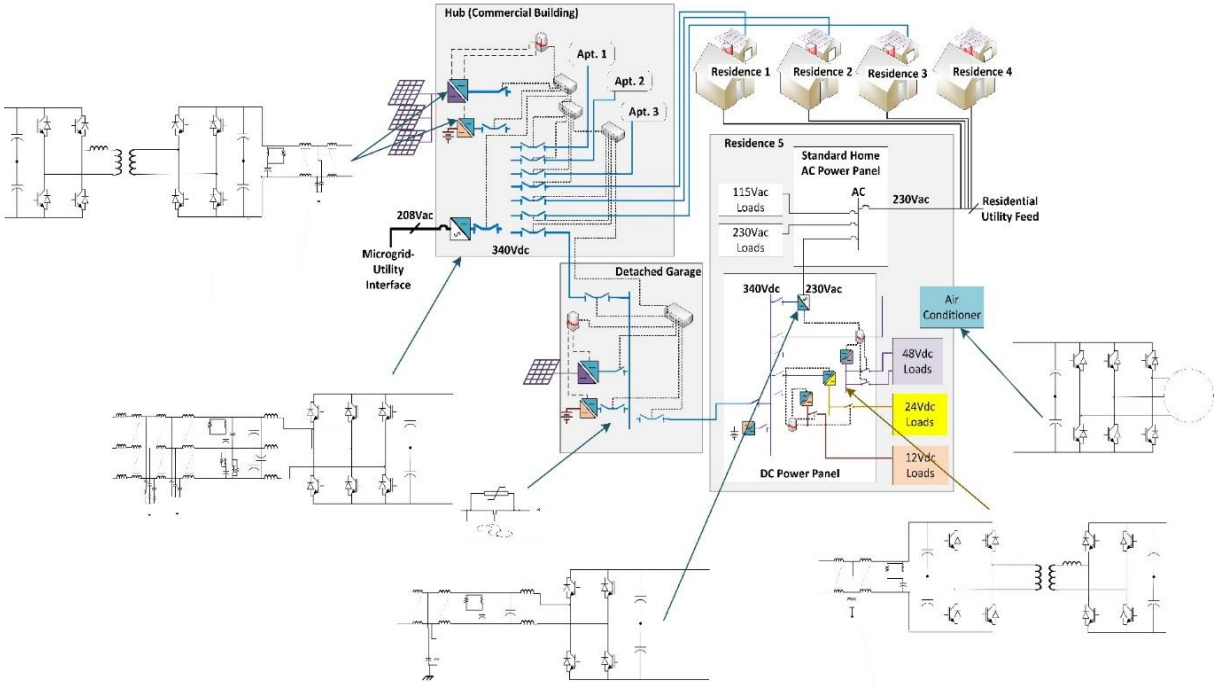

Figure 8-3 – DC Microgrid Emulation

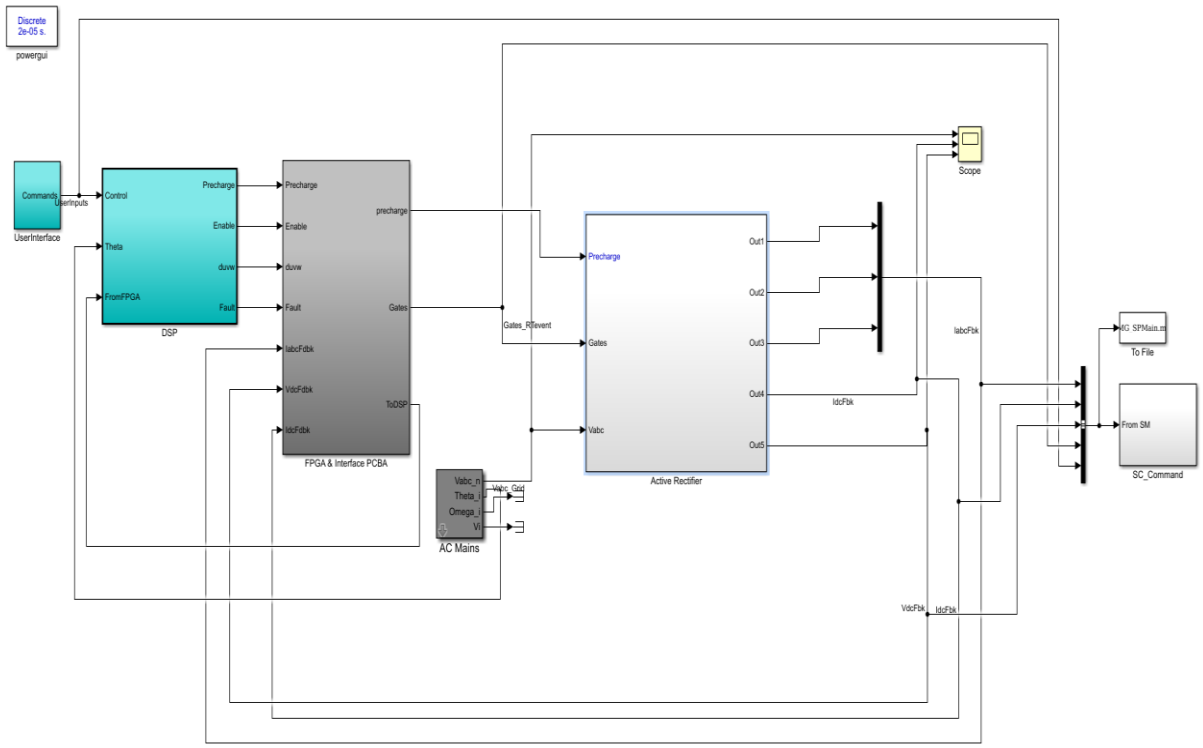

Figure 8-4 – Matlab Model for Comparison

The Matlab model for comparison with the Opal model is as given in Figure 8-4. The model, from left to right consists of a user interface subsystem to apply the fault and start and stop the system and present the system with aa command voltage. The signals then go to a DSP model which consists of a state machine to choose between online, standby, precharge, fault and online mode, a ramping state machine and a model for AC to DC converter control. The next part of the model is the FPGA interface, this is where the PWM for the system is generated. The last part is the Active Rectifier, this is where we have the AC converted o DC and feeds the DC loads in the system. This part extends out to be the heart of the DC microgrid. In this simulation, we just have one of them and a resistive load. The simple Hardware in the loop real time simulation set up with Opal-RT OP5600 system as shown in Figure 8-5. The figure also shows an OP4500 which has a Kintex 7 FPGA on it. This will be used to bring the HIL to action.

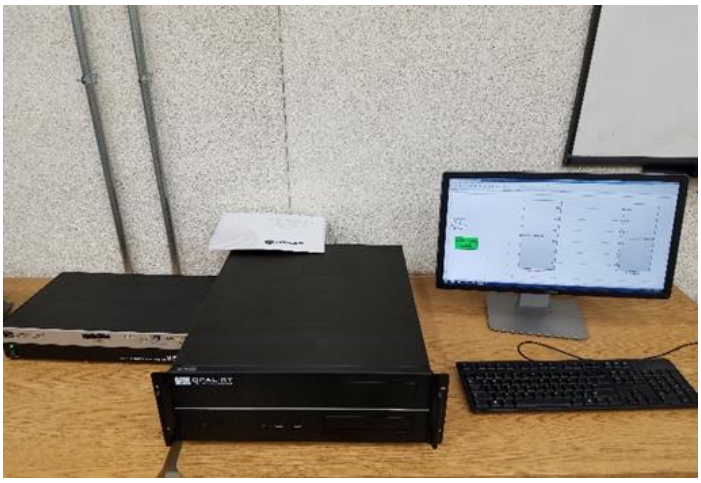

Figure 8-5 – HIL Lab Setup

There can be external PWM or other hardware which can be connected to the Opal system to do real time generation of PWM signals for the gates of the rectifier or other operations. The Opal system gives us the ability to be able to interface with various systems as long as the voltage and current requirements for the Analog and Digital Ins and Outs are satisfied. The Opal system allows us to use its inbuilt solver called the eHS. This approach uses the Pejovic method as indicated in [140]. It solves the conductance matrix of the network to find the voltage at each node and current from each of the sources. The Kintex 7 FPGA we have can have multiple solvers and it was one in this case and the simulated model can be modified without recompiling the bit stream on the FPGA. The active rectifier was modeled in the FPGA to test out the real time HIL capabilities of the Opal system. The outputs of the Matlab and the eHS Opal models are as given in the following figures. A fault was applied at 4s and we can see the response of both the systems. It is pretty similar and the Opal system was in real time so the data had to be captured and plotted separately.

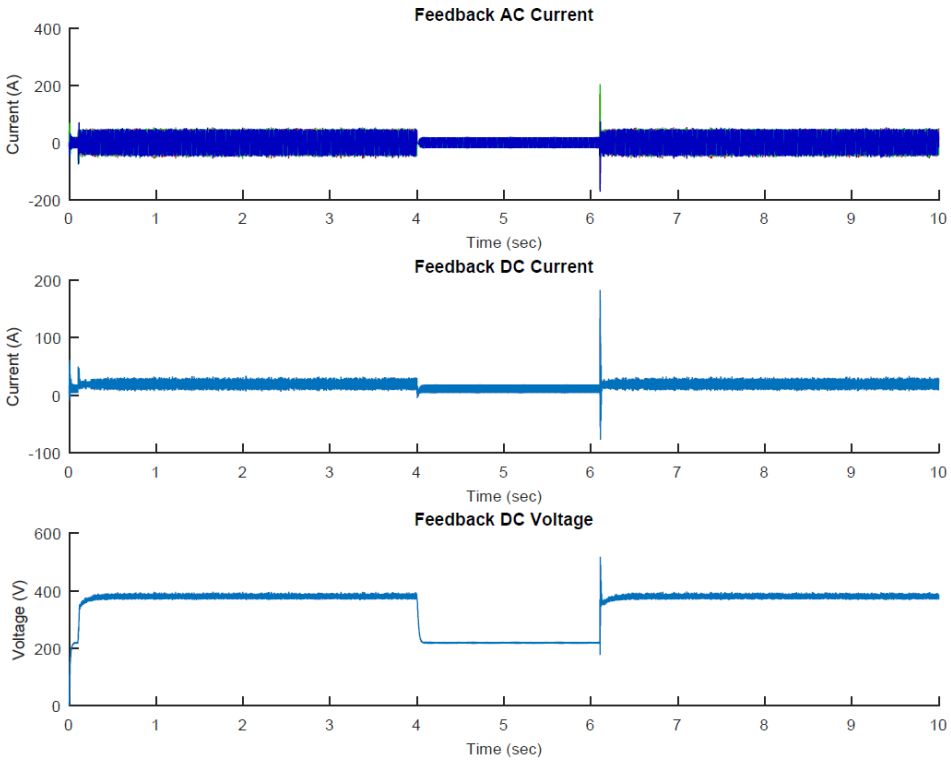

Figure 8-6 – Matlab/Offline Simulation

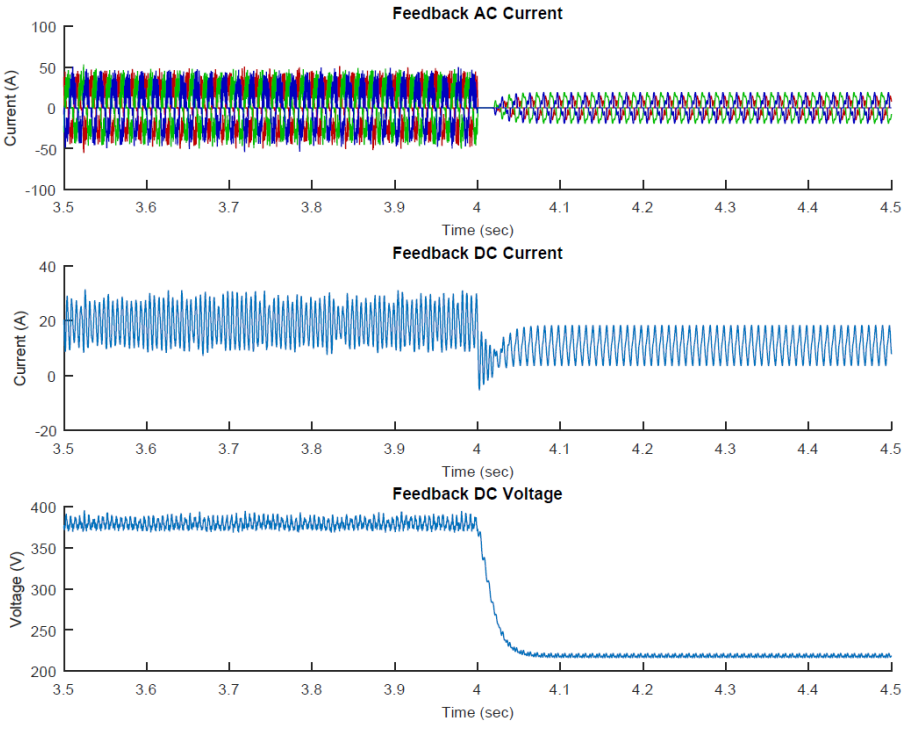

Figure 8-7 – Matlab/Offline Simulation - Zoomed

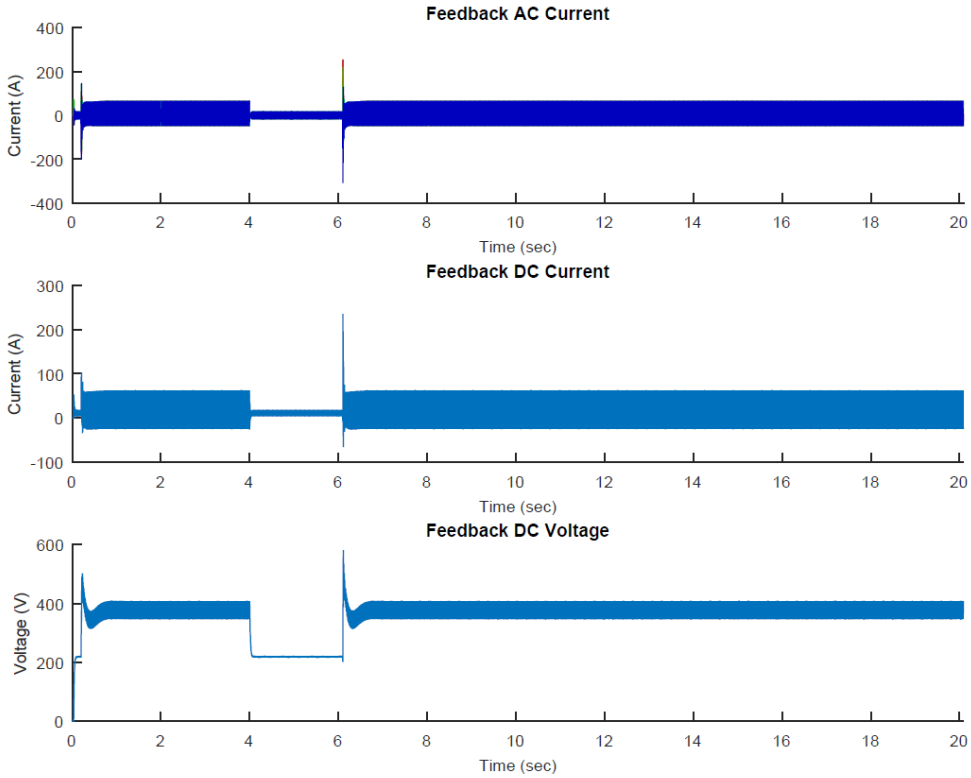

Figure 8-8 – OPAL eHS Simulation

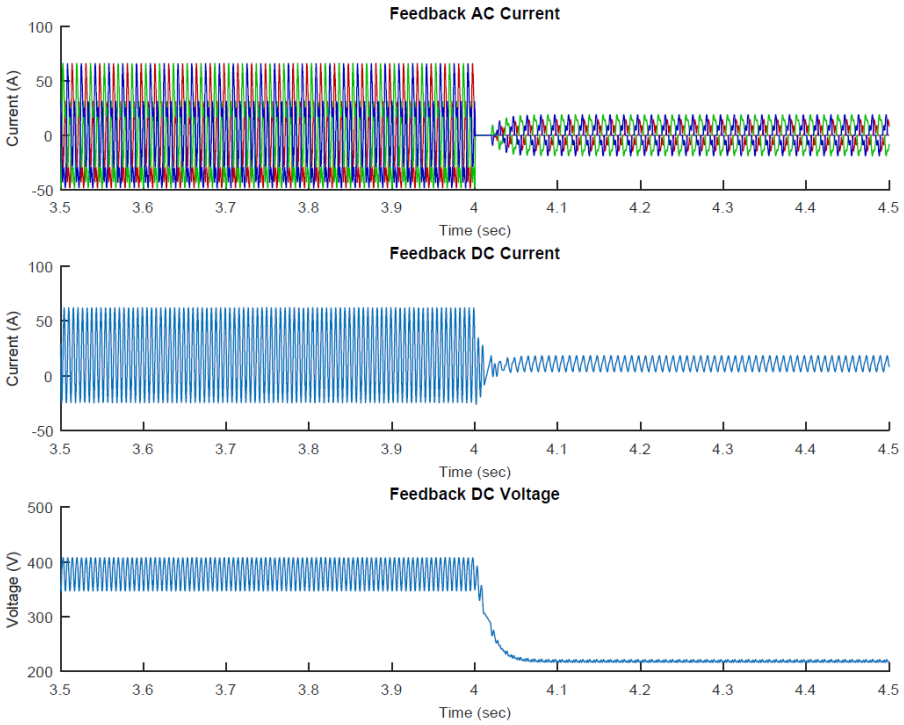

Figure 8-9 – OPAL eHS Simulation - Zoomed

8.3 Novel HIL Implementation

A novel HIL simulation model for the DC Community microgrid is as shown in Figure 8-10. The set up involves the Opal set system to be used as the base for the community with the connection to the DERs and the protection devices along with the MEMS and HEMS to implement the system side of the design. The converters in the individual houses themselves are implemented using a custom FPGA HIL system as shown in Figure 8-11. This model shows the case with one house but there can be N houses and the same model will be repeated.

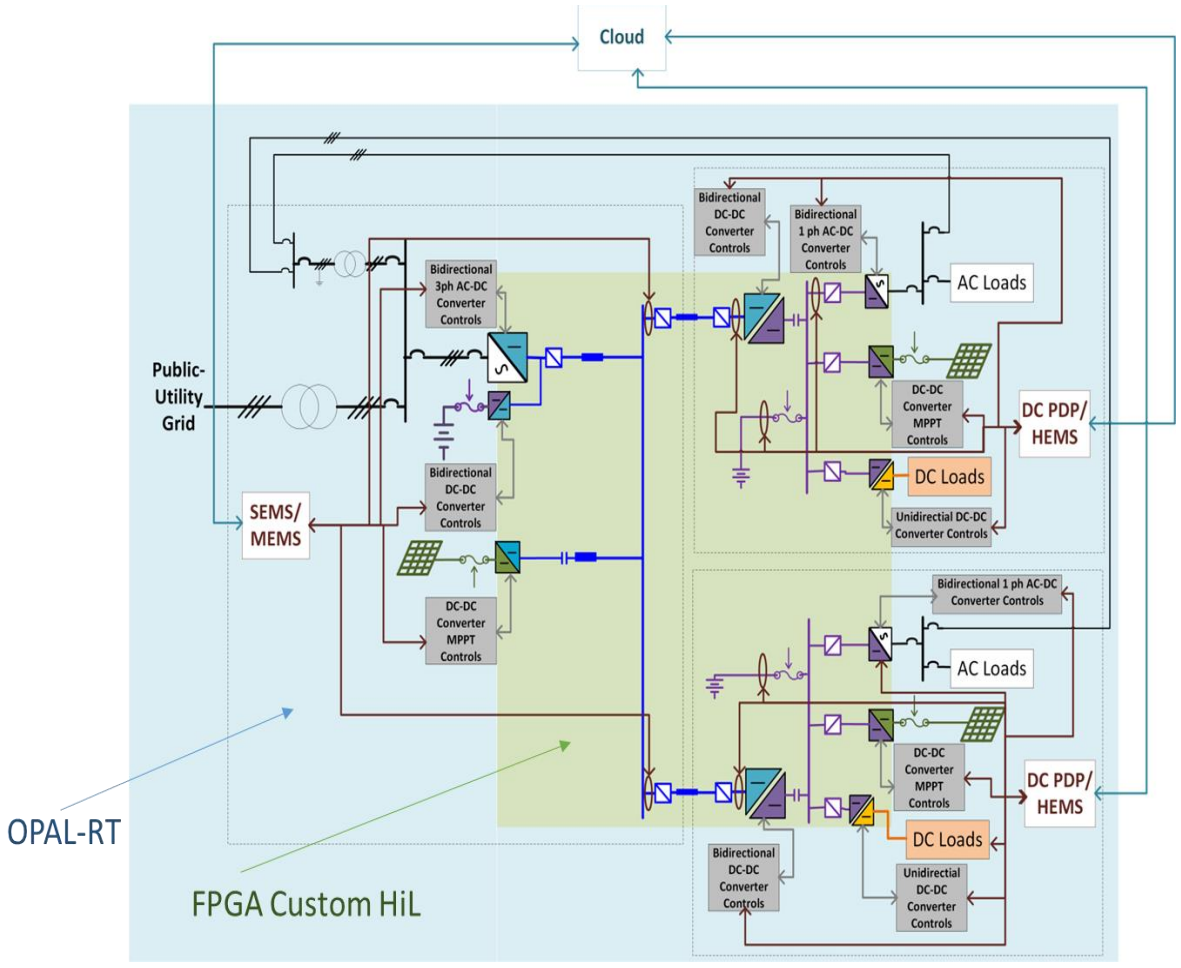

Figure 8-10 – HIL Simulation Model of the Community DC Microgrid

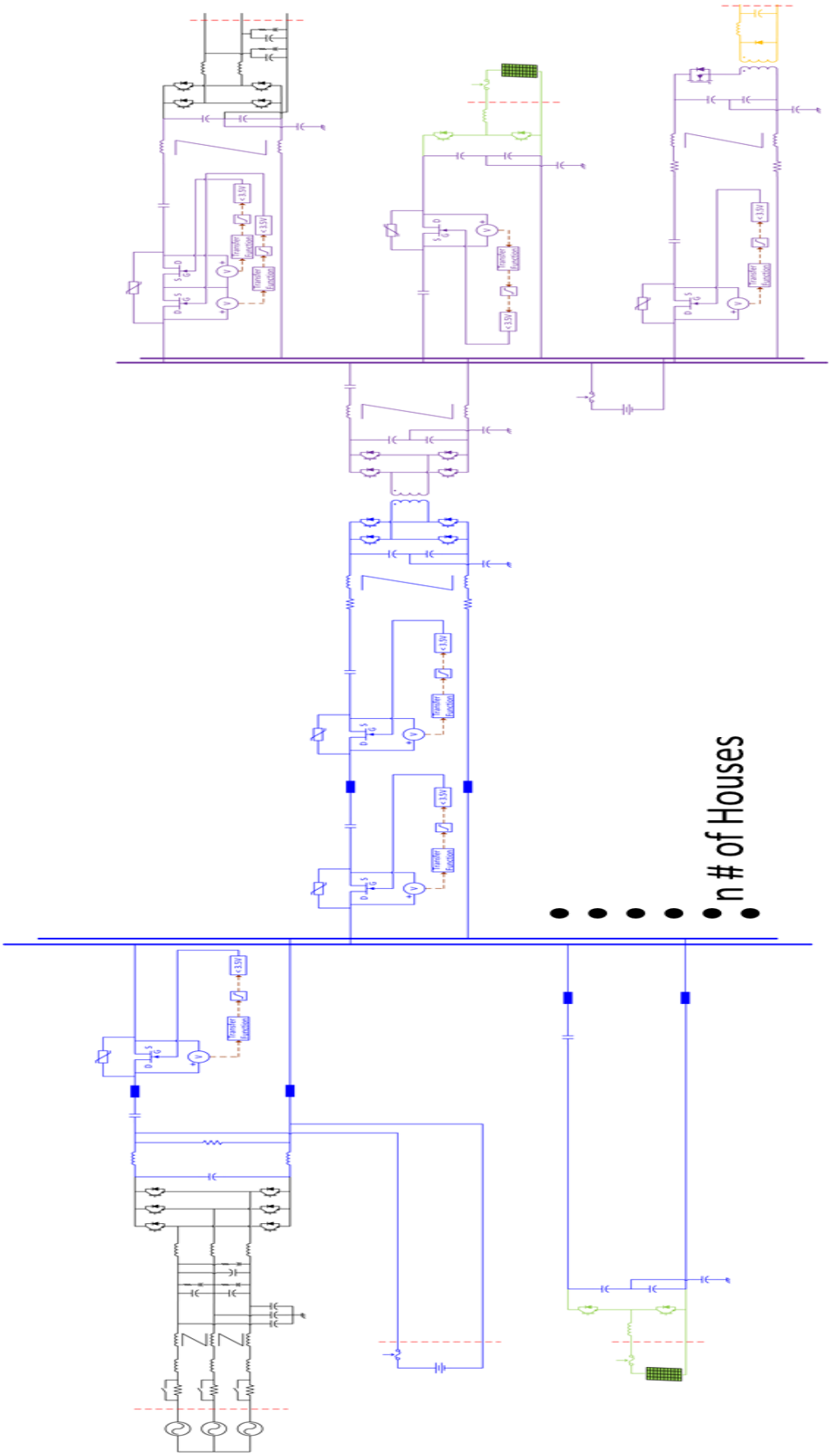

Figure 8-11 – System for FPGA Implementation

The basic components which make up the model are the three phase grid connected converter with some filters, unidirectional and bidirectional solid state circuit breakers as a transfer function because of the unavailability of JFETs, Dual Active Bridge to house feeds, three wire one phase grid connection at the house, point of load converters o DC loads and half bridge boost for PV connection along with the HEMS and MEMS. The proposed validation platform for the work is as given in Figure 8-12. The setup consists of the Opal system hosting he base of the microgrid and the FPGA simulator having the controls as discussed earlier. LabVIEW and Compact RIO may be used to make controllers and relays for the protective system design.

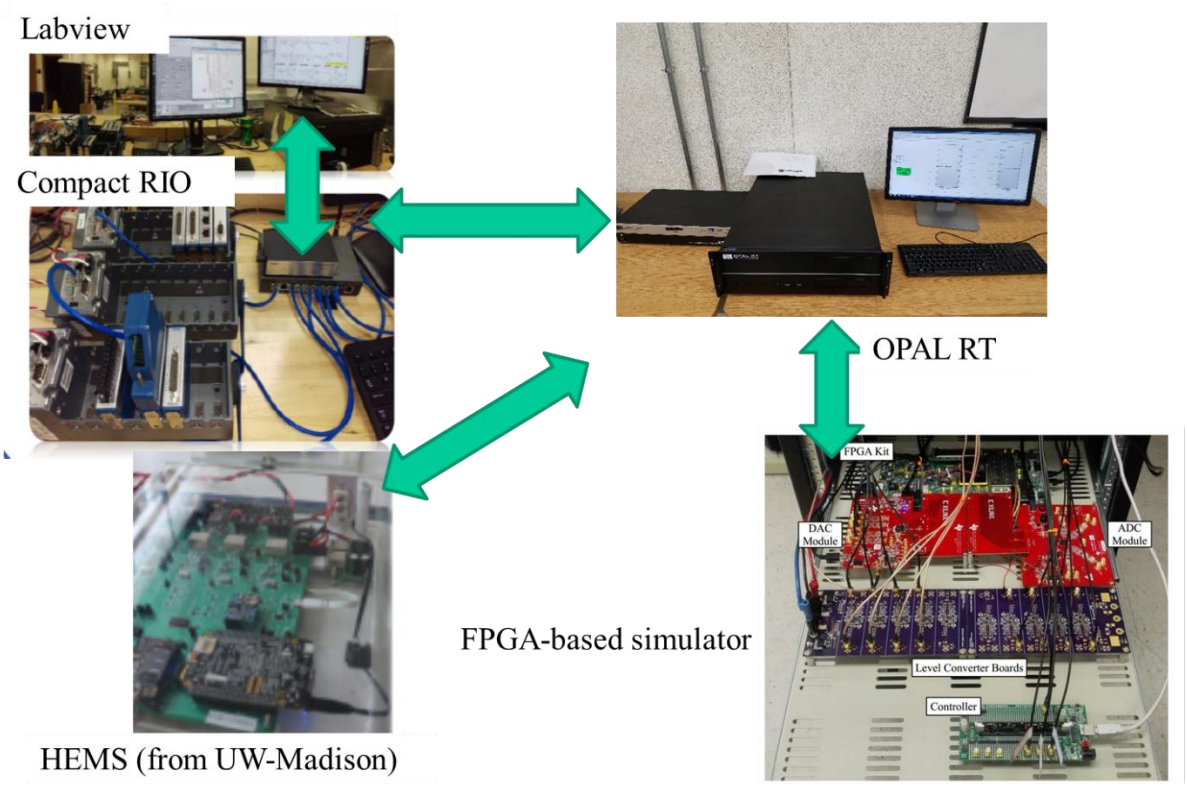

Figure 8-12 – Proposed HIL Validation Platform

8.4 Summary

This chapter presented a basic HIL emulation of the DC Community microgrid and compared the results from inducing fault in the microgrid using Matlab and eHS Opal system. This chapter also proposed a novel implementation and platform for doing a complete HIL of the DC MG.

Chapter 9 Societal Impact

9.1 Educational Impact

Electrification is indisputably one of the most effective ways to provide billions of people with clean water, sanitation, access to education, medical services, and communication technologies, which are objectives recently outlined in the United Nations Sustainable Development Goals. Electrification is also one of the integral parts in creating a solid educational foundation for vocational training and collaborative worldwide idea-sharing among current and future visionaries, entrepreneurs, and leaders striving to bring their communities together in creating community-based infrastructure and sustainable business opportunities [119]. The proposed community microgrid as shown in Figure 9-1will be used to train students who will learn about the various aspects of the specific DC community microgrid in great detail after going through a series of sessions on learning the basics of power, energy, grids and renewable energy. Topics related to Smart homes and loads will give them skills to compete in an increasingly knowledge-based economy and better equip them to be a part of this living laboratory so the entire community can be transferred to a smart community, one home at a time. The students will learn about smart devices and how the whole Internet of Things (IoT) approach will be applicable in a real world scenario. They will learn how the different aspects of the technology comes in to play by observing the various equipment and scenarios in practice. The students once educated will be living in these houses with their parents and teaching them how to use the smart loads in a DC community microgrid setting so they can learn the latest technology and work towards optimal using the energy so reduce costs.

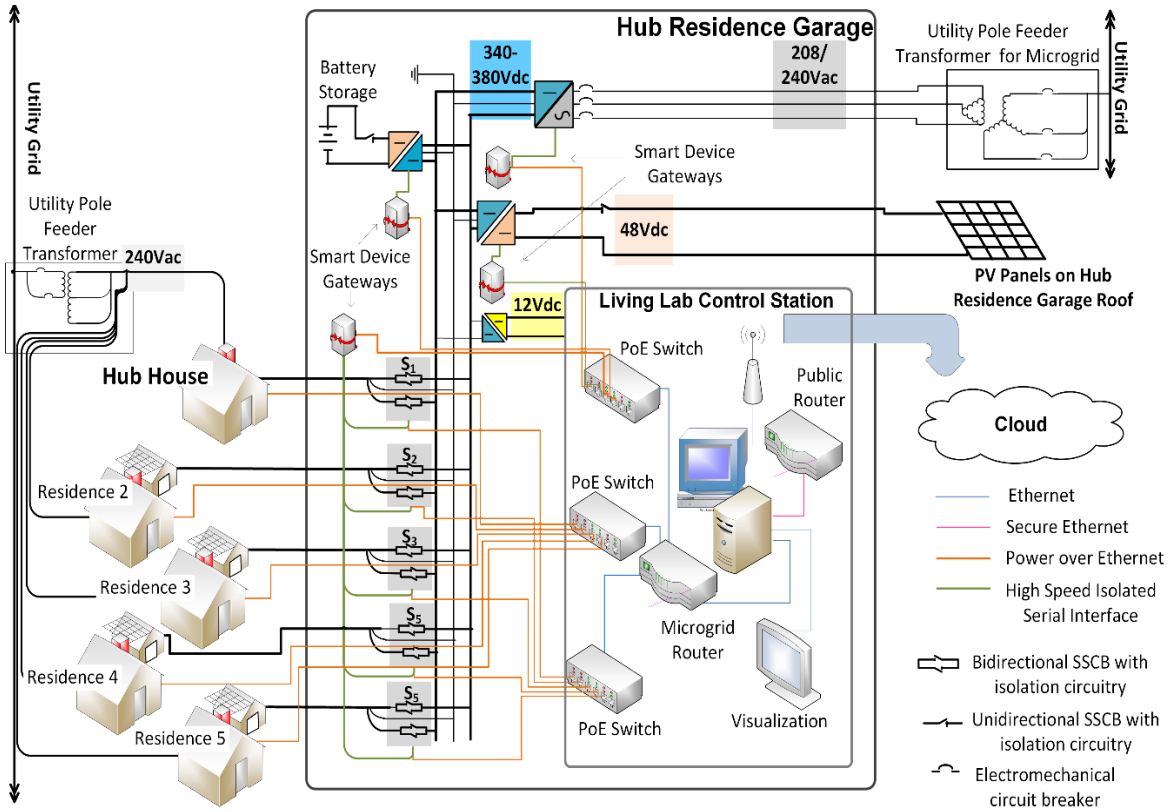

Figure 9-1 – DC Community Microgrid as a Living Laboratory

9.1.1 Motivation

According to the US Department of Energy “Smart Grid generally refers to a class of technology people are using to bring utility electricity delivery into 21st century using computer based remote control and automation” 159[120]. This initiative requires power engineers to have a good understanding of auxiliary fields like controls, information technology (IT), and communication networks, while being experts in the basic operations of the future power systems.

There is a great need in the power industry and not only for such cross-trained graduates and professionals to meet challenges and needs in the power gird modernization[121] - [125]. The high school students in this neighborhood will be trained in these fields so they are well equipped to

handle the ever changing world of technology and, through this process, we are hoping to develop an interest in the students so they can pursue a career in the STEM fields. This hands on living laboratory based training will help develop future engineers and scientists. The low income household students will not be left too far behind other young people who can afford such education. This will help these students stay ahead of the curve and compete in this world. Lack of education and exposure to technology contributes to loss of opportunity in reducing electricity costs and participating in the society's major undertaking of carbon emission reduction among the economically disadvantaged population. Increased visibility to future technology can provide a bridge to high-skill careers, which will lift youth out of poverty. This project combines renovation of vacated inner city homes with development of smart DC microgrid, brings new technology into under-served communities as a means to reduce economic and racial disparity, and bridges a growing "sustainability divide" among citizens with diverse socio-economic background.

The living laboratory environment of the proposed project will enable students from a STEM high school in the target community to work side by side with researchers, learn how to manage energy usage in their own homes to reduce electricity costs, and to gain exposure to future technology careers. Adult residents in the same community will be engaged through a similar learning practice with the assistance of the student early adopters who are often family members or neighbors. The project will encourage the community to become stakeholders in cooperative energy usage and, in the process, achieve a sustainable infrastructure that lowers barriers to economic mobility. The project will accelerate the adoption of renewables by enabling a paradigm shift towards smart consumption of electricity and immersing renewables into the daily lives of people of all socio-economic background.

9.1.2 Proposed Learning Objectives

The students will first understand the big picture of how each and everything in their house operates. For e.g., they will be able to understand how is their TV/Computer/Fridge and other electrical appliances powered. They will understand what is electricity and what are the ways it is generated and how does generation affect their daily life and about the different ways of electricity generation, mainly renewable energy generation. The students will learn how to calculate the energy loads in a typical house and understand how each of the appliances can affect the energy consumption of the individual houses. The students will then understand how power is delivered to their houses i.e., they will learn about what a transmission line is, what is a substation, what is a grid, what is a microgrid and what are the types. They will also understand what happens when power goes out and how we are affected by it and how is the power restored in such conditions. This will give the students a good perspective of the consumption of electricity and how they can optimally use the resources in hand to satisfy their energy needs in an efficient and socially amicable way as [126] discusses.

Then the students will learn how to model a house using software. This will give them an intuition about how things are done in the industry and about research in general. They will learn how to use different applications on the computer to their advantage. This will give the students a good insight to engineering and math. This part of the project will excite the most if we are not mistaken. This is the part where the children can experiment a lot of things and see how they can be a part of something big in the future. The approach is to have them learn and use specialized software like HOMER as used in [127] to better be able to model the entire house and eventually the entire microgrid, In this way, they are able to see how the individual loads in the different houses affect the output of the power consumption in the community as a whole. Visualization of

power usage within the microgrid will provide a means for explaining social responsibility as well. They will learn some other important tools like Matlab and Simulink and as shown [128] - [131], they will try to create some models in these software environments. The students apart from all this will be introduced to other relevant applications and topics in order to enhance their skills in which ever field is of interest to them. Throughout this project, they will be able to interact with people with experience in the engineering/math sector to give them insights and guide them on this project and outside if needed. The students, we hope will develop a new appreciation for math, science and engineering and will want to be doing things like this project and advanced stuff in their lives.

9.1.3 Implementation

This project is being implemented in four different phases. The first was when the authors visited the school to let the participating students know about the basics of electrical power systems and introduced some terminologies associated with the same. The students learned about the concept of microgrids in the context of the way power is distributed conventionally and how microgrids introduce renewables into the grid. The students were taught how personal devices can be used to monitor and control power usage. This was followed by giving students hands-on experience with solar panels, converters and IoT interfaces. The second phase was the start of an Energy club at the school.

Figure 9-2 – Energy club inaugural session

Figure 9-3 – Tour of Electrical Lab – 1

Figure 9-4 – Tour of Electrical Lab – 2.

Figure 9-5 – Tour of Electrical Lab – 3.

As shown in Figure 9-2 the students were taught the workings of a solar panel and had a set up where they tried to work with the battery and panel set up to run a small motor, which powered the fan. They were also learned how to control appliances over blue tooth using a smart plug-in device. The third phase was students toured the University's Sustainable Electrical Energy System laboratory in order to experience a research environment and observe undergraduate and graduate students at work in the lab. Figure 9-3 was when the students came in to the lab and we were given an explanation of some electrical machines and their operation and also about the DC Microgrid project details associated with the lab. The students were given some information about some of the software and hardware platforms we use in our lab, Matlab-Simulink, OPAL-RT Hardware-in-the-Loop and Labview, as seen in Figure 9-4. The students had a look at a working MATLAB-Simulink PV Model and were given an insight into how they relate to an actual PV Mode out there in the real world and how we can model the system in the software. In this phase, the students were then given an introduction to the physical workings of a mini-microgrid through the Alternative Energy System demonstration setup in the labs (Figure 9-5). The setup consists of a small wind turbine, a solar panel, battery and a few loads. The system shows how we can operate with either

just the batteries or solar and battery combo or wind and solar combo among other permutations and combinations. There are AC and DC loads on the system and it was very helpful to teach the students about the different types of loads and how they all get fed. The students were able to see how energy is transferred and they asked more questions and learned about the system. The last phase of the project is to select the interested students and bring them back and train to do research side by side with graduate students. This is all in preparation for the introduction of a learning laboratory that will be part of the planned residential DC microgrid implementation. The goal is for the high school students and their parents, who live in this community, to be stakeholders in the DC microgrid project and, as a result, teach tem valuable skills to not only sustain the community but also to prepare students for a brighter future.

9.2 Environmental Impact

Reduction in energy consumption reduces the electricity the power plant must supply. Coal, natural gas and petroleum are the main fuels used for electricity generation, making up about 81% of the electricity generated in Wisconsin in 2007 [111]. All fossil fuels release pollutants when burned to produce electricity. The Intergovernmental Panel on Climate Change (IPCC) concluded that human consumption of fossil fuels has led to climate change. Some of the effects of climate change include loss of glaciers, loss of species, increase in severe weather, increased flooding, acid rain, and respiratory problems in humans including higher incidences of asthma [112].The harmful emissions from power plants include carbon dioxide (CO2) gas which contributes to climate change, nitrous oxide (NOx) and sulfur oxide (SOx) which lead to acid rain, small particulates (< 10 μm [PM 10]) which cause respiratory irritation, volatile organic compounds (VOC), and mercury (Hg). As given in [113] CO2 reduction for electricity is 1.885 lbs /kWh. Thus, we do not only see a reduction in the cost but also a betterment in the carbon footprint through reduction of

energy consumption. Table 9-1 lists the energy consumption in a day for the total consumption listed in Table 4-3 and the difference in the CO2 emissions for an AC and a DC house in the summer and winter months. In the summer months we can save about 447.87 lbs/kWh and in the winter we can save about 393.8 lbs/kWh with the DC alternatives.

Table 9-1: Emission in Different seasons

Season	**Energy Consumption (kWh)**	**CO_2 Emissions Reduction (lbs/kWh)**
Summer AC	451.2	447.87
Summer DC	213.6	
Winter AC	369.6	393.58
Winter DC	160.8	

Chapter 10 Conclusions and Future Work

A Community DC Microgrid in the inner city of Milwaukee has been taken as the heart of this dissertation and the architecture and protection system design of it were presented. The community microgrid was built bottoms up and the loads were analyzed with a vision of reducing the electricity bills paid by the patrons of this underserved community. Monthly utility costs are compared on a hot summer day for a conventional AC home, smart AC home and the DC home concept. Notional load profiles in a 24-hour period based different usage habits and solar power generation based on location were developed and the optimal battery and solar combination for this Microgrid in Milwaukee was identified. The proposed changes in the load and the use of solar panels and batteries substantiate the claim that the system will help reduce utility bills for the customers. The customized bottoms down approach for load measurements was calculated and compared with the DOE database for the base house.

This dissertation proposed a unique protection device for a DC system and provided hardware results validating that the self-powered Ultra-Fast SiC JFET based SSCBs can successfully discriminate faults in a radially distributed network. The SiC normally on JFET-based SSCB was able to quickly act on the fault current and drive it to zero within a few microseconds. This is one of the desired characteristics of a DC protection device. A single SSCB, double SSCB and three cascaded SSCBs were implemented in series and it was shown that the one with the least resistance turns off and cuts the current to zero while the other two remain intact. It was also observed that the transient change in temperature, measured at the base of the transistor indicates that the fault condition will not have a significant impact. It is recognized that a transient change at the transistor junction may be occurring. If this transient change is significant a reduction in the lifetime of the device may occur as a result of fault mitigation. The measured result indicates that the thermal

effects were not quite visible due to the speed at which the transition happens during a fault. The end-use intention is to incorporate packaged SSCB modules into custom DC power panels at the hub, in the detached garages and in the homes. A full fault characterization has been performed on a detailed simulation of the proposed residential DC microgrid from which fault discrimination requirements were derived. A viable circuit for isolating the fault and enabling external shunt trip has been proposed.

The future work will focus on getting a house built with the smarts in them and starting to test the HEMS/MEMS. The immediate work will focus on developing the control algorithms for the / MEMS and finding the optimal energy sharing mechanisms within the DC MG with real constraints introduced into the system. Future work will increase the robustness of the circuit implementation and test the devices up to full ratings. The intended ratings of these SSCBs is 400V, 75A. The target application will have a nominal bus voltage of 320V. Future work will focus on the implementation and testing of these surrounding circuit features. A full-fledged hardware in the loop environment can be created as well and this will provide a test bed for a lot of the things going forward.

Students had started the energy club and the progress on the work and details about the steps pursue to educating the students were presented. This is a continual process and the hope is to at least influence in the interest in a few young people to think about college and pursue Electrical Engineering and getting jobs in the STEM area.

BIBLIOGRAPHY

[1] Frank Sharp, Dennis Symanski, “Scalable DC Micro Grids Provide Cost Effective Electricity in Regions without Electric Infrastructure”, IEEE Global Humanitarian Technology Conference.

[2] Chester, Lynne, and Alan Morris. "A new form of energy poverty is the hallmark of liberalised electricity sectors." Australian Journal of Social Issues 46, no. 4 (2011): 435-459.

[3] Kolokotsa, D., and M. Santamouris. "Review of the indoor environmental quality and energy consumption studies for low income households in Europe." Science of the Total Environment 536 (2015): 316-330

[4] Palaniappan, Karthik, Swachala Veerapeneni, Robert M. Cuzner, and Yue Zhao. "Viable residential DC microgrids combined with household smart AC and DC loads for underserved communities." Energy Efficiency (2018): 1-17.

[5] K. Palaniappan, W. Sedano, N. Hoeft, R. Cuzner and Z. J. Shen, "Fault discrimination using SiC JFET based self-powered solid state circuit breakers in a residential DC community microgrid," 2017 IEEE Energy Conversion Congress and Exposition (ECCE), Cincinnati, OH, 2017, pp. 3747-3753.

[6] T. S. Reynolds and T. Bernstein, “The damnable alternating current,”Proc. IEEE, vol. 64, no. 9, pp. 1339–1343, 1976.

[7] P. Fairley, “DC versus AC: the second war of currents has already begun [In My View],” IEEE Power Energy Mag., vol. 10, no. 6, pp. 104–103, Nov. 2012.

[8] Johnson K, Vossos V, Kloss M, Robinson G, Brown R, " Direct Current as an Integrating Platform for ZNE Buildings with EVs and Storage: DC Direct Systems – Abridge to a Low Carbon Future? – LBNL 100705.

[9] NextEnergy 2015.

[10] Ravula, S. 2015. "Direct Current Based Power Distribution Architectures for Commercial Buildings." presented at the Bosch DC Microgrid Project: EPC 14-053, November 12. http://www.energy.ca.gov/research/epic/documents/2015-12-03_symposium/presentations/Session_1A_4_Sharmila_Ravula_Robert_Bosch.pdf.

[11] Fregosi, D., S. Ravula, D. Brhlik, J. Saussele, S. Frank, E. Bonnema, J. Scheib, and E. Wilson.2015. "A Comparative Study of DC and AC Microgrids in Commercial Buildings across Different Climates and Operating Profiles." In 2015 IEEE First International Conference on DC Microgrids (ICDCM), 159–64. doi:10.1109/ICDCM.2015.7152031.

[12] Boeke, U., and M. Wendt. 2015. "DC Power Grids for Buildings." In 2015 IEEE First International Conference on DC Microgrids (ICDCM), 210–14. doi:10.1109/ICDCM.2015.7152040.

[13] Weiss, R., L. Ott, and U. Boeke. 2015. "Energy Efficient Low-Voltage DC-Grids for Commercial Buildings." In 2015 IEEE First International Conference on DC Microgrids (ICDCM), 154–58. doi:10.1109/ICDCM.2015.7152030.

[14] BUCEA. 2015. "DC Micro-Grid Photovoltaic Power Generation Efficiency Simulation Analysis Reports (Unpublished Manuscript)." Beijing University of Civil Engineering and Architecture.

[15] Noritake, M., K. Yuasa, T. Takeda, H. Hoshi, and K. Hirose. 2014. “Demonstrative Research on DC Microgrids for Office Buildings.” In Telecommunications Energy Conference (INTELEC), 2014 IEEE 36th International, 1–5. doi:10.1109/INTLEC.2014.6972180.

[16] Zhang, F., C. Meng, Y. Yang, C. Sun, C. Ji, Y. Chen, W. W., H. Qiu, and G. Yang. 2015. “Advantages and Challenges of DC Microgrid for Commercial Building a Case Study from Xiamen University DC Microgrid.” In 2015 IEEE First International Conference on DC Microgrids (ICDCM), 355–58. doi:10.1109/ICDCM.2015.7152068.

[17] E Hossain, E Kabalci, R Bayindir, R Perez “Microgrid testbeds around the world: State of art” Energy Conversion and Management, 2014:Vol 86, pg 156-183

[18] http://coe.miami.edu/simlab/mg.html

[19] http://energy.sandia.gov/energy/ssrei/gridmod/integrated-research-and-development/esdm/

[20] http://www.uta.edu/ee/powerlab/index.php?page=projects&id=3

[21] https://energy.fiu.edu/2014/12/smart-grid-test-bed-lab/

[22] http://www.hnei.hawaii.edu/projects/hawaii-hydrogen-power-park/

[23] Weiss, R; Ott, L.; Boecke, U., “Energy efficient low-voltage DC-grids for commercial buildings,” IEEE First International Conference on DC Microgrids, June 7-10 2015

[24] European Commission: Directive 2010/31/EU of 19 May 2010 on the energy performance of buildings, 2010, http://ec.europa.eu/energy/efficiency/buildings/buildings_en.htm.

[25] U.Boeke, M.Wendt: “DC power Grids for Buildings”, IEEE First International Conference on DC Microgrids, June 7-10 2015

[26] Adam Chandler, “Where the poor spend more than 10 percent of their income on energy”, The Atlantic, June 8, 2016, https://www.theatlantic.com/business/archive/2016/06/energy-povertylow-income-households/486197/

[27] A. Drehobl, “Explaining the unique energy burden of low-income households”, American Council for an Energy-Efficient Economy (ACEE), May 2016, https://aceee.org/blog/2016/05/explaining-unique-energy-burden-low

[28] A. Drehobl, F. Castro-Alvarez, “Low-income energy efficiency programs: a baseline assessment of programs serving the 51 largest cities”, American Council for an Energy-Efficient Economy (ACEE), July 11, 2017, https://aceee.org/white-paper/low-income-ee-baseline

[29] Kirubi, Charles, Arne Jacobson, Daniel M. Kammen, and Andrew Mills. "Community-based electric micro-grids can contribute to rural development: evidence from Kenya." World development 37, no. 7 (2009): 1208-1221.

[30] Van Acker, V.; Szablya, S.J.; Louie, H.; McLean Sloughter, J.; Pirbhai, A.S., "Survey of energy use and costs in rural kenya for community microgrid business model development," Global Humanitarian Technology Conference (GHTC), 2014 IEEE , pp.166,173, 10-13 Oct. 2014

[31] Vosloo, A.; Raji, K.A., "Intelligent central energy management system for remote community microgrid," Domestic Use of Energy (DUE), 2015 International Conference on the , pp.137,140, March 31 2015-April 1 2015

[32] Kumar, Y.V.P.; Bhimasingu, R., "Optimal sizing of microgrid for an urban community building in south India using HOMER," Power Electronics, Drives and Energy Systems (PEDES), 2014 IEEE International Conference on , pp.1,6, 16-19 Dec. 2014

[33] Unger, K.; Kazerani, M., "Organically grown microgrids: Development of a solar neighborhood microgrid concept for off-grid communities," IECON 2012 - 38th Annual Conference on IEEE Industrial Electronics Society , pp.5663,5668, 25-28 Oct. 2012

[34] Bahramirad, S.; Khodaei, A.; Svachula, J.; Aguero, J.R., "Building Resilient Integrated Grids: One neighborhood at a time.," Electrification Magazine, IEEE , vol.3, no.1, pp.48,55, March 2015

[35] Tiansong Cui; Yanzhi Wang; Nazarian, S.; Pedram, M., "An electricity trade model for microgrid communities in smart grid," Innovative Smart Grid Technologies Conference (ISGT), 2014 IEEE PES pp.1,5, 19-22 Feb. 2014

[36] Moutis, P.; Skarvelis-Kazakos, S.; Brucoli, M.; Hung, J.; Shu-Wei Wu, "Planned communities as microgrid applications," Innovative Smart Grid Technologies Conference Europe (ISGT-Europe), 2014 IEEE PES , pp.1,7, 12-15 Oct. 2014

[37] Khodaei, A.; Shahidehpour, M., "Optimal operation of a community-based microgrid," Innovative Smart Grid Technologies Asia (ISGT), 2011 IEEE PES , pp.1,3, 13-16 Nov. 2011

[38] Che, L.; Shahidehpour, M.; Alabdulwahab, A.; Al-Turki, Y., "Hierarchical Coordination of a Community Microgrid With AC and DC Microgrids," Smart Grid, IEEE Transactions on, No. 99, 6 March 2015

[39] Wunder, B.; Ott, L.; Kaiser, J.; Han, Y.; Fersterra, F.; März, M., “Overview of different topologies and control strategies for DC micro grids”, in *DC Microgrids (ICDCM), 2015 IEEE First International Conference on* (pp. 349-354). IEEE.

[40] Davies, R.; Sumner, M.; Christopher, E., "Energy storage control for a small community microgrid," Power Electronics, Machines and Drives (PEMD 2014), 7th IET International Conference on , pp.1,6, 8-10 April 2014

[41] Nejabatkhah, F.; Li, Y. W., “Overview of power management strategies of hybrid AC/DC microgrid”, *IEEE Transactions on Power Electronics, 30*(12), 7072-7089.

[42] Cuzner, R. M.; Venkataramanan, G., The status of DC micro-grid protection. In *Industry Applications Society Annual Meeting, 2008. IAS'08. IEEE* (pp. 1-8). IEEE.

[43] Hemamalini, S. "Review on Microgrid and its Protection Strategies." *International Journal of Renewable Energy Research (IJRER)* 6, no. 4 (2016): 1574-1587.

[44] Jianmin Zhu; Jafari, M.; Yan Lu, "Optimal energy management in community micro-grids," Innovative Smart Grid Technologies - Asia (ISGT Asia), 2012 IEEE , pp.1,6, 21-24 May 2012

[45] Huber, M.; Sanger, F.; Hamacher, T., "Coordinating smart homes in microgrids: A quantification of benefits," Innovative Smart Grid Technologies Europe (ISGT EUROPE), 2013 4th IEEE/PES , pp.1,5, 6-9 Oct. 2013

[46] C. D. Xu and K. W. E. Cheng, "A survey of distributed power system — AC versus DC distributed power system," Power Electronics Systems and Applications (PESA), 2011 4th International Conference on, Hong Kong, 2011, pp. 1-12

[47] D. Antoniou, A. Tzimas and S. M. Rowland, "Transition from alternating current to direct current low voltage distribution networks," in IET Generation, Transmission & Distribution, vol. 9, no. 12, pp. 1391-1401, 2015

[48] E. Rodriguez-Diaz, M. Savaghebi, J. C. Vasquez and J. M. Guerrero, "An overview of low voltage DC distribution systems for residential applications," 2015 IEEE 5th International Conference on Consumer Electronics - Berlin (ICCE-Berlin), Berlin, 2015, pp. 318-322

[49] Engelen, Kristof, Erik Leung Shun, Pieter Vermeyen, Ief Pardon, Reinhilde D'hulst, Johan Driesen, and Ronnie Belmans. "The feasibility of small-scale residential DC distribution

systems." In IEEE Industrial Electronics, IECON 2006-32nd Annual Conference on, pp. 2618-2623. IEEE, 2006.

[50] Kakigano, Hiroaki, Y. Miura, T. Ise, T. Momose, and H. Hayakawa. "Fundamental characteristics of DC microgrid for residential houses with cogeneration system in each house." In Power and Energy Society General Meeting-Conversion and Delivery of Electrical Energy in the 21st Century, 2008 IEEE, pp. 1-8. IEEE, 2008.

[51] Kakigano, H., Y. Miura, and T. Ise. "Configuration and control of a DC microgrid for residential houses." In Transmission & Distribution Conference & Exposition: Asia and Pacific, 2009, pp. 1-4. IEEE, 2009.

[52] Dong, Dong, Igor Cvetkovic, Dushan Boroyevich, Wei Zhang, Ruxi Wang, and Paolo Mattavelli. "Grid-interface bidirectional converter for residential DC distribution systems—Part one: High-density two-stage topology." IEEE Transactions on Power Electronics 28, no. 4 (2013): 1655-1666.

[53] Kaur, P.; Jain, S.; Jhunjhunwala, A., “Solar-DC deployment experience in off-grid and near off-grid homes: economics, technology and policy analysis,” IEEE First International Conference on DC Microgrids, June 7-10 2015

[54] Rodriguez-Diaz, Enrique, Juan C. Vasquez, and Josep M. Guerrero. "Intelligent DC homes in future sustainable energy systems: When efficiency and intelligence work together." IEEE Consumer Electronics Magazine 5, no. 1 (2016): 74-80.

[55] Arcidiacono, Vittorio, Antonello Monti, and Giorgio Sulligoi. "Generation control system for improving design and stability of medium-voltage DC power systems on ships." IET Electrical Systems in Transportation 2, no. 3 (2012): 158-167.

[56] Jin, Zheming, Giorgio Sulligoi, Rob Cuzner, Lexuan Meng, Juan C. Vasquez, and Josep M. Guerrero. "Next-generation shipboard dc power system: Introduction smart grid and dc microgrid technologies into maritime electrical netowrks." IEEE Electrification Magazine 4, no. 2 (2016): 45-57

[57] Zhang, He, Fabien Mollet, Christophe Saudemont, and Benoît Robyns. "Experimental validation of energy storage system management strategies for a local dc distribution system of more electric aircraft." IEEE Transactions on Industrial Electronics 57, no. 12 (2010): 3905-3916.

[58] Saeedifard, M.; Graovac, M.; Dias, R.F.; Iravani, R., "DC power systems: Challenges and opportunities," Power and Energy Society General Meeting, 2010 IEEE , pp.1,7, 25-29 July 2010

[59] Garbesi K, Vossos V, Shen H, “Catalog of DC Appliances and Power Systems”, LBNL-5364E, October 2011

[60] Joon-Young Jeon, Jong-Soo Kim, Gyu-Yeong Choe, Byoung-Kuk Lee, Jin Hur and Hyun-Cheol Jin, "Design guideline of DC distribution systems for home appliances: Issues and solution," Electric Machines & Drives Conference (IEMDC), 2011 IEEE International, Niagara Falls, ON, 2011, pp. 657-662

[61] Rodriguez-Otero, M.A.; O'Neill-Carrillo, E., "Efficient Home Appliances for a Future DC Residence," Energy 2030 Conference, 2008. ENERGY 2008. IEEE , pp.1,6, 17-18 Nov. 2008

[62] Dimeas, A.; Drenkard, S.; Hatzlargyrlou, N.; Karnouskos, S.; Kok, K.; Ringelstein, J.; Weldlich, A., "Smart houses in the smart grid: developing an interactive network" Electrification Magazine, IEEE , vol.2, no.1, pp.81,93, March 2014

[63] Wei Zhang; Lee, F.C.; Pin-Yu Huang, "Energy management system control and experiment for future home," Energy Conversion Congress and Exposition (ECCE), 2014 IEEE , pp.3317,3324, 14-18 Sept. 2014

[64] Makarabbi, G.; Gavade, V.; Panguloori, R.; Mishra, P., "Compatibility and performance study of home appliances in a DC home distribution system," Power Electronics, Drives and Energy Systems (PEDES), 2014 IEEE International Conference on , pp.1,6, 16-19 Dec. 2014

[65] E. Rodriguez-Diaz, J. C. Vasquez and J. M. Guerrero, "Intelligent DC Homes in Future Sustainable Energy Systems: When efficiency and intelligence work together.," in IEEE Consumer Electronics Magazine, vol. 5, no. 1, pp. 74-80, Jan. 2016

[66] J. Yamini and Y. R. Babu, "Design And implementation of smart home energy management system," 2016 International Conference on Communication and Electronics Systems (ICCES), Coimbatore, 2016, pp. 1-4

[67] Yardley, J., “Pope Francis to explore climates effect on the world’s poor”, The New York Times, June 13, 2015

[68] A. Drehobl, L. Ross, “Lifting the high energy burden in America’s largest cities: how energy efficiency can improve low-income and underserved communities”, American Council for Energy-Efficient Economy, 2016

[69] Heffner, Grayson, and Nina Campbell. "Evaluating the co-benefits of low-income energy-efficiency programmes." In Workshop Report, OECD/IEA, Paris. 2011.

[70] K. Palaniappan, S. Veerapeneni, R. Cuzner and Y. Zhao, "Assessment of the feasibility of interconnected smart DC homes in a DC microgrid to reduce utility costs of low income households," 2017 IEEE Second International Conference on DC Microgrids (ICDCM), Nuremburg, 2017, pp. 467-473.

[71] Shen, Z. J., Miao, Z., Roshandeh, A. M., Moens, P., Devleeschouwer, H., Salih, A., ... & Jeon, W. (2016, June). First experimental demonstration of solid state circuit breaker (SSCB) using 650V GaN-based monolithic bidirectional switch. In Power Semiconductor Devices and ICs (ISPSD), 2016 28th International Symposium on (pp. 79-82). IEEE

[72] Cuzner, Robert M., Karthik Palaniappan, Willy Sedano, Nicholas Hoeft, and Mengyuan Qi. "Fault characterization and protective system design for a residential DC microgrid." In Renewable Energy Research and Applications (ICRERA), 2017 IEEE 6th International Conference on, pp. 642-647. IEEE, 2017.

[73] Cuzner, R. M.; Palaniappan, K.; Shen, Z. J., "System Specification for a DC Community Microgrid and Living Laboratory Embedded in an Urban Environment ," International Conference on Renewable Energy Research and Applications (ICRERA) , November, 2015

[74] Baran, M.; Mahajan, N.R., "PEBB Based DC System Protection: Opportunities and Challenges," Transmission and Distribution Conference and Exhibition, 2005/2006 IEEE PES , pp.705,707, 21-24 May 2006

[75] Cuzner, R. M.; MacFarlin, D.; Clinger, D.; Rumney, M.; Castles, G., "Circuit Breaker Protection Considerations in Power Converter-Fed DC Systems," IEEE Electric Ship Technologies Symposium, 20-22 April 2009, Washington DC

[76] D. Salomonsson, L. Soder and A. Sannino, "Protection of Low-Voltage DC Microgrids," in IEEE Transactions on Power Delivery, vol. 24, no. 3, pp. 1045-1053, July 2009

[77] *IEEE Recommended Practice for the Design of DC Auxiliary Power Systems for Generating Stations*, IEEE Std. 946-2004, 2004.

[78] J. Morton, "Circuit breaker and protection requirements for dc switchgear used in rapid transit systems," *IEEE Trans. Ind. Appl.*, vol.IA-21, no. 5, pp. 1268–1273, Sep./Oct. 1985.

[79] P. Sutherland, “DC short-circuit analysis for systems with static sources,” *IEEE Trans. Ind. Appl.*, vol. 35, no. 1, pp. 144–151, Jan./Feb.1999.

[80] X. Feng, Z. Ye, C. Liu, R. Zhang, F. Lee, and D. Boroyevich, “Fault detection in dc distributed power systems based on impedance characteristics of modules,” in *Proc. Conf. Rec. IEEE Ind. Appl. Soc. Annu.Meeting*, Rome, Italy, Oct. 8–12, 2000, vol. 4, pp. 2455–3462.

[81] M. Baran and N. Mahajan, “Overcurrent protection on voltage-sourceconverter-based multiterminal dc distribution systems,” *IEEE Trans.Power Del.*, vol. 22, no. 1, pp. 406–412, Jan. 2007.

[82] L. Tang and B. Ooi, “Locating and isolating dc faults in multi-terminal dc systems,” *IEEE Trans. Power Del.*, vol. 22, no. 3, pp. 1877–1884,Jul. 2007.

[83] W. Litzenberger and P. Lips, “Pacific hvdc intertie,” *IEEE Power Energy Mag.*, vol. 5, no. 2, pp. 45–51, Mar./Apr. 2007.

[84] https://www.jsonline.com/story/entertainment/arts/art-city/2016/04/16/historic-garden-homes-district-struggles-to-find-its-future/84907374/

[85] J. Brozek, “DC overcurrent protection—Where we stand,” IEEE Trans.Ind. Appl., vol. 29, no. 5, pp. 1029–1032, Sep./Oct. 1993.

[86] 2007, Ferraz Shawmut North American Fuses and Fuseholders CHS Control. [Online]. Available: http://www.chscontrol.se.

[87] 2007, Fuses (in Swedish) IFO Electric. [Online]. Available:http://www.ifoelectric.se., Data sheet.

[88] 2007, Moulded Case Circuit Breakers Tmax and Isomax ABB [Online].Available: http://www.abb.com., Data sheet.

[89] 2007, Eaton's Cuttler-Hammer Series G Moulded Case Circuit Breaker, 15-630 A CHS Control. [Online]. Available:http://www.chscontrol.se.

[90] 2007, Sentron VL System Manual Siemens. [Online]. Available: http://www.automation.siemens.com.

[91] 2007, DC circuit breakers Sécheron. [Online]. Available: http://www.secheron.com., Data sheet.

[92] S. D. A. Fletcher, P. J. Norman, S. J. Galloway and G. M. Burt, "Determination of protection system requirements for dc unmanned aerial vehicle electrical power networks for enhanced capability and survivability," in IET Electrical Systems in Transportation, vol. 1, no. 4, pp. 137-147, December 2011

[93] Huang Zhiwei; Ma Junchao; Zeng Jiasi; Gao Yibo; Yuan Zhichang; Hu Ziheng; Zhao Yuming; Liu Guowei "Research status and prospect of control and protection technology for DC distribution network", Electricity Distribution (CICED), 2014 China International Conference on, pp. 1488-1493

[94] Beheshtaein, S.; Savaghebi, M.; Vasquez, J.C.; Guerrero, J.M. "Protection of AC and DC microgrids: Challenges, solutions and future trends", Industrial Electronics Society, IECON 2015 - 41st Annual Conference of the IEEE, pp. 5253-5260

[95] Satpathi, K.; Ukil, A. "Protection strategies for LVDC distribution system", PowerTech, 2015 IEEE Eindhoven, On page(s): 1 – 6

[96] Swierczek, J.-C.; Mollet, F.; Michaud, B.; Meuret, R.; Saudemont, C.; Robyns, B. "Protection of local high voltage DC regenerative network on MEA", Power Electronics and Applications (EPE), 2013 15th European Conference on, On page(s): 1 - 10

[97] Z. J. Shen, “Solid State Circuit Breakers for DC Micrgrids: Current Status and Future Trends,” 1st IEEE International Conference on DC Microgrids (ICDCM2015), 2015

[98] Schmerda, R.; Cuzner, R. M.; Clark, R.; Nowak, D.; Bunzel, S., "Shipboard Solid-State Protection: Overview and Applications," Electrification Magazine, IEEE , vol.1, no.1, pp.32,39, Sept. 2013

[99] P. Cairoli, I. Kondratiev and R. A. Dougal, "Coordinated Control of the Bus Tie Switches and Power Supply Converters for Fault Protection in DC Microgrids," in IEEE Transactions on Power Electronics, vol. 28, no. 4, pp. 2037-2047, April 2013

[100] Office of Energy Efficiency and Renewable Energy (EERE), “Building Characteristics for Residential Hourly Load Data”, https://openei.org/doe-opendata/dataset/eadfbd10-67a2-4f64-a394-3176c7b686c1/resource/cd6704ba-3f53-4632-8d08-c9597842fde3/download/buildingcharacteristicsforresidentialhourlyloaddata.pdf

[101] Office of Energy Efficiency and Renewable Energy (EERE) “Commercial and Residential Hourly Load Profiles for all TMY3 Locations in the United States”, https://openei.org/datasets/dataset/commercial-and-residential-hourly-load-profiles-for-all-tmy3-locations-in-the-united-states

[102] Manur, Ashray, Giri Venkataramanan, and David Sehloff. "Simple electric utility platform: A hardware/software solution for operating emergent microgrids." Applied Energy 210 (2018): 748-763.

[103] http://www.geinnovations.net/solar_air_conditioner.html

[104] R. Fu, D. Chung, T. Lowder, D. Feldman, K. Ardani, and R. Margolis, “U.S. Solar Photovoltaic System Cost Benchmark: Q1 2016”, National Renewable Energy Laboratory (NREL), Technical Report NREL/TP-6A20-66532, Sept. 2016.

[105] K. Ardani, E. O'Shaughnessy, R. Fu, C. McClurg, J. Huneycutt, and R. Margolis, "Installed Cost Benchmarks and Deployment Barriers for Residential Solar Photovoltaics with Energy Storage: Q1 2016", National Renewable Energy Laboratory (NREL), Technical Report NREL/TP-7A40-67474 February 2017.

[106] E. Wilson, C. Engebrect Metzger, S. Horowitz, R. Hendron, "2014 Building America house simulation protocols", National Renewable Energy Laboratory (NREL), NREL/TP-5500-0988, March 2014

[107] Office of Energy Efficiency and Renewable Energy (EERE) "Commercial and Residential Hourly Load Profiles for all TMY3 Locations in the United States", https://openei.org/datasets/dataset/commercial-and-residential-hourly-load-profiles-for-all-tmy3-locations-in-the-united-states

[108] S. K. Lin and C. R. Chen, "Optimal energy consumption scheduling in home energy management system," 2016 International Conference on Machine Learning and Cybernetics (ICMLC), Jeju, 2016, pp. 638-643

[109] http://www.geinnovations.net/solar-electricity-cost.html

[110] http://www.techadvantage.org/wp-content/uploads/2018/03/BO1D-63851-Andrew-Yip.pdf

[111] http://energyindependence.wi.gov/docview.asp?docid=15822&locid=160

[112] Edenhofer et. al, IPCC Special Report on Renewable Energy Sources and Climate Change Mitigation. Intergovernmental Panel on Climate Change, 2011.

[113] http://www.cleanerandgreener.org/resources/emissions-reductions-calculator.html (Rates are for the average kWh produced in Wisconsin power plants)

[114] Ferrer, H. J. A., & Schweitzer, E. O. (Eds.). (2010). Modern Solutions for Protection, Control, and Monitoring of Electric Power Systems. Schweitzer Engineering Laboratories.

[115] http://www.cooperindustries.com/content/dam/public/bussmann/Electrical/Resources/solutioncenter/technical_library/BUS_Ele_Tech_Lib_Circuit_Breakers_Instantaneous_Trip_Region.pdf

[116] Hudgins, J. L., Simin, G. S., Santi, E., & Khan, M. A. (2003). An assessment of wide bandgap semiconductors for power devices. *IEEE Transactions on Power Electronics*, *18*(3), 907-914.

[117] L. Zhang, K. Tan, X. Song and A. Q. Huang, "Comparative study on the turn-off capability of multiple Si and SiC power devices," 2017 IEEE 5th Workshop on Wide Bandgap Power Devices and Applications (WiPDA), Albuquerque, NM, 2017, pp. 295-299.

[118] Texas Instruments, Inc. Product Datasheet [Online]. Available: http://www.ti.com/product/tl494.

[119] A Andersen et al.," Empowering Smart Communities: Electrification, Education, and Sustainable Entrepreneurship in IEEE Smart Village Initiatives", IEEE Electrification Magazine 5 (2), 6-16, 2017

[120] Smart Grid, Department of Energy, available: http://energy.gov/oe/technology-development/smartgrid

[121] S.E. Collier, Ten steps to a smarter grid, IEEE Industry Applications Magazine, Vol. 16(2), pp. 62-68,2010.

[122] P. Sauer, G. Heydt, and V. Vittal, The state of electric power engineering education, IEEE Trans.Power Syst., vol. 19, no. 1, pp. 5–8, Feb. 2004.

[123] V.G. Agelidis, The future of power electronics/power engineering education: challenges and opportunities, in Proc. of IEEE Workshop on Power Electronics Education, 2005, p. 1-8.

[124] R.G. Belu - Renewable Energy Based Capstone Senior Design Projects for an Undergraduate Engineering Technology Curriculum, 2011 ASEE Conference & Exposition, June 26 - 29, Vancouver, BC, Canada (CD Proceedings).

[125] H. Gharavi and R. Ghafurian, Smart grid: the electric energy system of the future, Proceedings of the IEEE, Vol. 99(6), 2011, p. 917- 921

[126] B Buluc, H.I. Bulbul, "Increasing Social Awareness of Consumer Behaviors on Smart Grids Energy Systems", International Journal of Renewable Energy Research (IJRER), vol 6, no. 4, 2016

[127] J Barzola, M Espinoza, F Cabrera, "Analysis of Hybrid Solar/Wind/Diesel Renewable Energy System for off-grid Rural Electrification", International Journal of Renewable Energy Research (IJRER), vol 6, no.3, 2016

[128] T Salmi, M Bouzguenda, A Gastli, A Masmoudia, "MATLAB/Simulink Based Modelling of Solar Photovoltaic Cell", International Journal of Renewable Energy Research (IJRER), vol 2, no.2, 2012

[129] Y. Mizuno et al., "Evaluation and verification of an intelligent control system with modelling of green energy devices by constructing a micro-grid system in University Campus (report II)", in Renewable Energy Research and Application (ICRERA), 2013 International Conference on

[130] G. Graditi; R. Ciavarella; M. Valenti; A. Bracale; P. Caramia, "Advanced forecasting method to the optimal management of a DC microgrid in presence of uncertain generation", in Renewable Energy Research and Application (ICRERA), 2015 International Conference on

[131] R. Boukenoui; R. Bradai; A. Mellit; M. Ghanes; H. Salhi., "Comparative analysis of P&O, modified hill climbing-FLC, and adaptive P&O-FLC MPPTs for microgrid standalone PV system", in Renewable Energy Research and Application (ICRERA), 2015 International Conference.

[132] Syed Nabi, Mahesh Balike, Jace Allen and Kevin Rzemien. An Overview of Hardware-In-the-Loop Testing Systems at Visteon. SAE World Congress, Detroit, March 2004.

[133] Pouria Sarhadi, Samereh Yousefpou. State of the art: hardware in the loop modeling and simulation with its applications in design, development and implementation of system and control software. Int. J. Dynam. Control (2015) 3:470–479

[134] Michel Lemaire, Pierre Sicard, Jean Bélanger. Prototyping and Testing Power Electronics Systems using Controller Hardware-In-the-Loop (HIL) and Power Hardware-In-the-Loop (PHIL) Simulations. Vehicle Power and Propulsion Conference (VPPC), Montreal, 2015 IEEE

[135] Dominik S. Buse, Max Schettler, Nils Kothe, Peter Reinold, Christoph Sommer, Falko Dressler. Bridging Worlds: Integrating Hardware-in-the-Loop Testing with Large-Scale VANET Simulation. Wireless On-demand Network Systems and Services (WONS), 2018 14th Annual Conference on.

[136] Weihua Wang, Jin Zhu, Wei Li, Jean Bélanger. Analysis And Hardware-In-The-Loop Simulation Of A Pole-To-Pole DC Fault In MMC-Based HVDC Systems. Power Electronics Conference and 1st Southern Power Electronics Conference (COBEP/SPEC), 2015 IEEE 13th Brazilian

[137] R. Razzaghi, F. Colas, X. Guillaud, M. Paolone, and F. Rachidi. Hardware-in-the-Loop Validation of an FPGA Based Real-Time Simulator for Power Electronics Applications. 11th

International Conference of Power Systems Transients (IPST), Cavtat, Croatia, June 15-18, 2015

[138] Mahmoud Matar, Dominic Paradis, Reza Iravani. Real-time simulation of modular multilevel converters for controller hardware-in-the-loop testing. IET Power Electronics (Volume: 9, Issue: 1, 1 20 2016)

[139] Selimcan Deda, Guenter Prochart, Roland Greul. Fully Automated Testing of “AVL E-Storage BTE 1200V” with Parallelized Hardware-in-the-Loop Systems. PCIM Europe 2017; International Exhibition and Conference for Power Electronics, Intelligent Motion, Renewable Energy.

[140] Pejovic, P.; Maksimovic, D.; , "A new algorithm for simulation of power electronic systems using piecewise-linear device models," Power Electronics, IEEE Transactions on, vol.10, no.3, pp.340-348, May 1995

Appendix A

A.1 Spring Energy Consumption of the Dwellings

SPRING	House 1 (High)	House 2 Low	House 3 High	House 4 Low	House 5 Base	House 6 Base	House 7 High	House 8 Base	House 9 Low	Total Load	Total Spring Solar
1	0.51	0.27	0.51	0.27	0.40	0.40	0.51	0.40	0.27	3.56	0.00
2	0.46	0.26	0.46	0.26	0.36	0.36	0.46	0.36	0.26	3.23	0.00
3	0.44	0.25	0.44	0.25	0.34	0.34	0.44	0.34	0.25	3.10	0.00
4	0.44	0.24	0.44	0.24	0.34	0.34	0.44	0.34	0.24	3.06	0.00
5	0.47	0.26	0.47	0.26	0.37	0.37	0.47	0.37	0.26	3.29	0.17
6	0.58	0.30	0.58	0.30	0.46	0.46	0.58	0.46	0.30	4.00	3.40
7	0.73	0.34	0.73	0.34	0.58	0.58	0.73	0.58	0.34	4.97	10.68
8	0.78	0.33	0.78	0.33	0.62	0.62	0.78	0.62	0.33	5.20	17.34
9	0.77	0.28	0.77	0.28	0.62	0.62	0.77	0.62	0.28	5.03	19.93
10	0.78	0.27	0.78	0.27	0.63	0.63	0.78	0.63	0.27	5.02	21.07
11	0.79	0.27	0.79	0.27	0.65	0.65	0.79	0.65	0.27	5.12	21.27
12	0.79	0.26	0.79	0.26	0.64	0.64	0.79	0.64	0.26	5.08	20.33
13	0.76	0.27	0.76	0.27	0.62	0.62	0.76	0.62	0.27	4.94	21.31
14	0.74	0.27	0.74	0.27	0.60	0.60	0.74	0.60	0.27	4.85	20.04
15	0.76	0.29	0.76	0.29	0.61	0.61	0.76	0.61	0.29	4.96	19.83
16	0.85	0.32	0.85	0.32	0.69	0.69	0.85	0.69	0.32	5.57	16.37
17	1.03	0.39	1.03	0.39	0.83	0.83	1.03	0.83	0.39	6.74	12.80
18	1.13	0.45	1.13	0.45	0.91	0.91	1.13	0.91	0.45	7.47	7.27
19	1.17	0.50	1.17	0.50	0.93	0.93	1.17	0.93	0.50	7.81	1.48
20	1.25	0.55	1.25	0.55	0.98	0.98	1.25	0.98	0.55	8.32	0.03
21	1.26	0.56	1.26	0.56	0.98	0.98	1.26	0.98	0.56	8.40	0.00
22	1.08	0.49	1.08	0.49	0.85	0.85	1.08	0.85	0.49	7.25	0.00
23	0.86	0.41	0.86	0.41	0.67	0.67	0.86	0.67	0.41	5.80	0.00
24	0.64	0.32	0.64	0.32	0.50	0.50	0.64	0.50	0.32	4.38	0.00

A.2 Summer Energy Consumption of the Dwellings

SUMMER	House 1 (High)	House 2 Low	House 3 High	House 4 Low	House 5 Base	House 6 Base	House 7 High	House 8 Base	House 9 Low	0
1	0.49	0.24	0.49	0.24	0.34	0.34	0.49	0.34	0.24	3.20
2	0.45	0.23	0.45	0.23	0.31	0.31	0.45	0.31	0.23	2.96

3	0.43	0.22	0.43	0.22	0.31	0.31	0.43	0.31	0.22	2.88
4	0.43	0.22	0.43	0.22	0.30	0.30	0.43	0.30	0.22	2.84
5	0.47	0.24	0.47	0.24	0.34	0.34	0.47	0.34	0.24	3.15
6	0.59	0.28	0.59	0.28	0.43	0.43	0.59	0.43	0.28	3.90
7	0.76	0.31	0.76	0.31	0.53	0.53	0.76	0.53	0.31	4.80
8	0.78	0.28	0.78	0.28	0.51	0.51	0.78	0.51	0.28	4.71
9	0.80	0.24	0.80	0.24	0.49	0.49	0.80	0.49	0.24	4.60
10	0.92	0.24	0.92	0.24	0.50	0.50	0.92	0.50	0.24	4.96
11	1.03	0.24	1.03	0.24	0.51	0.51	1.03	0.51	0.24	5.33
12	1.14	0.24	1.14	0.24	0.51	0.51	1.14	0.51	0.24	5.65
13	1.22	0.24	1.22	0.24	0.49	0.49	1.22	0.49	0.24	5.84
14	1.32	0.25	1.32	0.25	0.49	0.49	1.32	0.49	0.25	6.19
15	1.39	0.28	1.39	0.28	0.54	0.54	1.39	0.54	0.28	6.61
16	1.61	0.34	1.61	0.34	0.67	0.67	1.61	0.67	0.34	7.84
17	1.75	0.40	1.75	0.40	0.82	0.82	1.75	0.82	0.40	8.93
18	1.72	0.45	1.72	0.45	0.84	0.84	1.72	0.84	0.45	9.01
19	1.59	0.47	1.59	0.47	0.82	0.82	1.59	0.82	0.47	8.63
20	1.57	0.51	1.57	0.51	0.86	0.86	1.57	0.86	0.51	8.79
21	1.55	0.53	1.55	0.53	0.89	0.89	1.55	0.89	0.53	8.89
22	1.25	0.44	1.25	0.44	0.72	0.72	1.25	0.72	0.44	7.23
23	0.95	0.35	0.95	0.35	0.55	0.55	0.95	0.55	0.35	5.59
24	0.70	0.27	0.70	0.27	0.40	0.40	0.70	0.40	0.27	4.10

A.3 Fall Energy Consumption of the Dwellings

FALL	House 1 (High)	House 2 Low	House 3 High	House 4 Low	House 5 Base	House 6 Base	House 7 High	House 8 Base	House 9 Low	0
1	0.45	0.30	0.45	0.30	0.38	0.38	0.45	0.38	0.30	3.39
2	0.40	0.28	0.40	0.28	0.34	0.34	0.40	0.34	0.28	3.05
3	0.38	0.26	0.38	0.26	0.32	0.32	0.38	0.32	0.26	2.91
4	0.38	0.26	0.38	0.26	0.32	0.32	0.38	0.32	0.26	2.87
5	0.41	0.27	0.41	0.27	0.35	0.35	0.41	0.35	0.27	3.10
6	0.53	0.32	0.53	0.32	0.44	0.44	0.53	0.44	0.32	3.87
7	0.69	0.39	0.69	0.39	0.58	0.58	0.69	0.58	0.39	5.00
8	0.74	0.42	0.74	0.42	0.63	0.63	0.74	0.63	0.42	5.36
9	0.72	0.38	0.72	0.38	0.62	0.62	0.72	0.62	0.38	5.19
10	0.73	0.37	0.73	0.37	0.63	0.63	0.73	0.63	0.37	5.19
11	0.81	0.38	0.81	0.38	0.64	0.64	0.81	0.64	0.38	5.49
12	0.85	0.38	0.85	0.38	0.64	0.64	0.85	0.64	0.38	5.61
13	0.87	0.38	0.87	0.38	0.61	0.61	0.87	0.61	0.38	5.59

14	0.89	0.38	0.89	0.38	0.59	0.59	0.89	0.59	0.38	5.58
15	0.94	0.38	0.94	0.38	0.61	0.61	0.94	0.61	0.38	5.79
16	1.02	0.43	1.02	0.43	0.69	0.69	1.02	0.69	0.43	6.41
17	1.17	0.54	1.17	0.54	0.85	0.85	1.17	0.85	0.54	7.69
18	1.28	0.66	1.28	0.66	0.97	0.97	1.28	0.97	0.66	8.74
19	1.29	0.72	1.29	0.72	1.01	1.01	1.29	1.01	0.72	9.05
20	1.29	0.71	1.29	0.71	1.01	1.01	1.29	1.01	0.71	9.04
21	1.20	0.68	1.20	0.68	0.95	0.95	1.20	0.95	0.68	8.48
22	0.99	0.60	0.99	0.60	0.82	0.82	0.99	0.82	0.60	7.23
23	0.77	0.49	0.77	0.49	0.64	0.64	0.77	0.64	0.49	5.70
24	0.55	0.38	0.55	0.38	0.47	0.47	0.55	0.47	0.38	4.22

A.4 Winter Energy Consumption of the Dwellings

WIN TER	House 1 (High)	House 2 Low	House 3 High	House 4 Low	House 5 Base	House 6 Base	House 7 High	House 8 Base	House 9 Low	0
1	0.60	0.32	0.60	0.32	0.47	0.47	0.60	0.47	0.32	4.16
2	0.51	0.28	0.51	0.28	0.40	0.40	0.51	0.40	0.28	3.60
3	0.48	0.27	0.48	0.27	0.38	0.38	0.48	0.38	0.27	3.37
4	0.46	0.27	0.46	0.27	0.36	0.36	0.46	0.36	0.27	3.28
5	0.46	0.26	0.46	0.26	0.36	0.36	0.46	0.36	0.26	3.25
6	0.52	0.28	0.52	0.28	0.41	0.41	0.52	0.41	0.28	3.65
7	0.69	0.34	0.69	0.34	0.54	0.54	0.69	0.54	0.34	4.73
8	0.89	0.40	0.89	0.40	0.71	0.71	0.89	0.71	0.40	6.01
9	0.89	0.36	0.89	0.36	0.71	0.71	0.89	0.71	0.36	5.88
10	0.83	0.30	0.83	0.30	0.67	0.67	0.83	0.67	0.30	5.41
11	0.84	0.30	0.84	0.30	0.69	0.69	0.84	0.69	0.30	5.48
12	0.86	0.30	0.86	0.30	0.70	0.70	0.86	0.70	0.30	5.58
13	0.85	0.29	0.85	0.29	0.69	0.69	0.85	0.69	0.29	5.48
14	0.82	0.30	0.82	0.30	0.66	0.66	0.82	0.66	0.30	5.33
15	0.81	0.31	0.81	0.31	0.65	0.65	0.81	0.65	0.31	5.32
16	0.86	0.33	0.86	0.33	0.69	0.69	0.86	0.69	0.33	5.66
17	1.05	0.41	1.05	0.41	0.85	0.85	1.05	0.85	0.41	6.93
18	1.39	0.54	1.39	0.54	1.11	1.11	1.39	1.11	0.54	9.10
19	1.51	0.62	1.51	0.62	1.19	1.19	1.51	1.19	0.62	9.98
20	1.46	0.64	1.46	0.64	1.14	1.14	1.46	1.14	0.64	9.74
21	1.39	0.63	1.39	0.63	1.09	1.09	1.39	1.09	0.63	9.34
22	1.29	0.58	1.29	0.58	1.02	1.02	1.29	1.02	0.58	8.68
23	1.06	0.49	1.06	0.49	0.83	0.83	1.06	0.83	0.49	7.15
24	0.83	0.41	0.83	0.41	0.65	0.65	0.83	0.65	0.41	5.64

A.5 Optimization Code

```
for j = 1:24
S(j,1) = L_Orig(2,j)/12;
L(j,1)=L_Orig(1,j);
end
for j = 1:15
          Pos (j,1)= 0;
        Neg (j,1) = 0;
        Solar_Number (j,1) = j;
end

for b = 1:51
    for j = 1:15
        Pos_adj(j,b) = 0;
    end
end

for b = 1:51
    Battery_Size (b,1) = (b-1)/5;
end

for j = 1:15
for i = 1:24
    Net_Load (i,j)=L(i,1)-S(i,1)*j;

    if Net_Load(i,j)>0
        Pos (j,1)= Pos(j,1) + Net_Load(i,j);
    else
        Neg (j,1) = Neg(j,1) + Net_Load(i,j);
    end
end
end
for k = 1:51
    c = (k-1)/5;
    for j = 1:15
    if c*9 > -Neg(j,1)
        Pos_adj(j,k) = Pos(j,1)+ Neg(j,1);
    else
        Pos_adj(j,k) = Pos(j,1)- c*9;
    end
    if c*471+j*300*2.93 > 10000
       Pos_adj(j,k)=0;
    else
        Pos_adj(j,k)=Pos_adj(j,k);
    end
    end
end
for j = 1:11
    P = j*300*2.93;
    S_N (j,1)= j;
    B_N (j,1)= (10000 - P)/471;

end

mesh(Battery_Size, Solar_Number, Pos_adj);
```

Appendix B

B.1 SSCB Components

V_{DC_bus}	V_{GS_JFET}	R_1	R_2	R_3	R_4	C_1
400 V	-18 V	15KΩ	6.1Ω	33Ω	240KΩ	1uF
C_2	C_3	D_1	D_2	D_3	D_4	L_1
0.1uF	4.7nF	PK1N5929	STPS1150	STPS1150	1N4747	22uH
L_2	L_3	Q_1	Q_2			
137.5uH	137.5uH	UJN1205	IRFD010			

Transformer which includes L_1,L_2,L_3= Q4436-BL (from Coilcraft)

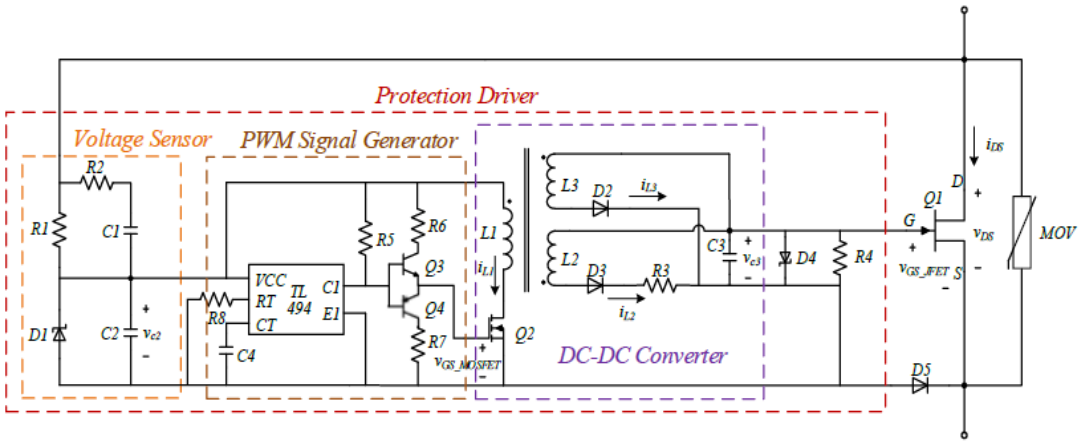

B.2 SSCB Schematic Prints

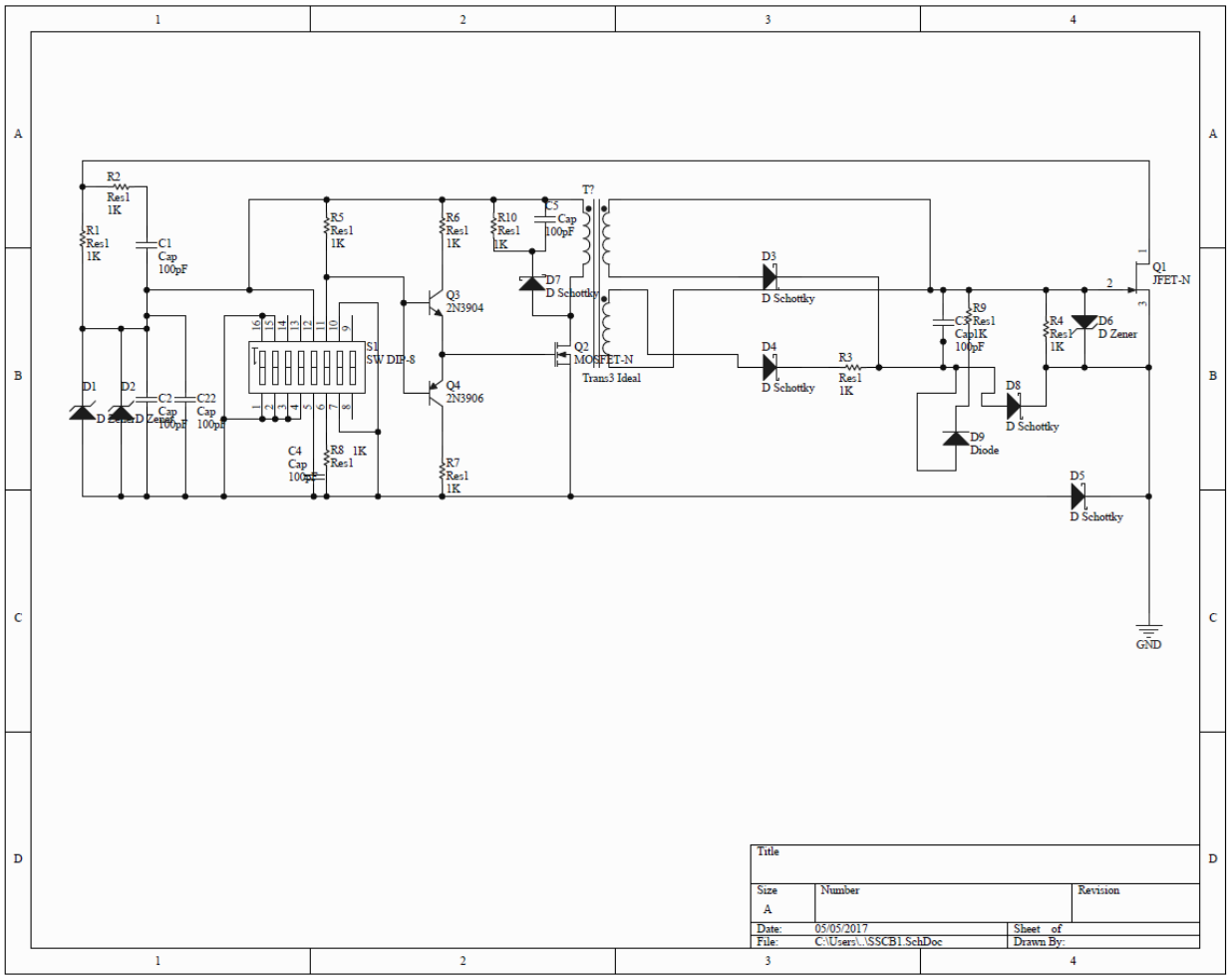

B.3 SSCB PCB Layout

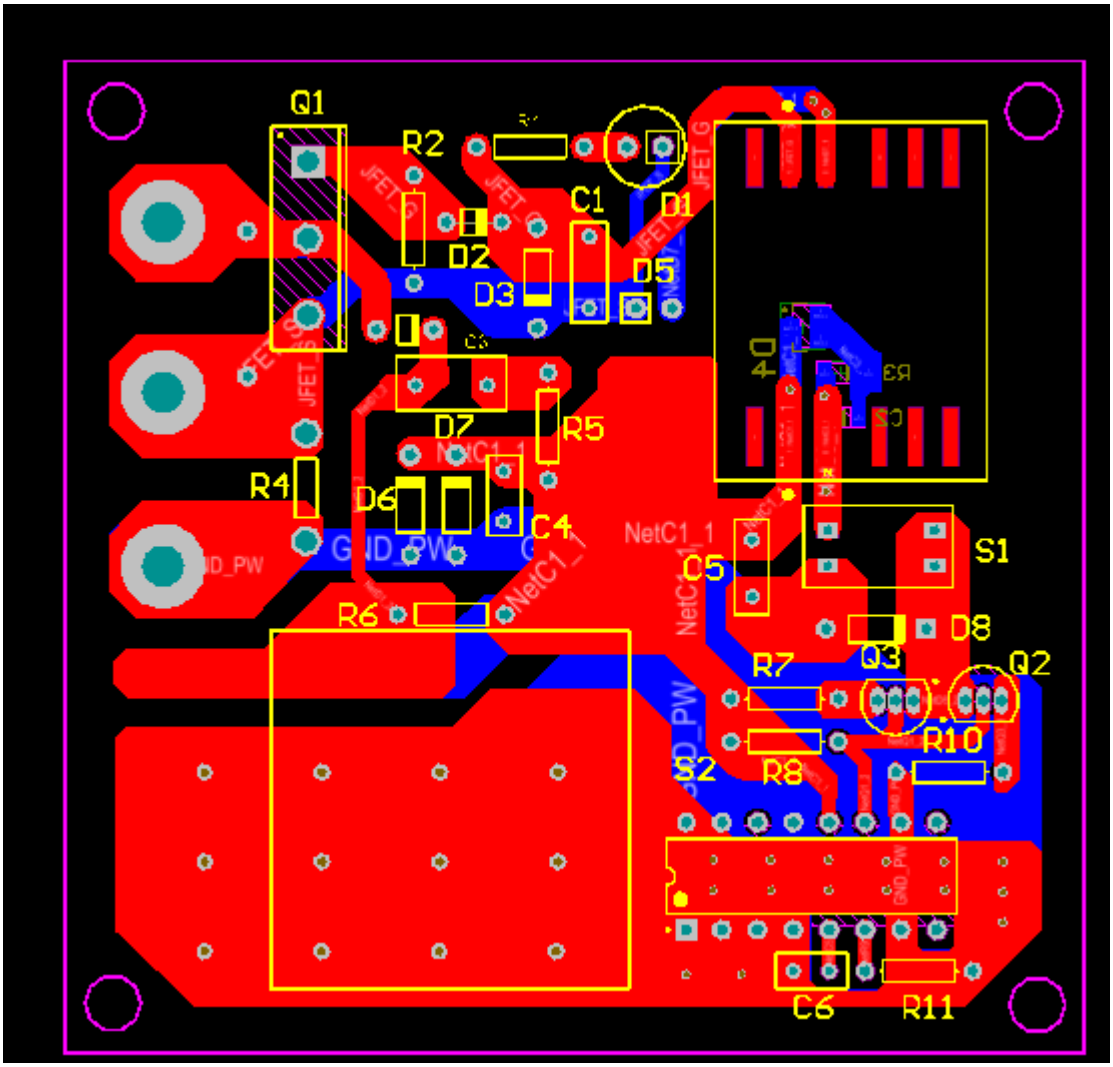

Curriculum Vitae

Karthik Palaniappan is currently a Ph.D. candidate in Electrical Engineering at University of Wisconsin - Milwaukee and also a Control Firmare engineer at Rockwell Automation working on Low Voltage Drives. He received his Master's of Science in Electrical Engineering from the University of Wisconsin – Milwaukee in 2011. He received a Bachelor's of Technology in Electronics and Communication from SRM University in India and was selected as one of three students to study on a study abroad programat UW Milwaukee as an undergraduate exchange student in Spring 2008. Karthik has worked as an Application Engineer at Elutions inc., working on SCADA controls and Energy monitoring of Verizon Data Centers from 2011 to 2012 returning to graduate school at UW-Milwaukee.

Publications

Journals:

Karthik Palaniappan, Swachala Veerapeneni, Robert M. Cuzner, and Yue Zhao. "Viable residential DC microgrids combined with household smart AC and DC loads for underserved communities." Energy Efficiency (2018): 1-17.

Swachala Veerapeneni, **Karthik Palaniappan**, Robert M. Cuzner. " Analysis of solar and battery requirements for hybrid DC/AC powered households in the USA." Energy Efficiency (2019): 1-19.

Karthik Palaniappan, Willy Sedano, Mark Vygoder, Nicholas Hoeft, Robert M. Cuzner, John Shen,"Short Circuit Fault Discrimination Using SiC JFET Based Self-Powered Solid State Circuit Breakers in a Residential DC Community Microgrid" – IEEE IAS (Second Review)

Conferences:

K. Palaniappan, B Seibel, M Cook, C Dufour, " Real Time Hardware-in-the-Loop Validation of Common Bus Inverter Low Voltage Drives," APEC 2019 -accepted.

K. Palaniappan, W. Sedano, N. Hoeft, R. Cuzner and Z. J. Shen, "Fault discrimination using SiC JFET based self-powered solid state circuit breakers in a residential DC community microgrid," 2017 IEEE Energy Conversion Congress and Exposition (ECCE), Cincinnati, OH, 2017, pp. 3747-3753.

K. Palaniappan and R. M. Cuzner, "Educating students as a means to help people in a low income community live in a DC microgrid laboratory," 2017 IEEE 6th International Conference on Renewable Energy Research and Applications (ICRERA), San Diego, CA, 2017, pp. 339-344.

Cuzner, Robert M., **Karthik Palaniappan**, Willy Sedano, Nicholas Hoeft, and Mengyuan Qi. "Fault characterization and protective system design for a residential DC microgrid." In Renewable Energy Research and Applications (ICRERA), 2017 IEEE 6th International Conference on, pp. 642-647. IEEE, 2017.

K. Palaniappan, S. Veerapeneni, R. Cuzner and Y. Zhao, "Assessment of the feasibility of interconnected smart DC homes in a DC microgrid to reduce utility costs of low income households," 2017 IEEE Second International Conference on DC Microgrids (ICDCM), Nuremburg, 2017, pp. 467-473.

Cuzner, R. M.; **Palaniappan, K**.; Shen, Z. J., "System Specification for a DC Community Microgrid and Living Laboratory Embedded in an Urban Environment ," International Conference on Renewable Energy Research and Applications (ICRERA) , November, 2015